The Institute of Paper Chemistry

Appleton, Wisconsin

Doctor's Dissertation

The Bond Structure in
The Alkaline-Ferric-Tartrate System

John E. Hanby, Jr.

June, 1968

THE BOND STRUCTURE IN
THE ALKALINE-FERRIC-TARTRATE SYSTEM

A thesis submitted by

John E. Hanby, Jr.

B.Ch.E. 1963, Georgia Institute of Technology
M.S. 1965, Lawrence University

in partial fulfillment of the requirements
of The Institute of Paper Chemistry
for the degree of Doctor of Philosophy
from Lawrence University,
Appleton, Wisconsin

June, 1968

SUMMARY

The bond structure of the complex in the alkaline-ferric-tartrate system (FeTNa) was examined and related to the cellulose-dissolving ability of the system.

The subject of bonding was approached by magnetic susceptibility and absorption spectrophotometric techniques. The magnetic measurements allowed classification of the bonding with respect to the electron spin-state in the iron. The absorption spectrophotometry was used for following general changes in the complex and for recording the FeTNa spectra. The spectrum of an alkaline FeTNa solution was analyzed in terms of the electron transitions, and the energies of these transitions were related to the interaction of the iron with its environment.

A ferric nitrate-tartrate acid solution (three moles of tartrate per mole of iron) was titrated potentiometrically with sodium hydroxide. The titration curve established that the solvent (or alkaline) FeTNa forms at the third equivalence point of the tartaric acid. The spin-state of the iron at this point was found to correspond with the high-spin type bond structure. With less than three equivalents of base, the magnetic susceptibility of the FeTNa showed suppressed values. This was attributed to the formation of polynuclear type complexes which have spin coupling.

In the alkaline FeTNa system, evidence was obtained for an equilibrium between various species of the complex. The iron in the solvent FeTNa was found to be co-ordinated with less than the maximum possible amount of tartrate. Additional tartrate in the solvent system then caused the equilibrium to shift and favor increased coordination between the iron and tartrate. (The complex which has maximum coordination between the iron and tartrate apparently does not dissolve cellulose.)

Finally, it was shown by magnetic and spectral measurements that glycerol coordinates with the solvent FeTNa in much the same manner as does additional tartrate. The same equilibrium mechanism must therefore be involved. Since the glycol pair of hydroxyl groups on the glycerol molecule is quite analogous to the glycol pair on the glucopyranoside repeating units of the cellulose molecule, it is expected that cellulose coordinates with the solvent FeTNa in a simmilar manner. Thus, the addition of cellulose to the solvent FeTNa apparently causes the equilibrium to shift, and the cellulose is carried into solution as the glycol pairs on its repeating units are incorporated into the complex.

INTRODUCTION

Until about the last fifteen years, the cellulose chemist had to choose between either cuprammonium hydroxide or cupriethylenediamine hydroxide as solvents for cellulose. The principal disadvantage with these solvents is the sensitivity of dissolved cellulose to oxidative degradation by air. This sensitivity is particularly severe with the cuprammonium hydroxide, and air must be excluded from the cellulose solutions at all times. The cupriethylenediamine solutions are less sensitive, and air contact can be tolerated for short periods. An additional disadvantage of these copper-based solvents is their intense color; studies employing spectrophotometric techniques are thus often difficult.

With the elimination of these disadvantages as a principal objective, Jayme and coworkers at Darmstadt began a systematic search for new cellulose solvents. Their general method of approach involved the substitution of other metal ions for the copper in the two copper-based solvents. In this manner, the cadmium-ethylene-diamine solvent system, which has proven quite successful, was discovered.

In addition, their search produced a quite different type of solvent, at least as compared with the copper-based systems. This solvent, which is abbreviated FeTNa (or EWNN in German), is formed by a combination of ferric ions and tartrate ions in a strong sodium hydroxide solution. Solutions of cellulose in the FeTNa are clear, green in color, odorless, and practically insensitive to atmospheric oxygen.

THE FeTNa SYSTEM

The discovery of the alkaline-ferric-tartrate solvent was reported by Jayme and Verburg (1) in 1954. Its method of preparation (2) and general properties as a cellulose solvent (3,4) were then described in publications which appeared during the next several years. By about 1957 the FeTNa system was established as a

cellulose solvent and, since that time, has been involved in numerous investigations. Almost entirely, however, these programs have been directed toward evaluation of the FeTNa as a solvent for various cellulosic materials. In general, emphasis has been placed on (1) the relation between solvent composition and dissolving power, (2) the use of the solvent in cellulose fractionation, and (3) the description of the hydrodynamic properties of cellulose solutions.

COMPOSITION

The dissolving power of the FeTNa solvent depends on the iron molarity, the iron-to-tartrate ratio, and the molarity of excess hydroxide. (The meaning of excess hydroxide is defined under the next heading.) The relation between the solvent composition and dissolving power has been examined in various programs (5-7). Though the agreement is not exact, an iron molarity of 0.5, an iron-to-tartrate mole ratio of 1 to 3, and an excess sodium hydroxide molarity of about 2, correspond to the general region of maximum solvent power.

The structure of the complex in the FeTNa solution is not known with any degree of certainty. Jayme and Bergmann (8) precipitated a material from the FeTNa by treatment of the solution with a large excess of alcohol. Analysis of the dried material revealed an iron-to-disodium tartrate mole ratio of 1 to 3. This led to the assumption that three moles of tartrate are coordinated with each mole of iron.

FeTNa NOMENCLATURE

An abbreviated method for describing the various iron-tartrate solutions is defined in this section. "FeTNa" applies to the iron-tartrate complex in general. The notation 1:3:13 FeTNa (0.5$\underline{M}$ Fe), for example, specifies a solution which is 0.5$\underline{M}$ with respect to the ferric ion and has a 1 to 3 to 13 mole ratio

of iron to tartaric acid to sodium hydroxide. Excess hydroxide is defined as the amount of sodium hydroxide in excess of that required to provide three moles for each mole of tartaric acid.

FeTNa solutions which have an excess of sodium hydroxide are referred to as "alkaline FeTNa" or "alkaline-ferric-tartrate" solutions. When the composition is such that the solution will dissolve cellulose, the notation "solvent FeTNa" or "cellulose-solvent FeTNa" is sometimes used. (The solvent FeTNa is always alkaline and green in color.) The word "iron," such as in "iron-tartrate," specifies the ferric ion.

GENERAL PROPERTIES

The principal advantages of the FeTNa system are as follows (4): (1) The solvent is easy to prepare and store; (2) dissolved cellulose is relatively insensitive to air and, in general, is stable. Jayme and Bergmann (3) showed that the cellulose in FeTNa is degraded only slightly by treatment of the solution with pure oxygen for 24 hours. The FeTNa solvent is thus ideally suited for viscosity determinations since air does not have to be excluded from the system. In addition, the concentration-viscosity relationships are linear over a wide range so that evaluation of the data is relatively simple (5,9).

The FeTNa solvent has found application in fractional solution and precipitation of cellulose according to chain length (10,11). The relation between the composition of FeTNa and its solvent power is frequently employed in these fractionations. Additions of aqueous glycerol to cellulose solutions provides a convenient means for effecting the fractional precipitation.

Certain hemicelluloses can be separated from a mixture of hemicelluloses with the FeTNa (12,13). The separation, which is only approximate, is based on the different solubilities of the various components.

A number of studies have been conducted in which the swelling and dissolution of various cellulosic fibers in FeTNa were followed microscopically ([14],[15]). In general, the results are described in terms of the fiber structure and solvent properties.

The solubility of cellulose in FeTNa is directly related to the structure of the cellulose. Water cellulose, which is favored at lower temperatures, is more soluble than cellulose II ([16]). Less crystalline cellulose samples are more soluble in FeTNa ([17]), and cellulose I will dissolve preferentially over cellulose II ([17],[18]). In fact, solubility data were found to be more sensitive in detecting the formation of cellulose II than was x-ray diffraction ([19]).

The industrial applications of the FeTNa solvent are generally in the categories of quality control and testing. The viscosities of chemical pulps and the swelling and dissolution behaviors of various fibers can sometimes be related to variables in the industrial process or to product specifications ([20-22]).

MECHANISM OF CELLULOSE DISSOLUTION

The description of cellulose dissolution in FeTNa is based predominantly on the work by Bayer ([23]). From a program of continuous variations, the optimum combining mole ratio of iron to tartrate in the FeTNa solution was found to be 1 to 4.5. This optimum solution had a total concentration (iron plus tartrate) of 0.40 mole per liter and a 2.0M excess of sodium hydroxide. A 1:4.5:17.5 FeTNa (0.5M Fe) solution failed to dissolve cellulose (cotton linters).

A 1:3:13 FeTNa (0.5M Fe) solution, however, dissolved cotton linters readily. In a continuous variations program with model compounds, this FeTNa was found to complex well with compounds containing a glycol pair of hydroxyl groups plus an additional oxygen atom. The glycol group appeared to be the active function in

the coordination between the FeTNa and model; the additional oxygen was thought to confer water solubility upon the new complex. The optimum combining ratio between the 1:3:13 FeTNa (0.5$\underline{M}$ Fe) and complexing model compounds was 1 to 1.5, as expressed on a mole basis. The mole ratio of iron to glycol-containing ligands (tartrate plus model) in the optimum solution was thus 1 to 4.5.

These results were interpreted in terms of a glycol-deficiency driving force for the dissolution of cellulose in the 1:3:13 FeTNa (0.5$\underline{M}$ Fe). Apparently, there is a deficiency of glycol groups in the solvent FeTNa which can be filled by glycol-containing compounds such as tartrate, glycerol, or methyl β-D-glucopyranoside. Similarly, the glycol pairs on the repeating units of the cellulose molecule can fill this deficiency; cellulose is then carried into solution as the new chelate forms.

FERRIC ION COMPLEXES

The tartrate complexes of the ferric ion have received attention in a large number of studies, most of which have been directed toward determining the structures and stabilities of the various complex species. In general, the agreement among the various studies is not good. It can, however, be concluded that the ferric-tartrate system forms a number of complexes and that these complexes are highly dependent on the pH of the system.

Bobtelsky and Jordan (24) reviewed the early work on ferric-tartrate and citrate complexes and proposed that three tartrate anions are coordinated with two ferric ions in the most stable species. Green and Parkins (25) examined the ferric-tartrate system at pH values between 1.5 and 4.0. Formulas having iron-to-tartrate mole ratios of 1 to 1, 1 to 2, and 1 to 3 were suggested. T erlake (26) proposed the existence of four complex species from an extensive st   in acidic media. The mole ratio of iron to tartrate in the species was unity; one

species was monomeric, two were dimeric, and one was trimeric. Pyatnitskii and Gorbataya (27) reported that the formula for the ferric-tartrate complex has a 1 to 1 iron-to-tartrate mole ratio as the pH varies from 4 to 8. From a thermometric titration over the pH range of 1.5 to about 11, Gallet and Paris (28) found evidence for the successive formation of five complexes which have iron-to-tartrate mole ratios of 1 to 0.5, 5 to 4, 1 to 1, 1 to 1.5, and 1 to 2. Lingane (29) and Yamada (30) examined the ferric-tartrate system by polarography and observed that the electrode processes are irreversible in alkaline media. Above a pH of 9, and with a large excess of tartrate, Yamada suggested the existence of only one complex species in which the tartrate is coordinated to the iron at the hydroxyl and carboxyl positions. Franke (31) and Pyatnitskii (32) suggested iron-to-tartrate mole ratios of 1 to 3 and 1 to 2, respectively, for complexes in alkaline media.

The complexes formed between ferric ions and fructose were examined as a function of pH in a series of experiments (33-35). With a large excess of fructose (10 to 20 moles per mole of iron), the color of the complex was found to be dark yellow and red-brown under acidic and alkaline conditions, respectively. At a pH of about 7, the ESR signal intensity, the NMR line width, and the magnetic susceptibility of the system went through minima. These results were attributed to the formation of a dimer which apparently breaks up at higher pH values. It was suggested that the ferric ions in the dimer are connected by hydroxo bridges.

Ferric-tartrate complexes are not well characterized in alkaline media. The principal reason for this is the strong affinity between hydroxide and ferric ions. The hydroxide thus becomes an additional ligand, and the number of possible species is substantially increased. It is felt, however, that the alcoholic hydrogen of the tartrate is replaced by the ferric ion at high pH levels (26,36,37). Structures involving bidentate chelation between the iron and tartrate, as suggested in Fig. 1, thus seems likely (8). With x equal to 3, both the coordination number and the

oxidation state of the ferric ion are satisfied. Such structures often show
enhanced stability ($\underline{38}$). With $\underline{x}$ less than 3, hydroxide ions and/or water mole-
cules probably fill the vacancies in the coordination sphere. The average value
of $\underline{x}$ in the alkaline FeTNa system very likely depends on the concentration of
iron, the iron-to-tartrate ratio, and the amount of sodium hydroxide in excess of
three moles per mole of tartaric acid. From equilibrium considerations (which are
discussed later) it is expected that $\underline{x}$ should increase as the ratio of iron to
tartrate in the solution decreases.
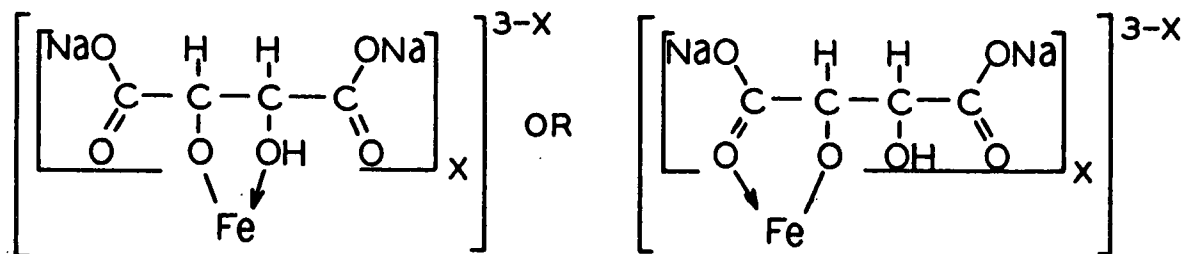
Figure 1. Possible Iron-Tartrate Coordination Structures

DEFINITIONS

In coordination compounds involving metal ions, the metal is frequently
surrounded by electron-donating groups or ligands. The coordination number is
the number of electron donating groups which surround the central species.
For the ferric ion, this number is usually 6. The electronic configuration of
the ferric ion is represented by $1s^2 2s^2 2p^6 3s^2 3p^6 3d^5$. Of principal importance
are the five electrons in the 3d orbitals.

Tartrate and glycerol are employed as ligands in the present study. The
structural formulas for tartaric acid and glycerol are:
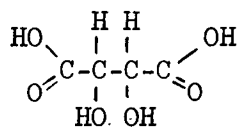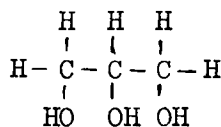
tartaric acid   glycerol

APPROACH TO THE STUDY

The solvent properties of the FeTNa system have been studied in considerable detail and seem to be sufficiently elucidated. It has also been shown that the FeTNa complex bonds chemically with cellulose as the latter is carried into solution. Little, however, is known about the alkaline-ferric-tartrate complex itself; a complete description of the reaction which occurs between cellulose and the complex is therefore not possible.

The complex in the alkaline FeTNa was given principal attention during the present study. The major objective of the program was examination of the bonding between the iron and tartrate. First, a description of this bonding has academic significance. Second, and more important, the bonding should be related to the cellulose-dissolving ability of the FeTNa. The latter aspect was pursued by examining the bond structure as the iron concentration and iron-to-tartrate ratio varied. This approach was suggested by the interdependence of the FeTNa composition and solvent properties. In addition, the effect of glycerol on the bond structure in the FeTNa system was studied. Glycerol complexes readily with the FeTNa solvent, is completely miscible with water (so that high concentrations are possible), and is easy to use. It was, therefore, employed as a model compound for cellulose.

The subject of bonding is an important aspect of this program. The methods for classifying the bond structure in coordination compounds are presented under the next heading. This section is then followed by a description of the experimental program.

CLASSIFICATION OF BONDING

HIGH-SPIN OR LOW-SPIN

A description of bonding in coordination compounds was first made by the electrostatic or crystal field approach (39). This involved an examination of

the influence of an electrostatic potential field on the various energy levels of the atom. Interaction between a potential field of octahedral symmetry and the d-electron wave functions produces a splitting of the initially degenerate d-orbitals into a higher energy, doubly degenerate set and a lower energy, triply degenerate set (40,41). This is shown schematically in Fig. 2, where Δ or 10Dq is the energy difference between the higher and lower energy sets. The higher energy set contains the $d_{x^2-y^2}$ and d_{z^2} atomic orbitals; the lower energy set contains the d_{xy}, d_{yz}, and d_{xz} atomic orbitals. (The octahedral symmetry is characteristic of the vast majority of ferric ion complexes.) Quantitative calculations based on the crystal field model generally give Δ values that are too small as compared with experiment. Nonetheless, the concept of the crystal field splitting energy has provided a useful means for classifying complexes. This somewhat surprising result is readily explained by application of the molecular orbital model (40,41). The central metal ion is now surrounded by six electron-donating groups rather than six point negative charges. With σ-type bonding, the d_{xy}, d_{yz}, and d_{xz} metal atomic orbitals become the non-bonding t_{2g} orbitals, and the $d_{x^2-y^2}$ and d_{z^2} metal orbitals overlap with ligand orbitals to form the e_g bonding and antibonding molecular orbitals (Fig. 3). The six ligand orbitals each contribute a pair of electrons, denoted by x which fill the bonding a_{1g}, t_{1u}, and e_g levels. (The a_{1g} and t_{1u} are formed by overlap of the 4s and 4p metal orbitals with ligand orbitals. The order of the levels with respect to energy is unknown, but fortunately unimportant for the present purposes.) The metal d-electrons are then fed into the t_{2g} and antibonding e_g orbital sets. The quantity Δ in the crystal field model now becomes the t_{2g}-antibonding e_g separation in the molecular orbital description. (The symbols given in Fig. 3 are frequently used in coordination chemistry. They are derived from group theory and describe the symmetries of various states (41,42). For the present discussions, these symbols, as well as others which will be introduced, can simply be regarded as convenient abbreviations.)
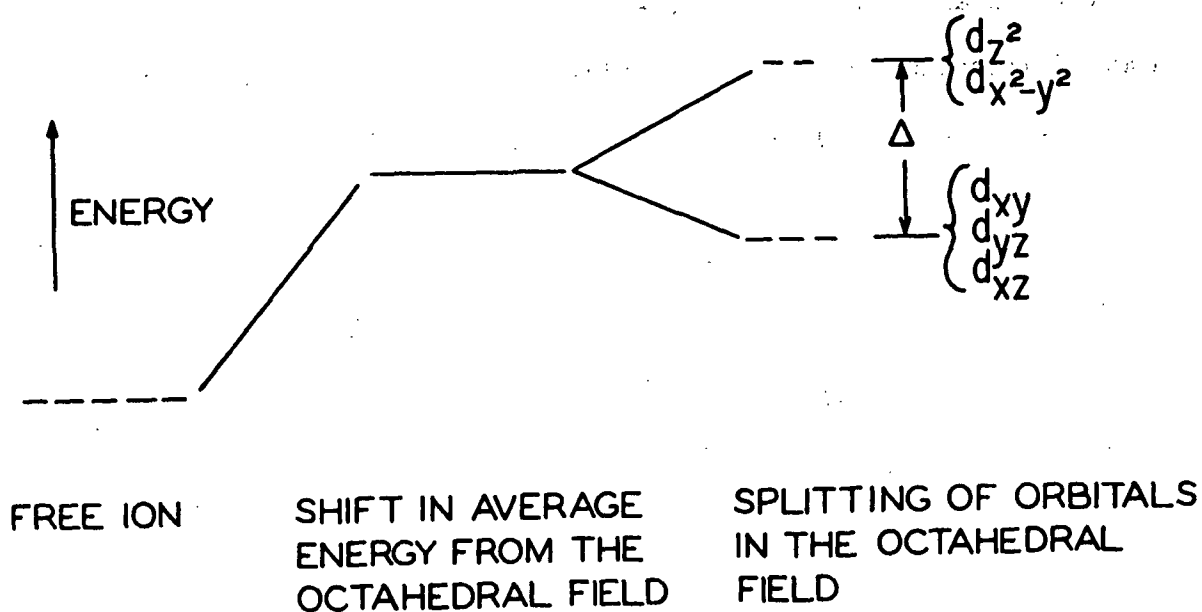
Figure 2. The Five d-Orbitals in an Octahedral Field
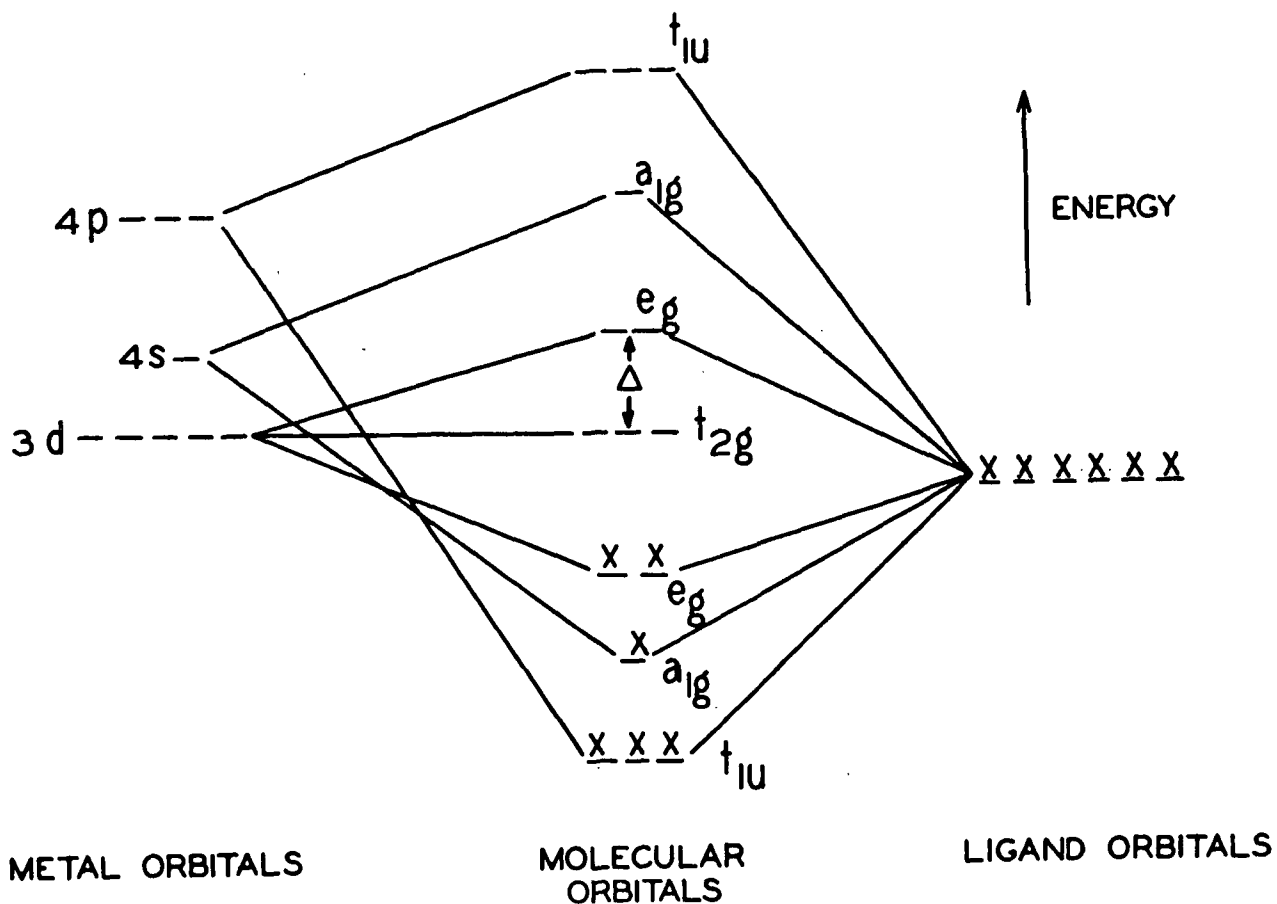
Figure 3. Molecular Orbital Diagram for σ-Bonding in an Octahedral Complex

With the ferric ion as the central metal in the complex, five d-electrons (often specified as d^5) must be fed into the t_{2g} and e_g orbitals. When Δ is small, these electrons occupy the orbitals in a spin-parallel or high-spin state, in accord with Hund's rule of maximum multiplicity. With Δ sufficiently large, it becomes energetically favorable for the electrons to pair spins, and the spin-paired or low-spin state exists. These two possibilities are illustrated in Fig. 4.

HIGH–SPIN STATE   LOW–SPIN STATE
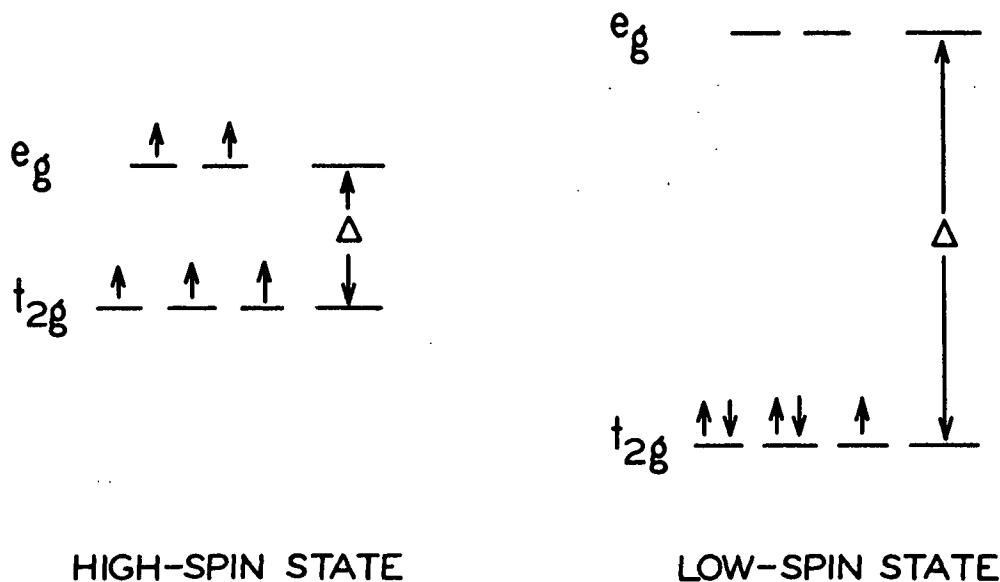
Figure 4. High- and Low-Spin States in a d^5 Octahedral Complex

ELECTRONIC PARAMETERS

A transition metal complex is characterized by two sets of parameters, the crystal field splitting energy, Δ, and the parameters of interelectronic repulsion. The excited state energies of electrons in the d-shell relative to the ground state have been expressed in terms of Δ, B, and C (43,44). B and C are calculated by the theory of Slater, Condon, and Shortley and of Racah and describe the interactions between these d-shell electrons. The ratio between the parameter B in the complex to the parameter B_0 in the corresponding gaseous metal ion is defined by β. Complex formation causes a reduction in B so that β is less than unity. This is generally interpreted by the nephelauxetic or "cloud-expanding" concept

(40,45,46); that is, the charge cloud of the d-electrons is spread by covalent inter-
actions with the ligands, and the repulsions between the d-electrons are decreased.
The complexes of a given metal ion are frequently arranged in order of decreasing β
values. The extent of covalent bonding is then considered as increasing along this
series.

LIGAND EXCHANGE

The exchange between a ligand, A, and a corresponding radioactively tagged
species, A*, is defined by

$$MA_n + A^* = MA_{n-1} A^* + A,$$
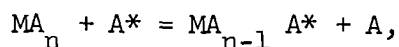
where M represents the metal ion. The equilibrium state is known since it corre-
sponds to a statistical distribution of A*. The rate of ligand exchange is related
to the electronic structure of the complex (47,48). Low-spin type complexes probably
undergo substitution by an activated complex mechanism which requires a vacant t_{2g}
orbital. The low-spin complexes of the ferric ion should thus be inert to substitu-
tion, and this has, indeed, been confirmed experimentally. The high-spin complexes
apparently substitute by a dissociation mechanism. The rate of exchange decreases
as the charge on the central metal increases. The high-spin ferric ion complexes
are classed as labile; that is, the rate of ligand exchange is rapid.

EXPERIMENTAL PROGRAM

The experimental program was divided into three sections. In the first, the
ferric-tartrate system was studied over a wide range of pH values by magnetic and
spectral measurements, and by a potentiometric titration. Examination of the effect
of pH on the bonding in the ferric-tartrate complex was the principal objective of
the section. The region between the second and third equivalence points of the

tartaric acid was given special attention; it was felt that the behavior of the complex in this region is probably related to the bonding in the alkaline system.

In the second section, the bond structure in the alkaline-ferric-tartrate complex was examined by magnetic, spectral, and ligand exchange techniques. The magnetic techniques, which employed the Gouy and Faraday methods, were used to determine the spin state of the d-electrons in the ferric ion. The Gouy magnetic system was operated at room temperature and utilized the iron-tartrate samples in solution form. The Faraday measurements, which were made on solid specimens of the complex, were conducted from -77.6 to about 50°C. The two methods provided a means of check and, more importantly, the measurements over a range of temperatures were needed for an unambiguous description of the electron spin configuration. The magnitudes of the crystal field splitting parameter, Δ, and the electronic repulsion parameter, $\underline{B}$, were estimated from the energies of d-electron transitions. These transitions were observed by absorption spectrophotometry and assigned after reference to appropriate literature sources. The ligand exchange study employed radioactively tagged tartrate for determining the degree of exchange.

In the third phase, the effect of an additional ligand on the bonding between the ferric ion and its environment was examined. Again, the techniques of magnetic susceptibility and absorption spectrophotometry were employed. Glycerol was chosen as the additional ligand since it is capable of complexing readily with the iron in the FeTNa solvent system ($\underline{23}$).

BASIS FOR EXPERIMENTAL PROGRAM

MAGNETIC METHODS

RELATION BETWEEN STRUCTURE AND MEASURABLE QUANTITIES

Coordination compounds involving the transition series metals are frequently examined by the methods of magnetochemistry (49,50) for the determination of bond type. Diamagnetism is exhibited by all substances and arises from the motion of the electrons. Paramagnetism is associated with the spin and orbital angular momenta of the electrons. For many complexes, and particularly for those involving first transition series metal ions, the orbital angular momentum is assumed to be quenched by the ligands. The magnetic moment of the ion, μ_{eff}, is then given as a function of the spin angular momentum by the "spin-only formula,"

$$\mu_{eff} = [4S(S + 1)]^{1/2}. \qquad (1)$$

$\underline{S}$ is the quantum number specifying the total spin angular momentum and is simply $\Sigma \underline{s_i}$, where $\underline{s_i}$ is the spin angular momentum of the $\underline{i}$th electron. Use of the spin-only formula requires that the complex be "magnetically dilute." That is, the paramagnetic centers must be sufficiently separated by the ligand atoms so that any interactions between these centers are effectively eliminated. When this is the case, the magnetic behavior of the complex is independent of the strength of an external magnetic field. For magnetically dilute complexes of the ferric ion, the magnetic moment is 5.92 B.M. and about 2.0 to 2.5 B.M. for high-spin and low-spin states, respectively. (The orbital angular momentum is identically zero for the high-spin state, but finite for the low-spin state. The spin-only formula thus applies less accurately to the latter case.)

If a substance is placed in a magnetic field of intensity $\vec{H}$, the field inside the specimen, commonly termed the magnetic induction $\vec{B}$, differs from the external

field according to the relation

$$\vec{B} = (1 + 4\pi\kappa)\vec{H}, \tag{2}$$

where κ is the magnetic susceptibility per unit volume. The magnetic susceptibility per unit mass or specific susceptibility, χ, equals κ divided by the density of the material. The susceptibilities per gram atom, χ_A, or per mole, χ_m, are obtained, respectively, by $\chi_A = \chi$ (atomic weight) and $\chi_m = \chi$ (molecular weight). There is some confusion concerning the units of κ and χ. χ is expressed in c.g.s. em. (electromagnetic) units and κ in c.g.s. em. units times density through the present study.

The magnetic moment of a paramagnetic ion is related to the atomic paramagnetic susceptibility of the ion, $\chi_{A'}$, by (50)

$$\mu_{eff} = \left[\frac{N\beta^2}{3k}\right]^{-1/2} (\chi_A' T)^{1/2}, \tag{3}$$

where $\underline{N}$ is Avogadro's number, β the Bohr Magneton, $\underline{k}$ Boltzmann's constant, and $\underline{T}$ the absolute temperature. χ_A' is a susceptibility which has been corrected for diamagnetic contributions. The paramagnetic susceptibility is related to temperature because thermal motion opposes alignment of the moments of the electrons with an external magnetic field. This is expressed semiempirically by the Curie-Weiss law (49,50)

$$\chi_A' = C/(T + \theta), \tag{4}$$

which applies to many paramagnetic substances over a considerable range of temperature. $\underline{C}$ is the Curie constant and θ is a quantity of usually less than 20 to 30°. When the Curie-Weiss law is obeyed, and the magnitude of θ is small, μ_{eff} is independent of temperature, which indicates a well-defined paramagnetic material. The effective magnetic moment, μ_{eff}, can then be related to the total spin quantum number by Equation (1), according to the limitations previously discussed.

The experimental methods for examining magnetic susceptibilities are usually based on force measurements. Insertion of a body into a nonuniform magnetic field produces a force which tends to move the body. The magnitude of this force, F_x, along an arbitrary direction, x, is given by (51)

$$F_x = [1/2(\kappa - \kappa_a)v] \left[\frac{dH_x^2}{dx} + \frac{dH_y^2}{dx} + \frac{dH_z^2}{dx} \right] , \qquad (5)$$

where κ is the volumetric susceptibility of the body, κ_a the volumetric susceptibility of the displaced air (or other substance), and v the volume of the body.

THE GOUY METHOD

The Gouy magnetic balance (49-51), which finds frequent use, is especially well suited for measurements involving liquids. A cylindrical sample is suspended from a balance so that one end is in a region of large field strength and the other in a region of negligible field (Fig. 5). The magnetic pull or force, F, upon application of the magnetic field is expressed as an apparent weight change, Δw, times the gravitational constant. With H and H_o the field strengths at the base and upper surface of the sample, respectively, Equation (5) can be applied to a differential sample volume element, $dy = \alpha dx$, and integrated from H to H_o, where α is the cross-sectional area. Recognizing that the field is essentially unidirectional ($dH_z^2/dx \gg dH_x^2/dx$ and dH_y^2/dx) and letting $f(H)$ define the magnetic behavior of the sample container, the magnetic force measured by the Gouy balance is given by

$$F = f(H) + (\kappa - \kappa_a) [(1/2)\alpha(H^2 - H_o^2)]. \qquad (6)$$
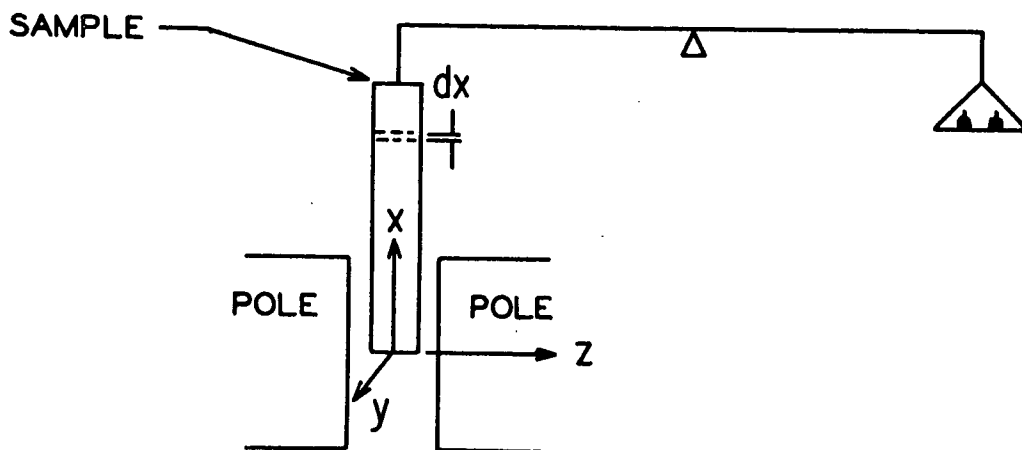
Figure 5. The Gouy Magnetic Balance

THE FARADAY METHOD

The Faraday magnetic method (49) allows the use of small sample quantities and gives the specific susceptibility directly so that separate density determinations are not required. This latter aspect makes the method particularly suitable for measurements on powders and other solid materials. The sample is suspended within a nonhomogenous magnetic field (Fig. 6) in a region over which dH_z^2/dx is fairly constant. The small sample size requires that a sensitive microbalance be used for determining the magnetic pull and that any disturbing factors, such as convection currents and electrostatic effects, be eliminated. The specific susceptibility of the sample in the Faraday system can be related to the magnetic pull (51) by application of Equation (5). The term $(\kappa - \kappa_a)v$ is replaced by $(\chi m - \chi_a m_a)$, where χ_a and m_a are the specific susceptibility of air and the mass of air displaced, respectively. The value of $\chi_a m_a$ is negligible compared to χm, the product of the specific susceptibility and mass of the sample, and dH_z^2/dx is again much larger than dH_x^2/dx plus dH_y^2/dx. Letting $f(H)$ describe the magnetic behavior of the sample bulb, the magnetic pull measured by the Faraday system (51) is defined by

$$F = f(H) + m\chi \ [H_z(dH_z/dx)]. \qquad (7)$$

MICROBALANCE
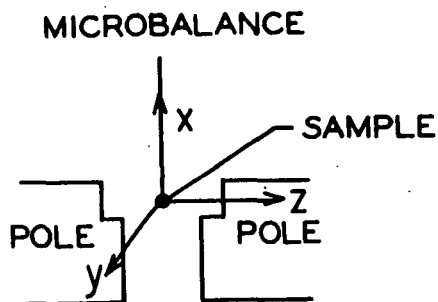
Figure 6. The Faraday Magnetic Balance

DETERMINATION OF Δ AND β

The magnitudes of the parameters, Δ and β, for a transition metal complex are usually estimated by relating the energies of observed d-electron transitions to the Tanabe-Sugano energy level diagrams (41). These diagrams have been derived for certain values of the interelectronic repulsion parameters, B and C (44). For d^5- type complexes, the values used for B and C apply well for manganous ion complexes, but not to complexes of the ferric ion. It was therefore necessary to solve the secular determinants of Tanabe and Sugano (43) for the energy of each level involved in the observed transitions. For complexes of the ferric ion, these transitions are specified by (52)

$$^{6}A_{1g} \rightarrow \, ^{4}T_{1g}$$

$$^{6}A_{1g} \rightarrow \, ^{4}T_{2g}$$

$$^{6}A_{1g} \rightarrow \, ^{4}A_{1g}, \, ^{4}Eg.$$
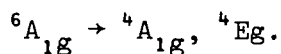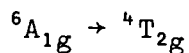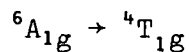
[The above symbols represent the combined symmetries of the t_{2g} and antibonding e_g states at various energy levels. The superscript specifies the multiplicity of the

level and is defined by $(2\underline{S} + 1)$, where $\underline{S}$ is the total spin quantum number. For the ground state, $\underline{S} = 5/2$, and the multiplicity thus equals 6.]

Solution of the Tanabe-Sugano determinants gave Equations (8) through (12), where $\underline{E}$ in each equation represents the energy of the state specified in the left column. For the equations with more than one root, the lowest energy value is compatible with the expected transition.

$^6A_{1g}$: $E = -35B$ $\hspace{8cm}$ (8)

$^4T_{1g}$: $-E^3 + (-66B + 19C)E^2 + (-1389B^2 + 842BC - 119C^2$
$\hspace{1.5cm} + \Delta^2)E + (16B - 7C)\Delta^2 - 9100B^3 + 8995CB^2$
$\hspace{1.5cm} - 2660C^2B + 245C^3 = 0$ $\hspace{5cm}$ (9)

$^4T_{2g}$: $-E^3 + (-56B + 17C)E^2 + (-1009B^2 + 646BC - 95C^2$
$\hspace{1.5cm} + \Delta^2)E + (22B - 5C)\Delta^2 - 5850B^3 + 5945CB^2$
$\hspace{1.5cm} - 1830C^2B + 175C^3 = 0$ $\hspace{5cm}$ (10)

^4Eg: $E^2 + (43B - 10C)E + 450B^2 - 215BC + 25C^2 = 0$ $\hspace{2cm}$ (11)

$^4A_{1g}$: $E + 25B - 5C = 0$ $\hspace{6cm}$ (12)

EXPERIMENTAL TECHNIQUES

All chemicals were of reagent grade. Triply distilled water was used at all points in the experimental program, except for the tartrate, glycerol, and nickel analyses. It was prepared by distillation of ordinary distilled water from an alkaline permanganate solution, followed by a distillation in which the water had been acidified with a few drops of sulfuric acid.

GENERAL

FeTNa PREPARATION

Preparation of the various iron-tartrate solutions followed the direct procedure (23,53) in which no intermediate is isolated. The reaction was conducted in an appropriately sized volumetric flask which had been wrapped with aluminum foil to exclude light. The flask contained a magnetic stirring bar which was activated throughout the entire course of the reaction. A weighed amount of d-tartaric acid was quantitatively introduced into the flask and dissolved in slightly more than the minimum amount of water. Ferric nitrate monohydrate was then quantitatively transferred to the flask with a few milliliters of water. (The calculated amounts of tartaric acid and ferric nitrate reagents were weighed to an accuracy of about 0.001 g. on an ordinary analytical balance.) After brief agitation, the flask was immersed in an ice bath, and a sodium hydroxide solution was introduced dropwise. The addition rate was adjusted to prevent the temperature of the reaction mixture from exceeding about 20°C. It was important to begin the sodium hydroxide addition immediately after dissolving the ferric nitrate in the tartaric acid solution. The combination of nitrate ions and high acidity appeared to cause slow oxidation of the tartrate anion. This was evidenced by nitrous oxide gases dissolved in a ferric nitrate-tartaric acid solution which had stood for several hours. The sodium

hydroxide solution was usually prepared by appropriate dilution of a commercially
standardized concentrate. When this was prevented by the need for higher concen-
trations, a weighed amount of sodium hydroxide pellets was dissolved in water.
At the termination of the sodium hydroxide addition, the stirring bar was removed
(by means of a large external magnet), and the solution temperature was adjusted
to 20°C. in a temperature bath. Water was then added in small portions, with
mixing between each addition, until the solution was diluted to the mark. The
completed solution was stored in a plastic bottle and kept under refrigeration.
(During synthesis, storage, and use, the iron-tartrate solutions were kept out of
the light as much as possible. This precaution was taken to minimize photochemical
reduction of the ferric ions.)

ISOLATION OF THE COMPLEX

The iron-tartrate complex was isolated from solution by an alcohol precipita-
tion technique adapted from Jayme and Bergmann (8). Basically, the technique
consisted of extracting sodium nitrate from the ferric-tartrate solution with small
additions of aqueous alcohol followed by precipitation of the complex with a large
excess of alcohol. The extractions were conducted by adding a 70% (v/v) ethanol-
water solution to an iron-tartrate solution contained within a separatory funnel.
The mixture was shaken vigorously and then maintained stationary. After standing
for a short time, two liquid phases formed, separated by a sharp demarcation line.
The lower, heavier phase contained the complex, water, and salts; the upper layer
consisted of alcohol, water, and the various salts, but contained practically no
complex. The complex-containing phase was separated and reextracted with the
alcohol-water solution. These extractions were continued to a total number of
between 8 and 12. The volume ratio of the aqueous alcohol solution to the iron-
tartrate solution was 1 to 2 for the first extraction. All further extractions

were conducted with an aqueous alcohol volume which equaled one half of that used

in the first extraction. After the final extraction and phase separation, the

complex was precipitated from the heavier phase by addition of a large excess of

alcohol. The precipitate was collected, dried to constant weight at 80°C. under

the vacuum of a water aspirator, and stored in a closed weighing bottle within a

desiccator.

<p style="text-align:center">MAGNETIC</p>

THE GOUY SYSTEM

Construction

The Gouy magnetic system utilized an electromagnet and matching power supply

built by Alpha Scientific Laboratories, Inc. The magnet, model 9500, produces a

precise, homogeneous magnetic field. Six-inch cylindrical pole tips with a two-

inch gap were employed. The magnetic field between these tips and not more than

about 1.5 in. from the center is extremely uniform. The power supply, model 100-20A,

provides up to 20 amperes at 100 volts with a regulation of 1 part in 10^5. The

magnetic pull was measured with an ordinary analytical balance. The balance was

mounted on a movable carriage which allowed positioning of the sample within the

magnetic field. Once positioned, the sample container could be removed from the

system and reinserted at the same position and orientation. The carriage consisted

of two aluminum plates, one above the other, connected by a screw mechanism (Fig. 7).

The upper plate supported the balance and the lower was provided with a wheel assembly

that fit onto steel tracks. The tracks were supported in a wooden frame (Fig. 8).

Brass stops, which attached to the tracks with set screws, prevented the carriage

from moving. The sample container (Fig. 9) was suspended from the left arm of the

balance by an aluminum rod which passed through a hole in the base of the balance

and through holes in the aluminum plates. The sample tube and suspending rod were
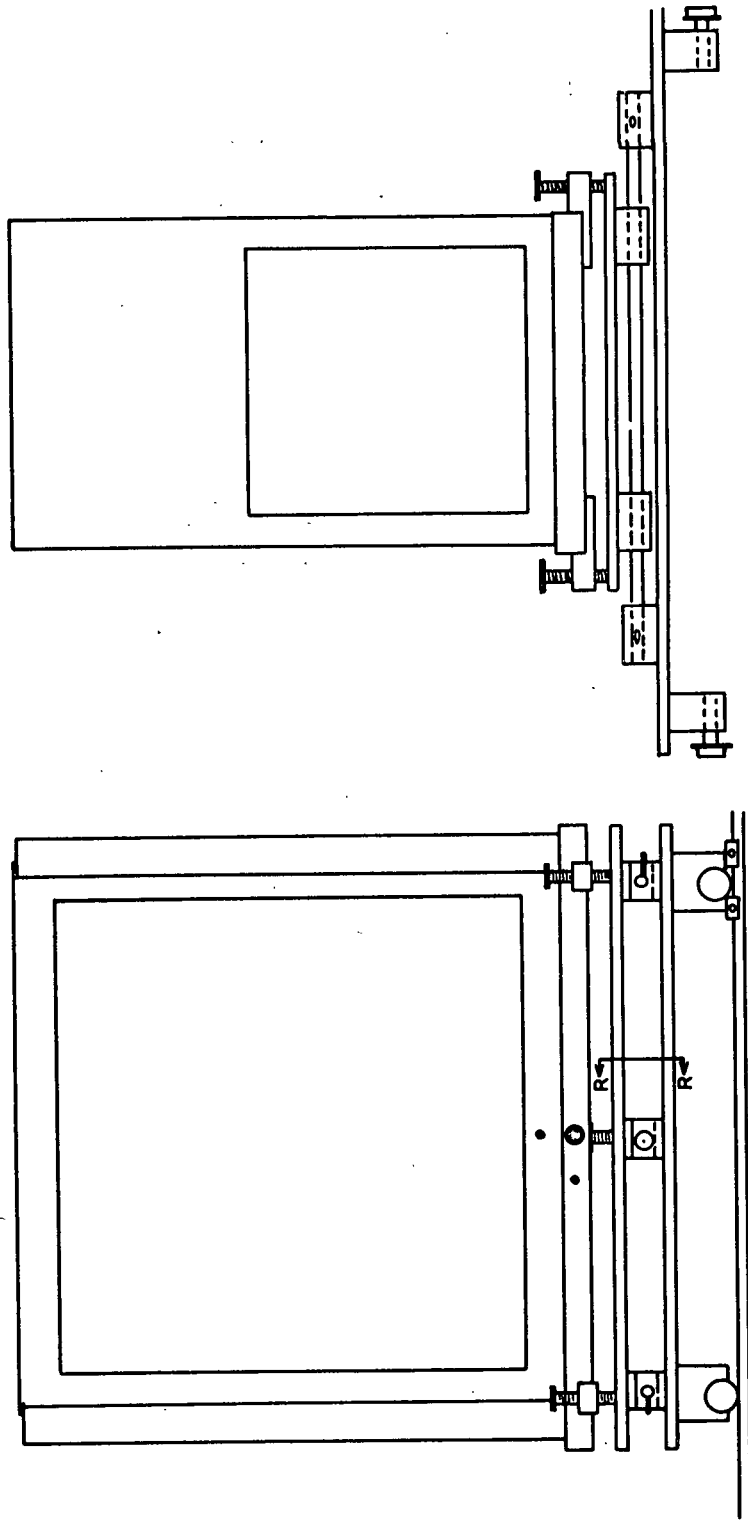
SECTION RR

APPROXIMATE SCALE: 0.25 in. = 1 in

Figure 7.   Balance and Carriage for the Gouy System
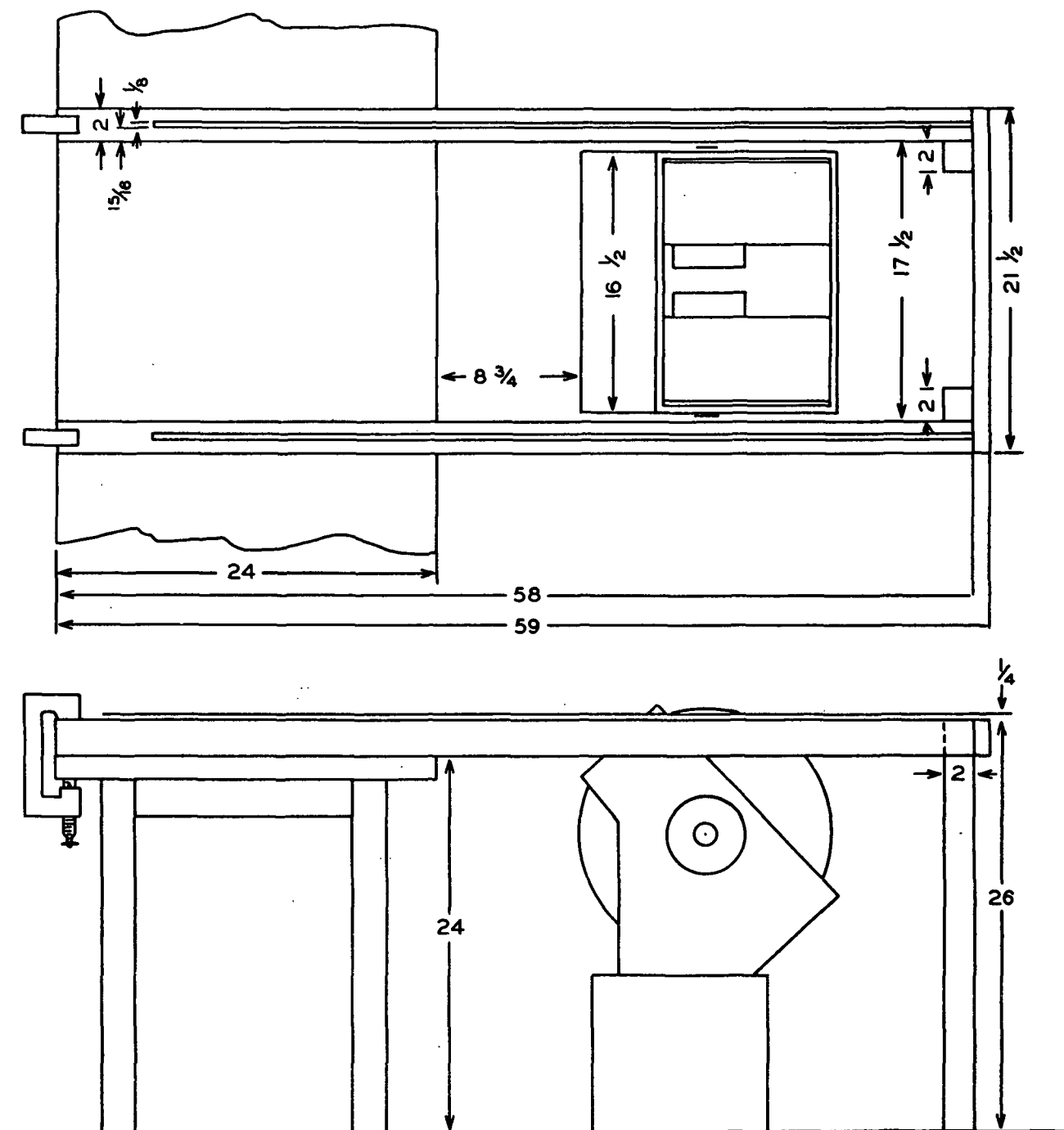
ALL DIMENSIONS IN INCHES.   SCALE: $\frac{1}{8}$ IN. = 1 IN.

Figure 8.   Frame and Magnet for Gouy System

GG FITTING

THERMOMETER
TUBE WITH
GG FITTING

RUBBER STOPPER

47

35

27

4.8

MATERIAL: PYREX GLASS
ALL DIMENSIONS IN CM.

Figure 10. Gouy Draught Shield

GG FITTING

22.6

16

3.1
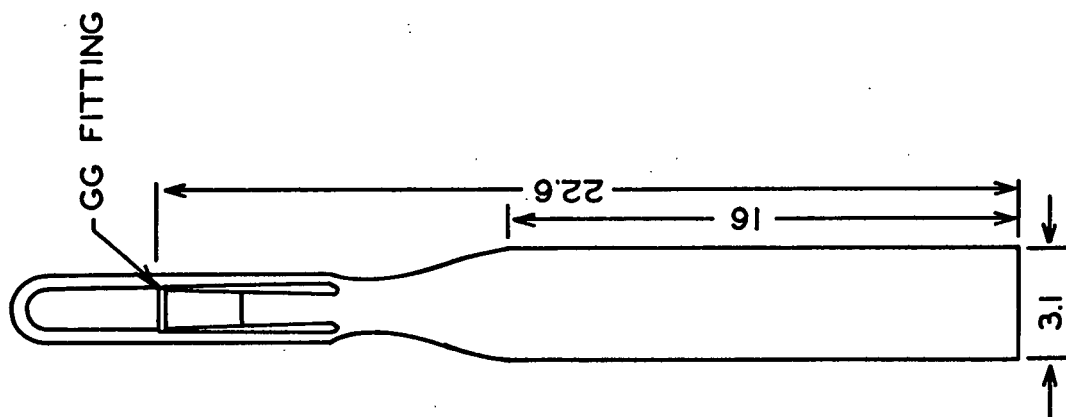
MATERIAL: PYREX GLASS
ALL DIMENSIONS IN CM.

Figure 9. Gouy Sample Tube

enclosed in a draught shield (Fig. 10). The shield was provided with a side arm for holding a thermometer with the bulb positioned directly below the base of the sample container. Access to the sample was gained by removing the thermometer and rubber stopper from the draught shield and lowering the sample tube by means of the aluminum rod. Electrostatic effects in the system were controlled by treatment of the draught shield with a glass-cleaning compound (GTC-59, manufactured by Beaver Laboratories, Inc., Long Island, New York). Previous use of this compound with the Faraday system had shown that it is effective.

Operation

The Gouy sample container was filled so that the upper surface of the solution was always at the same level. This minimized any errors resulting from the finite value of $\underline{H}_o$. The test solution was siphoned into the sample container by means of a small glass tube, which prevented splashing. After withdrawal of this first tube, a second glass tube was inserted into the sample container. This second tube had a drawn-out tip and a collar which accurately controlled the length of tube within the container. Suction was applied to the tube, and the test solution was withdrawn to a constant and reproducible level. After removal of the tube, a ground-glass stopper was fit into the opening of the sample container, and the container was placed inside the draught shield and lifted into position with the aluminum rod. After insertion of the thermometer and rubber stopper into the draught shield, the system was ready for operation. The weight of the sample and sample container was determined at zero magnetic field followed by weight measurements at increasing field strengths. After the measurement at maximum field, the field was reduced to zero, and the power supply unit was switched off and on several times. Then with the unit off, the weight of the sample and container was redetermined. This constituted one set of measurements. Two or more such sets were conducted on a given test solution.

Measurements at zero field strength were always made with the line voltage to the power supply switched off. With the field activated, it was important that successive measurements be made at increasing field strengths. Otherwise, hysteresis effects would cause false readings. The strength of the magnetic field was controlled by the vernier current adjustment on the power supply.

All Gouy system measurements were made at room temperature, which remained at about 21°C. The temperature of the magnet was maintained close to this by means of cooling water circulated from a controlled temperature bath. This was necessary because the test solution was located between the coils of the magnet. The temperature of the test solution was determined immediately before and after the Gouy measurements; the average value was used in the subsequent calculations.

Equation (6) was used for determining the volumetric magnetic susceptibility of the test solution. The magnetic force or pull, $\underline{F}$, equaled the apparent weight change of the sample and container times the gravitational constant. The terms $f(\underline{H})$ and $1/2\alpha(\underline{H}^2 - \underline{H}_o^2)$ were known from the calibration.

Calibration

The term $f(\underline{H})$ in Equation (6) for the Gouy system was determined by measuring the magnetic pull on the empty sample container as a function of the field strength, or experimentally, as a function of the current supplied to the magnet. The value of $1/2\alpha(\underline{H}^2 - \underline{H}_o^2)$ was determined as a function of current by utilizing a solution of known susceptibility and the function $f(\underline{H})$. Aqueous nickel chloride was used as the known. Its specific susceptibility has been accurately determined as a function of concentration and temperature (54) and is expressed empirically by

$$\chi = \left[\frac{10,030p}{T} - 0.720(1 - p)\right] 10^{-6} , \qquad (13)$$

where $\underline{p}$ is the weight fraction of nickel chloride. The nickel chloride solutions used for the calibration were prepared by dissolving $NiCl_2 \cdot 6H_2O$ in water and diluting to volume. Since this nickel reagent has a certain variation in its water of hydration, the nickel contents of the solutions were determined by the dimethylglyoxime gravimetric procedure (55). In weakly alkaline solutions, dimethylglyoxime quantitatively forms a voluminous precipitate with nickel which has the composition $C_8H_{14}N_4O_4Ni$. The standard quantitative procedure was revised slightly by incorporating urea (56) for raising the pH during digestion; the resulting nickel precipitate was more compact and easier to handle. In addition, small amounts of dilute NH_4OH were used as necessary to further adjust the pH.

Use of $f(\underline{H})$ and $1/2\alpha(\underline{H}^2 - \underline{H}_o^2)$ required that the sample container was always filled to the same level and located at the same position within the magnetic field. Errors resulting from any deviations in the location of the sample container were minimized by the uniform character of the field in the vicinity of the base of the container.

THE FARADAY SYSTEM

Construction

The Faraday magnetic system (Fig. 11), including the magnet, was built by Dr. R. W. Zuehlke at Lawrence University. The magnet was activated with the previously described Alpha 100-20A power supply unit. The maximum allowable current was 7 amperes. Weight changes were recorded by the Cahn RG Electrobalance. The instrument, which is based on the null-balance principle, has a capacity of 1 g. and measures weight changes of 1×10^{-6} g. with a sensitivity of about 3×10^{-7} g. The sample and counterweight bulbs were suspended from the balance by finely-drawn glass fibers. These bulbs, which weighed about 100 mg. apiece, were blown glass bubbles having a hook and small opening at one end. The

CAHN RG ELECTRO-MICROBALANCE

GLASS FIBERS

SAMPLE DRAUGHT SHIELD

SAMPLE AND SAMPLE BULB

COUNTERWEIGHT DRAUGHT SHIELD

COUNTERWEIGHT

TO VAC., ETC.

MAGNET POLE PIECES
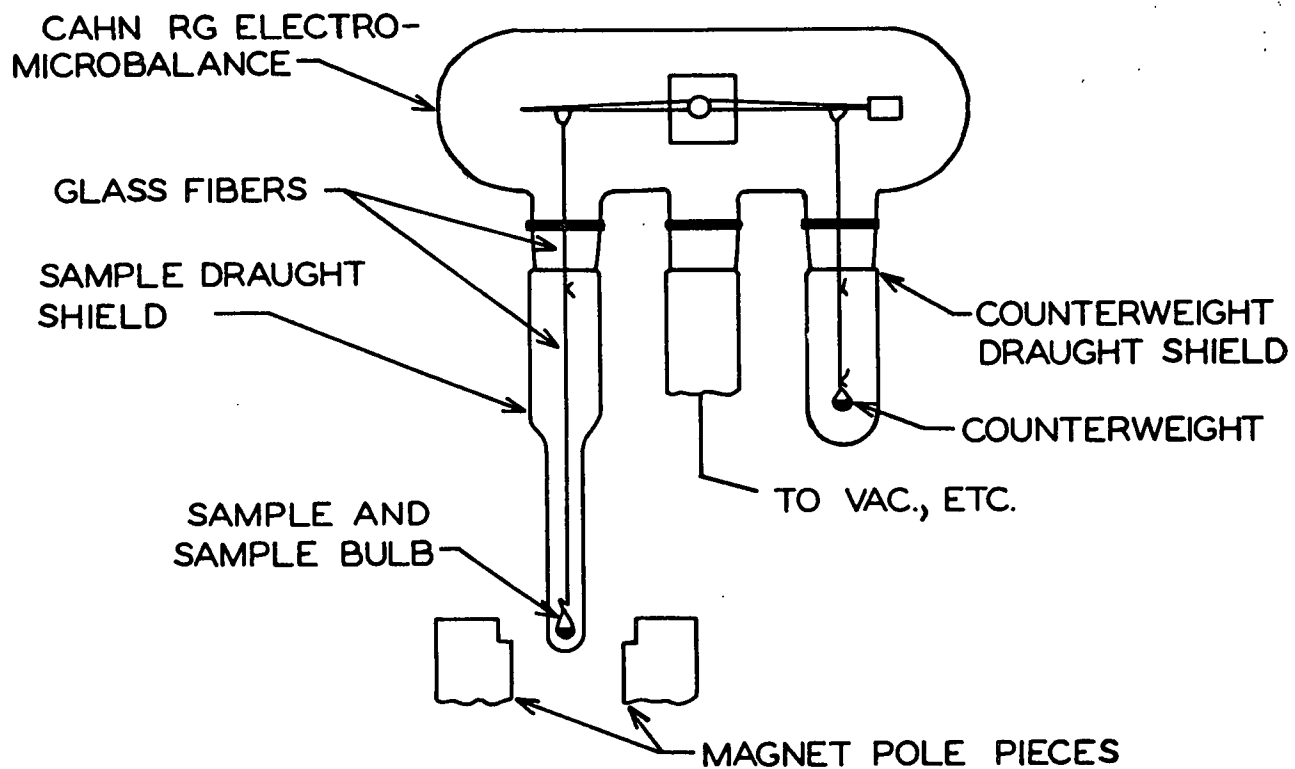
Figure 11. The Faraday Magnetic Balance

counterweight bulb was adjusted as necessary with small bits of broken glass. The sample bulb was positioned so that $H_z(dH_z/dx)$ was approximately constant over the region occupied by the sample. This was verified by showing that the value of $H_z(dH_z/dx)$ did not depend on the amount of material within the bulb. The balance and suspended bulbs were enclosed in glass. The sample draught shield was treated with GTC-59 compound (Beaver Laboratories) for controlling electrostatic charges.

Operation

Considerable care was required while filling and positioning the sample bulb. Very slight pressures would shatter the bulb or suspension fibers. In addition, allowance had to be made for the hygroscopic character of the iron-tartrate solids, which greatly increased the handling difficulties. The dried iron-tartrate sample was powdered thoroughly and weighed into the sample bulb. A weight of about 150 to 160 mg. was used. These operations were conducted within a large plastic bag that was filled with dry nitrogen. The bag had been fitted with plastic gloves and contained an analytical balance as well as other tools. (The sample bulb was suspended from the balance by a glass fiber during the weighing operations.) After being filled, the sample bulb was kept in a closed weighing bottle until it was transferred to the Faraday system. This transfer was conducted as rapidly as possible to minimize moisture pickup by the sample. The draught shields of the Faraday system contained a layer of P_2O_5 which had been within the system for at least 12 hours. Several additional hours then elapsed after suspension of the sample for moisture equilibrium. Attainment of equilibrium was indicated by an approximately constant sample weight. (A small amount of moisture pickup by the sample was not critical. The requirement for equilibrium was based on the necessity for a constant sample weight during the measurements.) As with the Gouy system, measurements at zero field strength were made with the power supply unit switched off; successive measurements were made at increasing field strengths.

Temperature control from 0 to about 50°C. was maintained by a water jacket which surrounded the sample draught shield. Water from a temperature bath was circulated through this jacket. The temperature of the water within the jacket was measured and recorded as the sample temperature. Lower temperatures were obtained by use of various slush mixtures contained in a Dewar flask, which also fit around the sample draught shield. The upper end of the flask was approximately 6 inches above the sample. A temperature of -77.6°C. was provided by a mixture of dry ice and ether. Relatively higher temperatures were achieved by using mixtures of a frozen organic solvent in thermal equilibrium with the same solvent in liquid form. These mixtures were prepared by stirring finely powdered dry ice into the solvent. Experimentally, it was necessary to precool the Dewar with an initial slush mixture. This was followed by fitting a frozen plug of the solvent into the bottom of the Dewar. The flask was then positioned around the sample draught shield and filled with slush. These slush mixtures provided a constant temperature for short periods only, as indicated by reproducible weight measurements followed by drifting values. A thermocouple in place of the sample had shown that adequate temperature control was possible. Proper use of the slush mixtures, however, was difficult and required practice. Chloroform, chlorobenzene, and carbon tetrachloride were employed as the solvents with slush temperatures of -63.5, -45.2, and -22.5°C., respectively.

Calibration

The pull on the empty sample bulb, $f(\underline{H})$ in Equation (7), was determined at various levels of the magnetic field. The function $\underline{H}_z(d\underline{H}_z/dx)$ was then evaluated by utilizing $f(\underline{H})$ and a material of known susceptibility. Hydrated ferrous ammonium sulfate was chosen as the standard. Its specific susceptibility is given by (57)

$$\chi = 9500 \times 10^{-6}/(T + 1), \tag{14}$$

where $\underline{T}$ is the absolute temperature. Approximately 160 mg. of the ferrous ammonium sulfate, in the form of small crystals, were weighed into the sample bulb. The magnetic measurements were conducted with the temperature bath operating in the vicinity of room temperature.

ANALYTICAL

Various chemical analyses comprised an important aspect of the experimental program. The percentage of iron in the materials examined by the magnetic methods had to be known accurately. In addition, correction of the magnetic data for diamagnetic contributions depended on the total composition of the test material. Small analytical errors could be tolerated in the diamagnetic corrections; it was more important that the material have a 100% summation. The compositions of the solutions examined by the Gouy technique were known so that analyses were unnecessary, except for iron. The iron was determined because of the variable water of hydration in the reagent. The solids subjected to the Faraday measurements were analyzed for iron, tartrate, sodium, and nitrate, and for glycerol when applicable. The ligand exchange study required analyses for iron and tartrate.

IRON

Quantitative analysis for iron was conducted by the o-phenanthroline colorimetric technique (58-60). o-Phenanthroline forms a very stable, highly colored complex with the ferrous ion in weakly acidic to weakly alkaline media. The complex obeys Beer's law and has an absorption maximum at 508 nm. Sodium and nitrate ions do not interfere and tartrate does not if the pH is kept above 3.0 (58,60). Hydroxylamine hydrochloride was used for reducing the ferric ion to the ferrous state. The procedure is described in Appendix I. The colorimetric method was calibrated with a standard iron solution (0.0992 mg. iron/ml.). This solution

was prepared by dissolving primary standard electrolytic iron in dilute nitric acid, boiling to expel the nitrogen oxides, and diluting to volume. The standard iron solution was checked by a calibration with a second known solution which was prepared from ferrous ammonium sulfate. The two calibrations agreed well.

The o-phenanthroline colorimetric technique for iron has a high sensitivity (61). A total of eight determinations made on two FeTNa (0.5$\underline{M}$ Fe) solutions showed a standard deviation of 3.9×10^{-3} moles of iron per liter. This represents a deviation which is approximately 0.8% of the mean.

TARTRATE

Tartrate was determined by an oxidation method employing the perchlorate-cerate ion, $Ce(ClO_4)_6^{-2}$, in 2$\underline{M}$ perchloric acid. The procedure is described in detail by Smith (62). Briefly, a specimen of the tartrate-containing material in 4$\underline{M}$ perchloric acid was reacted with an excess of a standard perchlorate-cerate solution. At 26°C., the reaction reached completion in 10 minutes. The excess of oxidant was then determined by titration with a standard oxalate solution. The titration was followed potentiometrically and with a nitro-ferroin indicator. Both methods have very sharp end points and gave equivalent results. Two solutions having known tartrate contents were analyzed by this oxidation procedure. Approximately 99.7% of the tartrate was found. The reaction equations are as follows:

$$COOH \cdot CHOH \cdot CHOH \cdot COOH + 6H_2Ce(ClO_4)_6 + 2H_2O \rightarrow$$
$$6Ce(ClO_4)_3 + 2CO_2 + 2HCOOH + 18HClO_4$$

$$COOH \cdot COOH + 2H_2Ce(ClO_4)_6 \rightarrow 2CO_2 + 2Ce(ClO_4)_3 + 6HClO_4 .$$
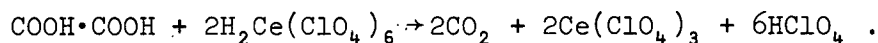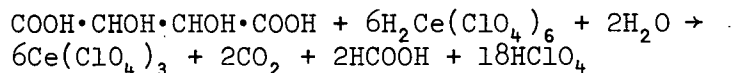
GLYCEROL

Certain samples contained both tartrate and glycerol. These were oxidized by the perchlorate-cerate ion to give the total organic content. The glycerol was

then determined by periodate oxidation and the tartrate was obtained by difference.

The perchlorate-cerate oxidation is described in the previous section; conditions

of 28°C. for 30 minutes were found to give quantitative reaction with both the

tartrate and glycerol. The equation for the glycerol oxidation is given by

$$CH_2OH \cdot CHOH \cdot CH_2OH + 8H_2Ce(ClO_4)_6 + 3H_2O \rightarrow$$
$$3H\overset{\smile}{C}OOH + 8Ce(ClO_4)_3 + 24HClO_4 \ .$$
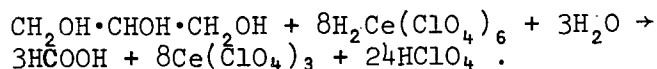
For the glycerol determinations with periodate, an aqueous aliquot of the sample

was oxidized at room temperature with periodic acid for 80 minutes (63), the excess

acid was reduced by sodium arsenite (63), and the reaction mixture was analyzed

colorimetrically for formaldehyde with the chromotropic acid reagent (64,65). The

oxidation converted the tartrate to glyoxylic acid and the glycerol to formic acid

and formaldehyde. The reactions are described by

$$glycerol + 2HIO_4 \rightarrow 2HCHO + HCOOH + 2HIO_3 + H_2O$$

$$tartaric\ acid + HIO_4 \rightarrow 2CHO \cdot COOH + HIO_3 + H_2O$$

$$HIO_4 + Na_3AsO_3 \rightarrow Na_3AsO_4 + HIO_3.$$
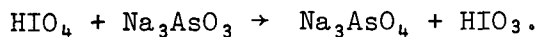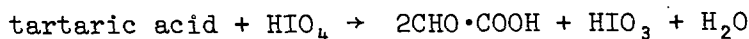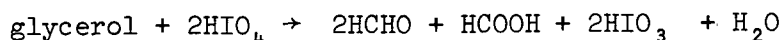
Chromotropic acid forms an intense, violet-red color with formaldehyde when heated

in the presence of sulfuric acid. The color obeys Beer's law over moderate concen-

tration ranges at 570 nm. The reaction is quite specific; formic acid and glyoxylic

acid were found not to interfere. Calibration of the colorimetric technique was

conducted by oxidizing known glycerol solutions with periodic acid, followed by

treating the reaction mixtures with chromotropic acid, and measuring the optical

densities at 570 nm. The procedure for the glycerol analysis is given in Appendix I.

SODIUM

Sodium was determined quantitatively by flame photometry. Basically, the

technique consisted of introducing an aqueous solution of the sample into an

oxygen-acetylene flame and measuring the emission intensity of the sodium line at 589 nm. The intensity was then related to the sodium concentration by comparison with a calibration curve. An internal standard is frequently employed in flame photometric determinations for sodium. This minimizes disturbing effects due to variations in spray rate, drop size, and fuel gas pressures (66). Initial attempts were made with lithium as internal standard. The method, however, was abandoned because the peak emission of the sodium band could not be reproducibly selected. (Normally, the internal standard is used in conjunction with a specially designed spectrophotometer.)

Diluted aliquots from a standard sodium chloride solution were used for the calibration. The standard solution had a sodium concentration of 200 p.p.m.; the calibration measurements were made over a range of 10 to 30 p.p.m. of sodium. The tartrate in the various iron-tartrate samples was oxidized with nitric and perchloric acids (67) before the flame analyses. Organic matter can cause errors by altering the flame temperature and the rate of introduction of the sample into the flame (67,68). The experimental procedure was conducted according to the considerations given by Dean (68). All glassware was washed carefully and leached for at least 24 hours in distilled water before use. Disposable plastic gloves were used during the various handling operations to minimize contamination. The flame emission intensities were measured by a Beckman DU spectrophotometer with flame attachment. The instrument settings were as follows: photomultiplier sensitivity at 1; zero suppression control off; slit width, 0.045 mm.; selector switch at 0.1; wavelength setting, 589 nm.; oxygen pressure, 16 p.s.i.; and acetylene pressure, 5 p.s.i.

NITRATE

The possible presence of nitrate in the various iron-tartrate materials was investigated by quantitative analysis for nitrogen. The analyses followed the procedure of Timell and Purves (69), modified to a semimicro basis, and were conducted by the Institute Analytical Group.

ABSORPTION SPECTROPHOTOMETRY

The absorption spectra of various iron-tartrate solutions were recorded from about 220 to 1200 nm. The measurements were made at room temperature with the Beckman Ratio Recording Spectrophotometer, model DK-2. Matched standard silica cells of 0.1, 1, and 10 cm. path lengths were used as required. The chart paper for the DK-2 is marked along the abscissa in nanometers. The pen is aligned on the chart by means of a friction clutch. Slippage of the clutch, expansion or contraction of the paper, misalignment of the pen, etc., can cause faulty readings. These possible difficulties were eliminated by marking the wavelengths directly on the paper as the spectrum was recorded. This was accomplished by disengaging the motor, setting the wavelength dial, and rotating the scale selection knob. The pen then marked that wavelength with a vertical line.

Initial absorbance measurements were made on iron-tartrate solutions that were 0.5M with respect to iron. The reference solution was triply distilled water since sodium tartrate is not sufficiently soluble for the required concentrations. The spectra showed two weak absorption bands in the region from about 800 to 1100 nm. Analysis of these bands was attempted, but failed. It was then discovered that a sodium tartrate solution has a lower absorbance than triply distilled water in two sections of this region. These sections corresponded with minima in the iron-tartrate spectrum. One of these minima split a true absorption band, creating the

appearance of two bands. Further spectral measurements were thus made at decreased iron molarities and with a corresponding alkaline tartrate solution in the reference cell. The difficulty encountered with the water reference was eliminated, and satisfactory spectra were recorded.

LIGAND EXCHANGE

The general approach to the ligand exchange study was as follows: A radioactively tagged alkaline tartrate solution, designated as the control, was mixed with a FeTNa solution. After a given time interval, a portion of the tartrate was extracted from the mixture, and its specific activity was determined. The amount of ligand exchange was then estimated by a comparison of the specific activity of the control with that of the extracted tartrate. [Specific activity is defined as the disintegrations per minute (DPM) per millimole (mM) of tartrate.]

The control had a tartrate molarity of 1.200 and contained 3 moles of sodium hydroxide per mole of tartaric acid, plus an additional 0.5 mole of sodium hydroxide per liter. Its activity was supplied by dl-tartaric acid-1,4-C14, which was purchased from Nuclear-Chicago Corporation. (l-Tartaric acid is the mirror image of the d-form and should fit into the coordination sphere of the ferric ion in a similar manner.) The iron-tartrate solution, 1:3:10.25 FeTNa (0.4M Fe), had a tartrate molarity of 1.200 and a sodium hydroxide excess of 0.5 mole per liter.

Success of the exchange technique depended on separation of excess tartrate from tartrate coordinated with the iron. Initially, it was proposed to effect the separation by the alcohol precipitation technique. Analysis of the precipitates, however, revealed that most of the tartrate was removed with the complex. Next, it was attempted to preferentially precipitate either the complex or the excess tartrate with a suitable cation. After a comparison of solubility data for many

cations, barium and strontium were chosen as reasonable possibilities. Both produced precipitates which appeared likely, but analysis revealed little selection between excess tartrate and the complex. Finally, a FeTNa-sodium tartrate powder was extracted with a series of ethyl alcohol-dilute sodium hydroxide solutions. It was found that 60 and 70% (v/v) alcohol-2.0$\underline{N}$ sodium hydroxide solutions preferentially extracted the sodium tartrate. This suggested the possibility of extracting excess tartrate directly from the FeTNa solution with a proper volume of alcohol. After a substantial amount of trial and error, an alcohol-to-FeTNa ratio was found which provided a satisfactory separation. The mole ratio of iron to tartrate in the extract was usually in the vicinity of 1 to 35; the ratio in the solution before extraction was 1 to 6. The principal difficulty with the technique was that only about 2% of the total tartrate was extracted, which increased the possibilities for experimental error.

The specific activity of the tartrate in the various specimens was determined by the Van Slyke manometric and the liquid scintillation counting methods. With the Van Slyke procedure (70), the tartrate was oxidized to CO_2, which was then collected and counted. The scintillation method utilized the Beckman DPM liquid scintillation counter. Considerable difficulty was encountered with this method because the samples were not completely soluble in the generally used scintillation cocktail D. (This cocktail contains 10 g. of naphthalene and 0.5 g. of 2,5-diphenyloxazole in 100 ml. of 1,4-dioxane.) Partial success was attained by suspending the sample in a gel formed by mixing Cab-O-Sil, a silica compound supplied by Beckman, Inc. (Catalog No. 161408), with the cocktail D. The system, however, was difficult to handle, and the method was abandoned when a toluene-Triton X-100 cocktail proved adequate. This cocktail was prepared by mixing a standard toluene cocktail (0.5 g. of 2,5-diphenyloxazole per 100 ml. of toluene) with Triton X-100 in the volume ratio of 2 to 1. Solutions of the tartrate samples in the cocktail gave very high initial count rates, presumably due to some form of chemiluminescence.

The solutions were thus allowed to stand until the count rate became stable. The scintillation method was calibrated with a C-14 tagged toluene solution of known activity. This allowed conversion of the registered CPM (counts per minute) to DPM. The procedure for the exchange study is described in Appendix II.

EXPERIMENTAL RESULTS

EFFECT OF pH ON THE COMPLEX

POTENTIOMETRIC TITRATION

In the synthesis of FeTNa, the initial ferric nitrate-tartaric acid solution is highly acidic and has an intense, bronze-orange color; the final solution is alkaline and green in color. The properties of the system between these points were unknown. A study was therefore initiated in which sodium hydroxide was volumetrically added to the ferric nitrate-tartaric acid system, while measuring the pH and noting physical changes.

The initial ferric-tartrate solution contained the same reagent concentrations as employed by Bayer (23) in his FeTNa syntheses; i.e., 0.379 and 0.126 mole of tartaric acid and ferric nitrate, respectively, in about 60 ml. of water. It was recognized that a quantitative interpretation of the results would not be possible since solution properties are not well defined at these high concentrations. The relative pH values, however, should be meaningful. The titrant contained 0.0188 mole of sodium hydroxide per milliliter. The delivery buret, which had a 50-ml. capacity, was fitted with a teflon stopcock. During the titration the temperature was maintained close to 20°C., agitation was provided by a magnetic stirring bar, and the pH was monitored with a Beckman battery-powered pH meter. The results of the titration, including the physical observations, are shown in Fig. 12. The green solution is the cellulose solvent FeTNa. Appearance of the yellow-orange precipitate was unexpected. Analysis of the material showed that it was primarily composed of sodium tartrate. It could be dissolved by dilution of the mixture.
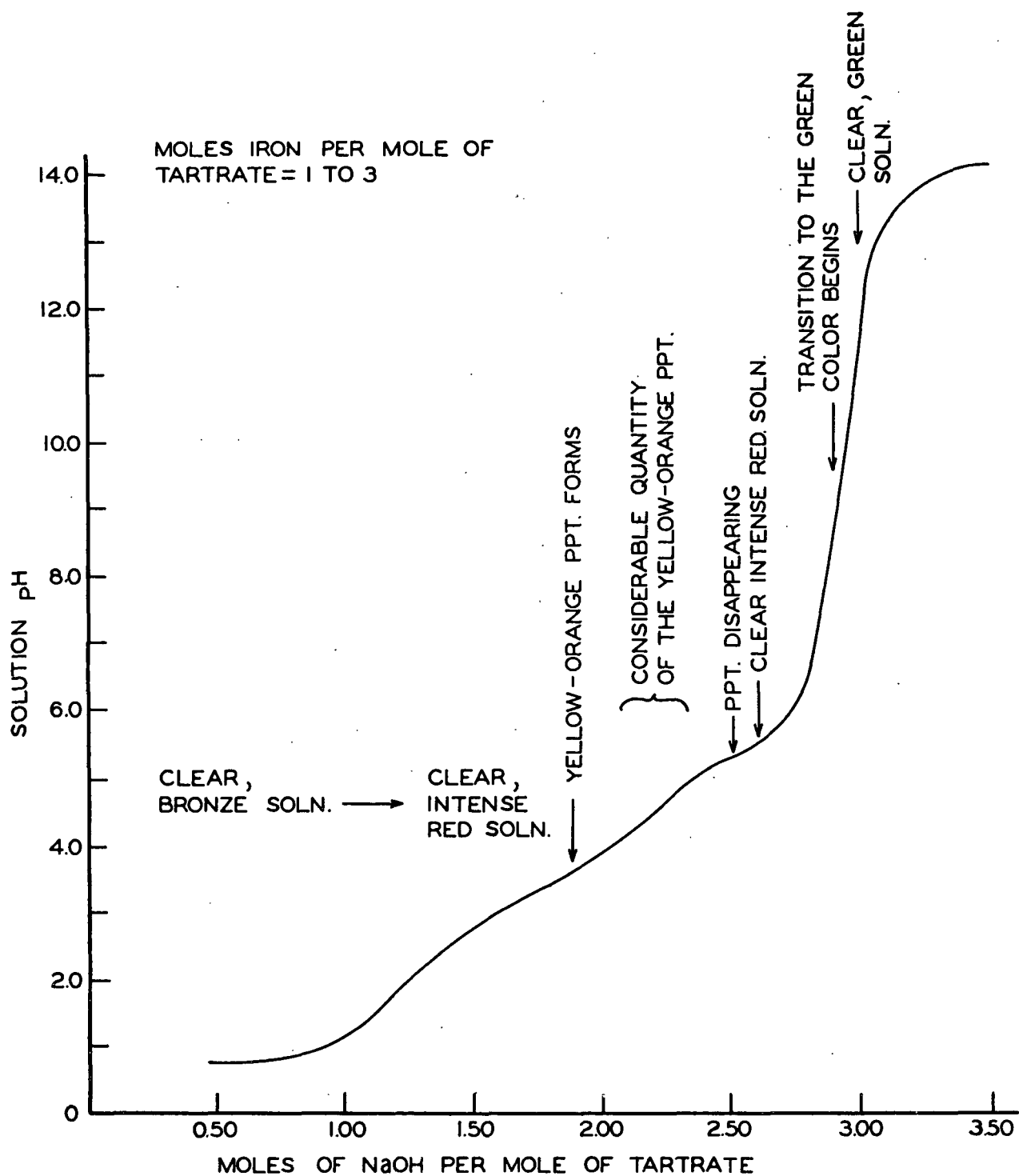
Figure 12. Potentiometric Titration of Ferric-Tartrate with NaOH

MAGNETIC AND SPECTRAL MEASUREMENTS

Changes in the bond structure of the iron-tartrate complex seemed especially

likely in the region over the red to green color transition (Fig. 12). The

initial series of magnetic measurements was thus made on solutions beginning in

this region and continuing through formation of the green complex. A ferric

nitrate-tartaric acid solution was prepared and reacted with just sufficient

alkali to cause disappearance of the yellow-orange precipitate. The solution was

divided into aliquots of equal volume, which were then treated with various amounts

of sodium hydroxide, diluted to a constant volume, and finally subjected to measure-

ments by the Gouy technique. The aliquot volumes were of such size that dilution

to 100 ml. gave solutions with iron and tartrate molarities of 0.5 and 1.5,

respectively. The compositions and physical descriptions of the solutions are

given in Table I. (The numbering of the solutions is arbitrary. These numbers

will be continued through the study and used as necessary in the various discussions.)

TABLE I

SOLUTIONS FOR MAGNETIC INVESTIGATION

Soln.	Iron Molarity	Tartaric Acid Molarity	Moles NaOH per Mole Tart. Acid	Solution Color
1	0.495	1.487	2.76	Intense red
2	0.500	1.505	2.77	Intense red
3	0.495	1.487	2.84	Intense red
4	0.495	1.487	2.93	Rust-red
5	0.495	1.487	3.00	Brownish-red
6[a]	0.495	1.487	3.07	Brownish-green
7[a]	0.495	1.487	3.15	Brownish-green
8	0.495	1.487	3.24	Brown tint in green
9	0.495	1.487	3.61	Green
10	0.500	1.505	3.88	Green
11	0.500	1.505	4.43	Green

[a]
A fine precipitate formed in Solutions 6 and 7 so that magnetic measurements
could not be made. The remaining solutions gave no indication of instability.

The results from the magnetic measurements are shown in Fig. 13. The experimental data are tabulated in the first section of Appendix IV, and the method of data treatment is illustrated in the second section. Each data value represents an average of at least two, and usually three, measurements. The calibration results for the Gouy magnetic system are given in Appendix III. From Fig. 13 it is noted that the magnetic susceptibility of the iron-tartrate system increases markedly over the region in which the solution color changes from dark red to green. The electronic structure of the ferric ion is thus changing in some manner over this region. Approximate calculations, however, showed that the observed susceptibility increase accounted for only about 27% of the increase expected for a transition from the low-spin to the high-spin state.

Since the region of minimum susceptibility was probably not included in the above measurements, a study was initiated in which solutions from the entire pH range were examined. These solutions, which had an iron molarity of 0.1 instead of 0.5, were subjected to the following experimental measurements: Gouy magnetic, optical absorbance from about 400 to 1200 nm., pH, density, and analytical for iron. The reason for the dilution was twofold. First, it was desired that formation of the solid phase over certain pH values be eliminated, and second, sodium tartrate is not sufficiently soluble for preparation of the necessary spectrophotometer reference solutions at the higher concentration. (These reference solutions had the same concentrations of alkali and tartaric acid as the corresponding test solutions.)

The compositions, pH values, and colors of the test solutions are listed in Table II. The magnetic data are treated in the second section of Appendix IV. The absorption spectra of Solutions 12 through 19 were roughly similar to the spectra shown in Fig. 14, which applies specifically to Solution 16. Analysis of these
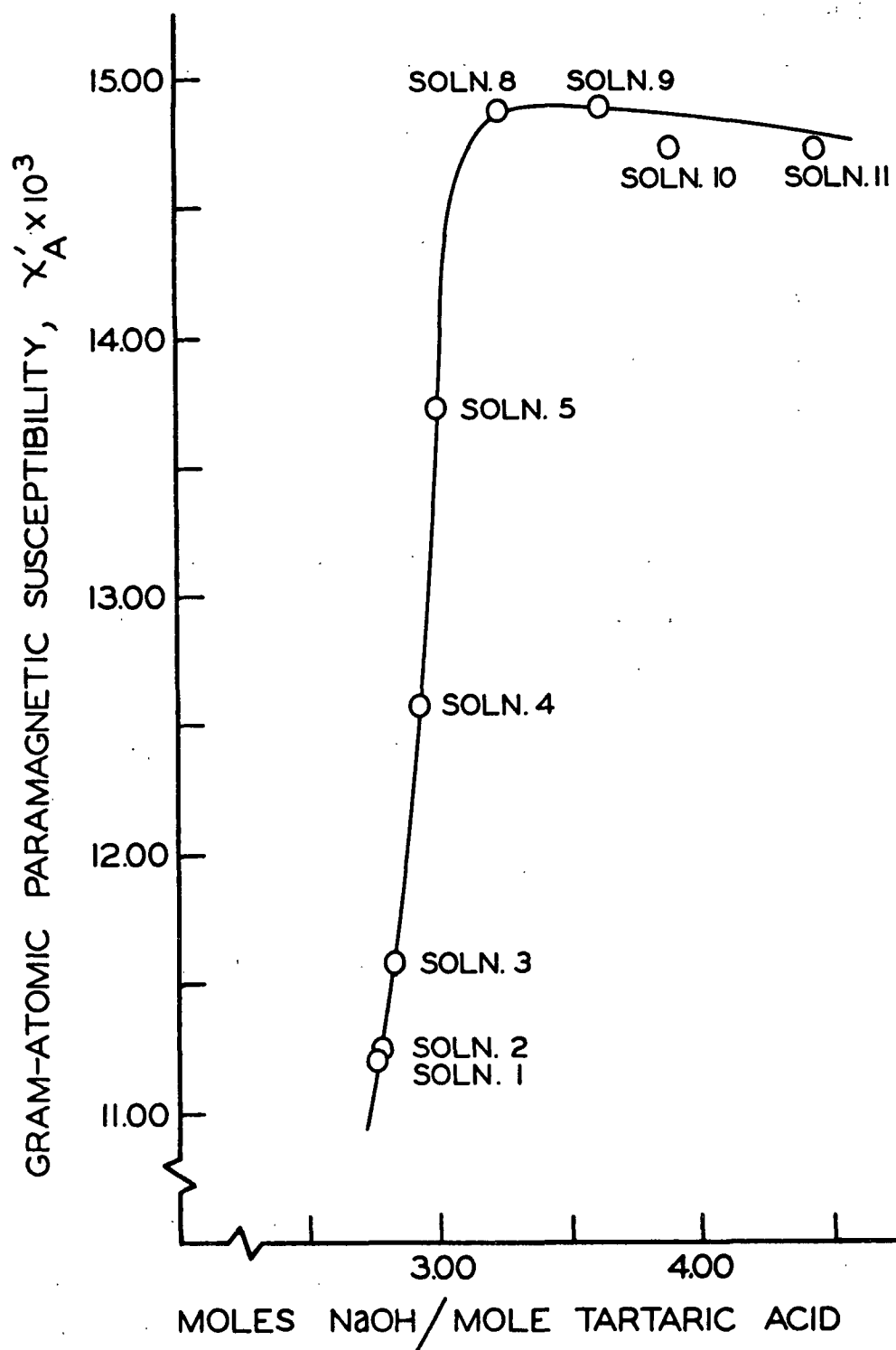
Figure 13. Magnetic Susceptibilities of Solutions 1-11

spectra was not attempted. The strength and position of the band in the vicinity of 1,000 cm.$^{-1}$, however, seemed interesting. The position of the maximum shifts slowly to higher energies as the pH increases, while the extinction coefficient of the maximum appears to correlate approximately with the paramagnetic susceptibility. This latter aspect is illustrated in Fig. 15; the solutions with lower susceptibilities have larger absorbances around 10,000 cm.$^{-1}$. The values of the paramagnetic susceptibilities (at 20°C.) and the corresponding effective magnetic moments are given in Table III. It is noted that the minimum magnetic moment is not consistent with the ferric ion in either a high-spin or low-spin state (p. 17).

TABLE II

EFFECT OF pH ON IRON-TARTRATE SOLUTIONS

Soln.	Iron Molarity[a]	Tartaric Acid Molarity	Moles NaOH per Mole Tart. Acid	pH	Solution Color
12	0.100	0.300	0.17	0.71	Bronze-orange
13	0.103	0.300	0.50	1.10	Bronze-orange
14	0.100	0.300	1.00	1.79	Intense red
15	0.101	0.300	1.50	2.52	Intense red
16	0.100	0.300	2.00	3.63	Wine red
17	0.099	0.300	2.50	4.27	Bronze
18	0.100	0.300	3.00	11.13	Bronze
19	0.100	0.300	3.67	12.30	Bronze
20	0.099	0.350	3.57	12.30	Yellow-orange
21	0.100	0.400	3.50	12.37	Green
22	0.099	0.600	3.33	12.31	Green
23	0.100	1.200	3.42		Green

a
Determined colorimetrically.
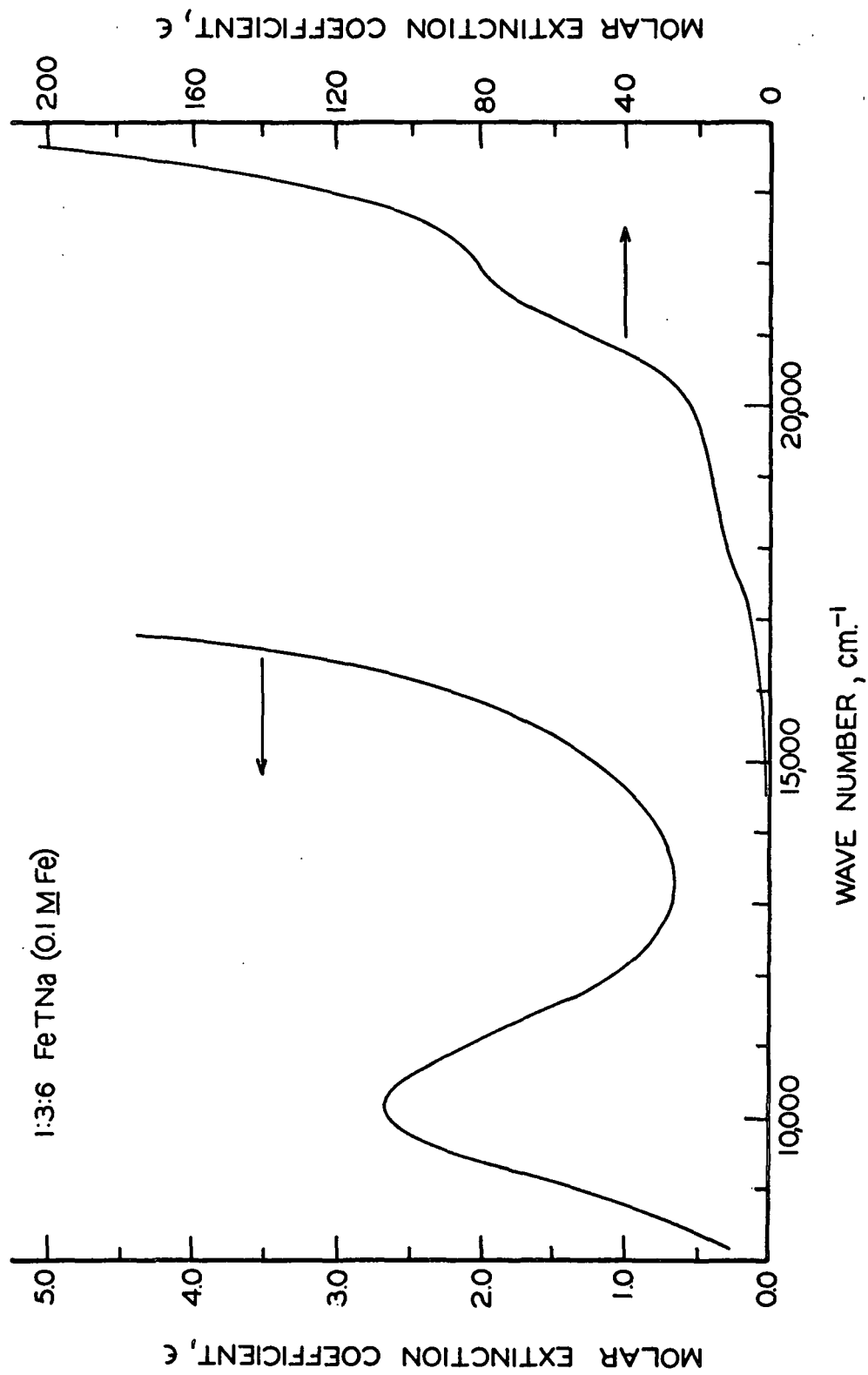
Figure 14. Absorption Spectrum of Solution 16
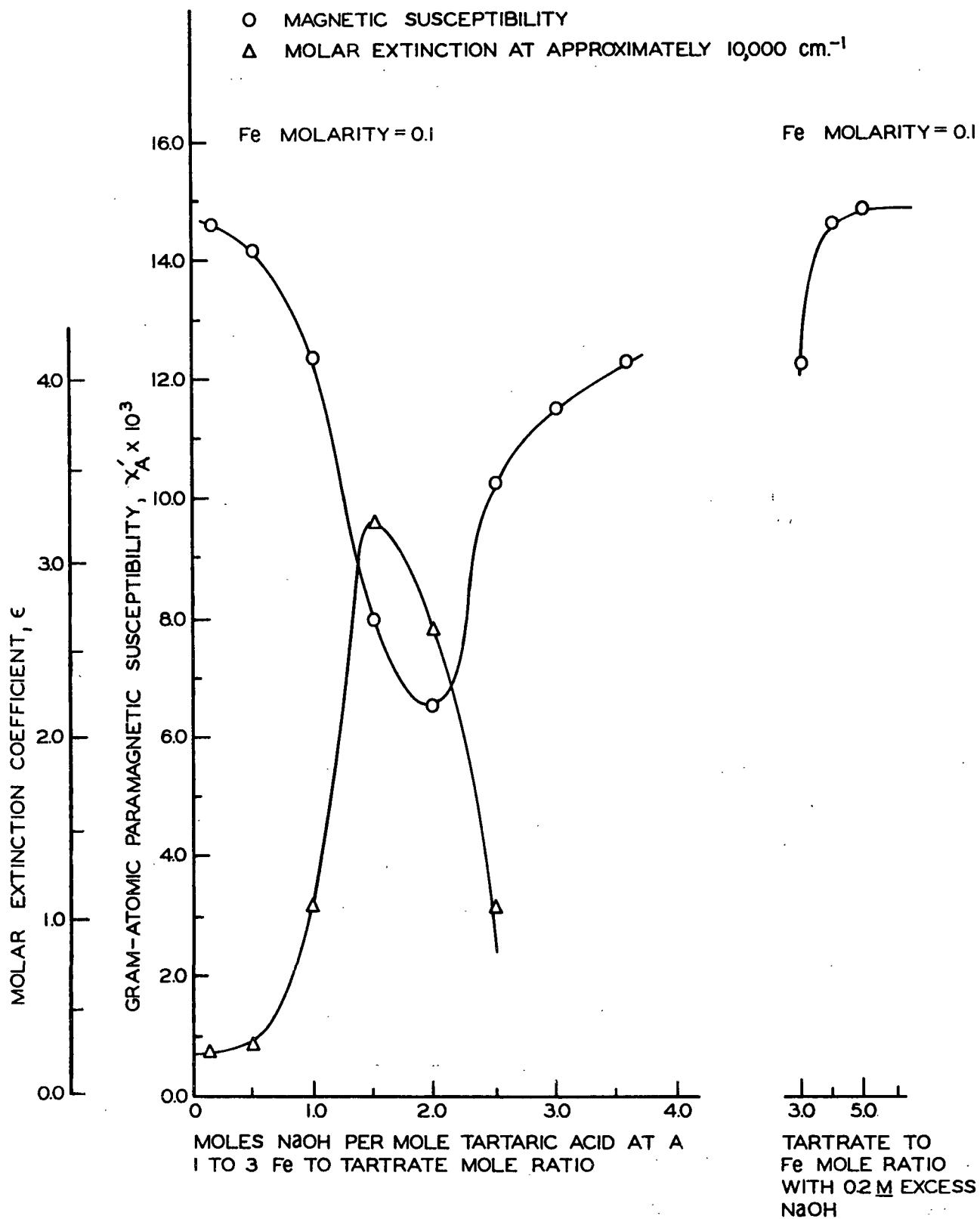
Figure 15.   Relation Between FeTNa Composition and Solution Properties

TABLE III

MAGNETIC PROPERTIES

Soln.	Para. Sus.[a], $X_A' \times 10^3$, c.g.s. em. units	Eff. Mag. Moment, B.M.
12	14.69	5.87
13	14.13	5.76
14	12.39	5.39
15	7.97	4.32
16	6.53	3.91
17	10.22	4.90
18	11.49	5.19
19	12.27	5.36
20	14.57	5.85
21	14.81	5.89
22	14.84	5.90

a.

Per gram-atom of ferric ions in the complex at 20°C.

Two iron-tartrate samples from the region of lower magnetic susceptibility were examined by the Faraday method. Sample I was a specimen of the solid phase which appeared during the potentiometric titration. It was obtained by filtration of a mixture which corresponded approximately to the center of the region over which the solid existed. The mole ratios of iron to tartrate to sodium hydroxide in this mixture were 1 to 3 to 6.74. Sample II was isolated by alcohol treatment of the red iron-tartrate solution which was observed immediately after disappearance of the yellow-orange solid (Fig. 12). The solution was 0.5M in iron and had iron to tartrate to sodium hydroxide mole ratios of 1 to 3 to 8.16. The alcohol treatment was conducted according to the previously described procedure. Samples I and II were dried to constant weight, analyzed quantitatively, and examined by the Faraday method. The results of the analyses, which were conducted for iron, tartrate, sodium, and nitrate, are presented in Appendix V. The magnetic data and the average values for the calculated gram-atomic paramagnetic susceptibilities are included in

Appendix VI. (The calibration results for the Faraday system are given in Appendix III, and the method for treating the experimental data is illustrated in Appendix VI.)

The Curie-Weiss law, Equation (4), predicts a linear relation between the reciprocal of the gram-atomic paramagnetic susceptibility and the absolute temperature. The susceptibilities for Samples I and II follow this relation reasonably well (Fig. 16). The data points were fitted to the linear form of the Curie-Weiss law by the method of least squares to give the following values for the constants C and θ:

	C	θ
Sample I	3.759	84.20
Sample II	4.545	157.82

In both cases the magnitude of θ is substantially larger than expected for a true paramagnetic material.

The effective magnetic moments of the ferric ions in Samples I and II were evaluated from the gram-atomic paramagnetic susceptibilities by substitution into Equation (3):

Sample I	μ_{eff} = 4.84 B.M.
Sample II	μ_{eff} = 4.88 B.M.

Neither value is consistent with the ferric ion in a high- or low-spin state, which is in accord with the Gouy system measurements and the large magnitudes obtained for θ.

At this point a slight digression is made by pointing out that the Gouy and Faraday magnetic measurements were conducted at three or usually more external field strengths for all specimens examined in this study. In each case the
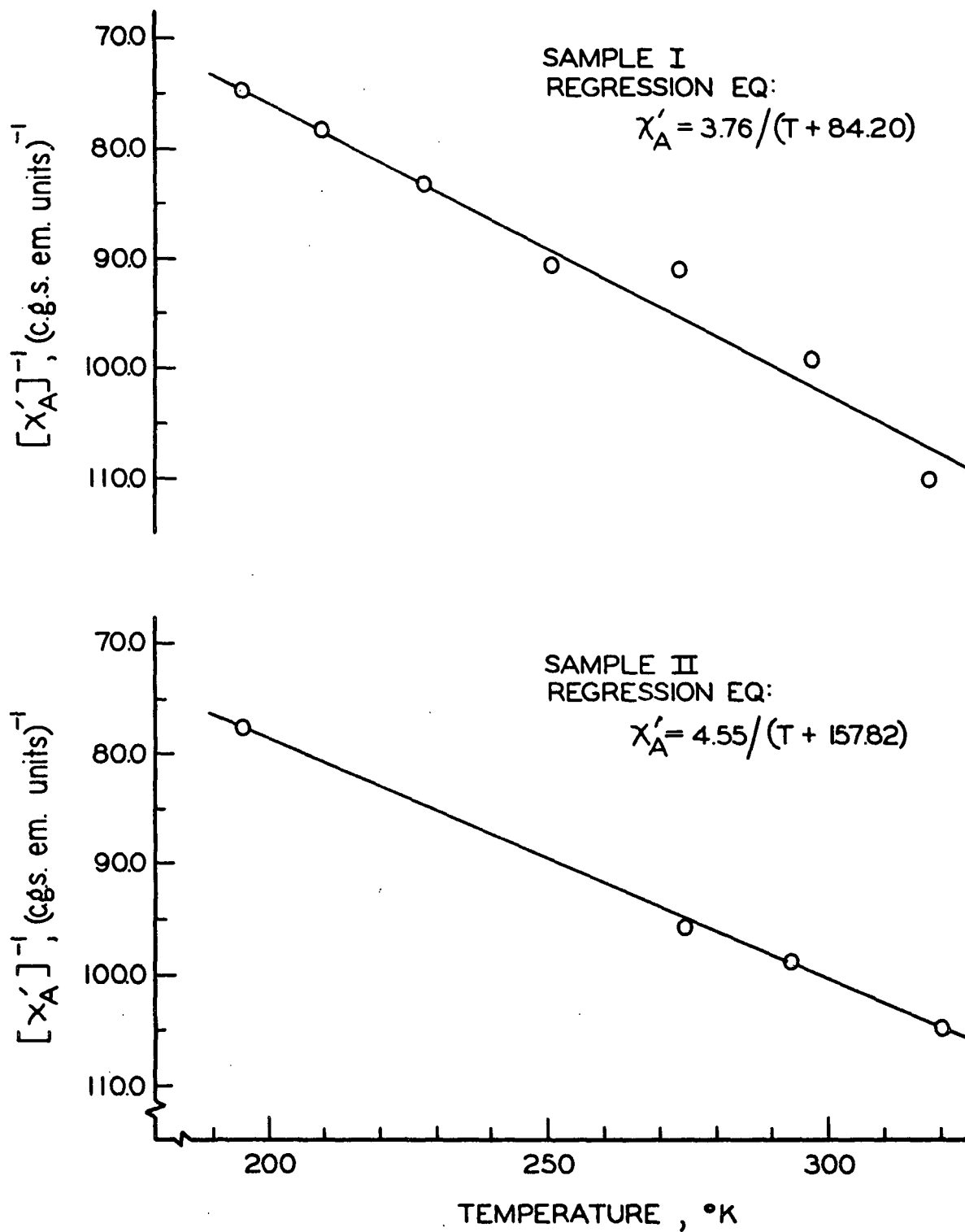
Figure 16.   Temperature-Susceptibility Relations for Samples I and II

susceptibility of the specimen was independent of the external field. This establishes that ferromagnetic impurities were not present in any of the samples (50). Trace amounts of a ferromagnetic material can substantially alter the measured properties; it was thus absolutely necessary to take these precautions.

THE ALKALINE-FERRIC-TARTRATE SYSTEM

The results given in this section, which apply to the alkaline FeTNa system, are divided into two categories. In the first, evidence is presented which suggests the existence of an equilibrium between various species of the complex. In the second, the bonding in the system is examined specifically.

EQUILIBRIUM CONSIDERATIONS

As the study progressed it became increasingly apparent that the structure of the complex in the alkaline FeTNa system depends on the total iron concentration and the iron-to-tartrate ratio. The 1:3:13 FeTNa (0.5$\underline{M}$ Fe) is the normally used cellulose solvent. Its absorption spectrum between 14,000 and 20,000 cm.$^{-1}$ is shown in Fig. 17 and compared with that of a 1:3:14 FeTNa (0.4$\underline{M}$ Fe) solution. The latter solution has the characteristic green color, but with a brownish tint. The amount of excess sodium hydroxide and the iron-to-tartrate ratio are the same for the two solutions; the second solution simply represents a dilution with 2$\underline{M}$ alkali. In Fig. 18 the spectra between 14,000 and 20,000 cm.$^{-1}$ of a series of FeTNa solutions are shown. The solutions have the same iron molarities (0.40) and the same amounts of excess sodium hydroxide (2.0$\underline{M}$); only the iron-to-tartrate mole ratio varies. It is noted that the edge of the strong absorption moves to higher energies as the tartrate-to-iron ratio increases. (These spectra were recorded with triply dis-tilled water in the reference cell. The absorbance of disodium tartrate over this region is very small and essentially constant.) The absorption spectra of Solutions 20, 21, 22, and 23 are compared in Fig. 19. (Alkaline tartrate solutions were used
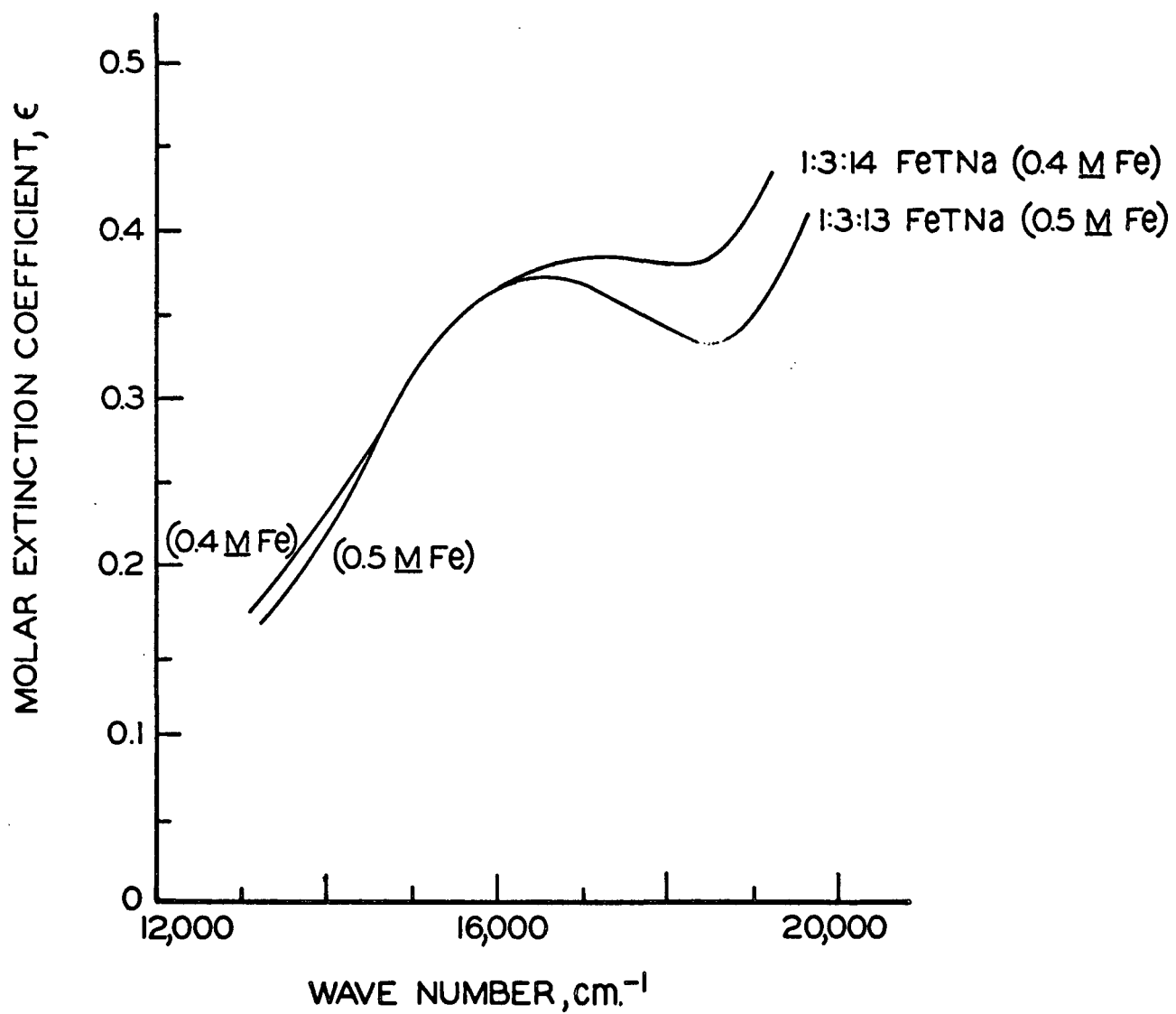
Figure 17. Effect of Dilution on the FeTNa Absorption
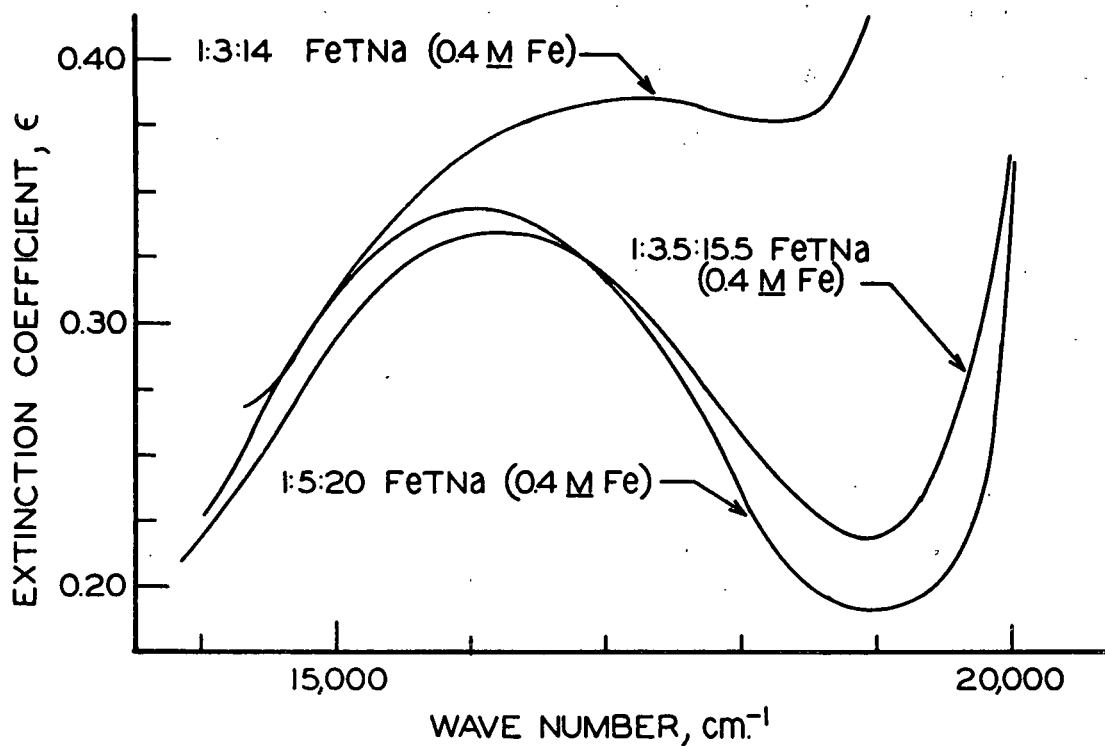
Figure 18. Spectra of FeTNa Solutions Which Are 0.4$\underline{M}$ in Fe
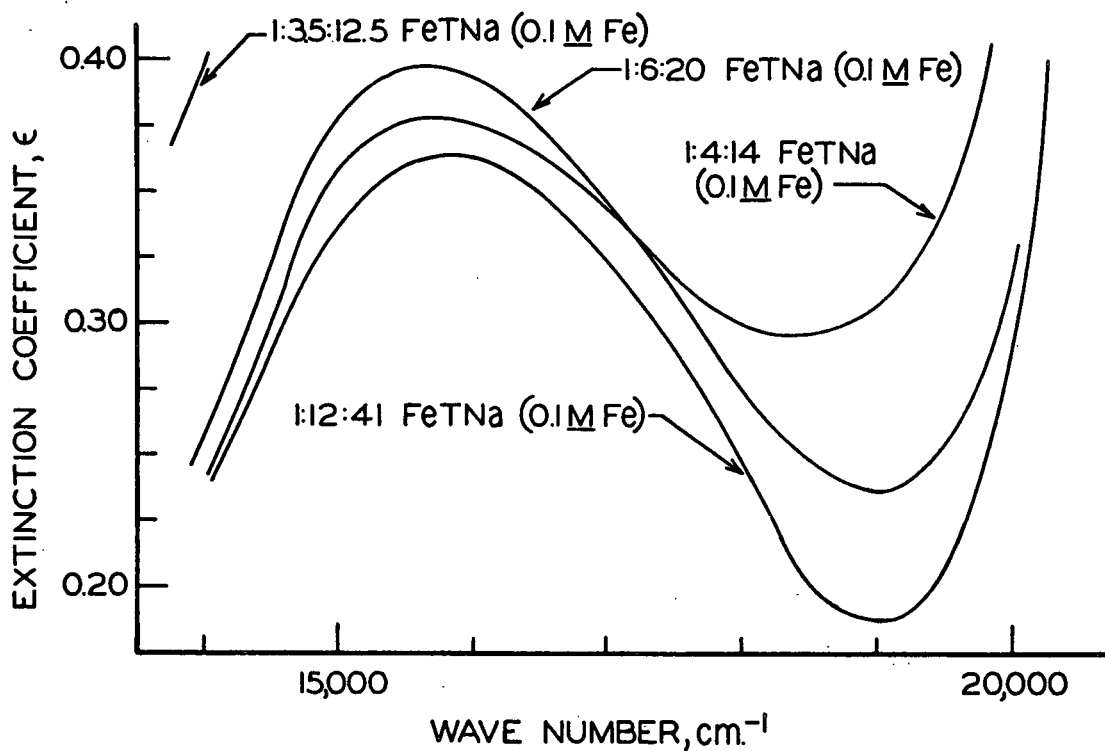
Figure 19. Spectra of FeTNa Solutions Which Are 0.1$\underline{M}$ in Fe

in the reference cell for these measurements.) It is noted from Table II that these solutions are 0.1M in iron and 0.2 or 0.5M in excess alkali. A 1 to 4 iron-to-tartrate mole ratio is required for the characteristic green color; the 1 to 3 solution is bronze in color. The spectral characteristics of these solutions are in agreement with the behavior observed for the 0.4M iron solutions (compare Fig. 18 and 19). The relation between the composition of alkaline FeTNa solutions and their resulting colors and magnetic properties is summarized in Table IV.

TABLE IV

DEPENDENCE OF FeTNa PROPERTIES ON COMPOSITION

Soln.	Molarity	Moles Tartrate per Mole Iron	Molarity of Excess NaOH	μ_{eff}, B.M.	Solution Color
19	0.1	3.0	0.20	5.36	Bronze
20	0.1	3.5	0.20	5.85	Yellow-green
21	0.1	4.0	0.20	5.89	Green
22	0.1	6.0	0.20	5.90	Green
8	0.5	3.0	0.36	5.92	Green
9	0.5	3.0	0.91	5.92	Green
10	0.5	3.0	1.33	5.90	Green
11	0.5	3.0	2.16	5.89	Green

BOND STRUCTURE

Magnetic Measurements

A 1:3:13 FeTNa (0.5M Fe) solution was examined magnetically by the Gouy method. The experimental data are presented in Appendix IV. An iron molarity of 0.503 was used in the calculations. This value was determined from four quantitative analyses, which gave results of 0.501, 0.509, 0.503, and 0.501. The gram-atomic paramagnetic susceptibility and the effective magnetic moment of the system were found to equal 14.69 x 10^{-3} c.g.s. em. units and 5.89 B.M., respectively.

Two 1:3:13 FeTNa (0.5M Fe) solutions were treated with alcohol by the previously described precipitation technique. The resulting solids, Samples III and IV, were dried, analyzed quantitatively, and examined magnetically by the Faraday method. The results of the analyses, which were conducted for iron, tartrate, sodium, and nitrate, are listed in Appendix V. The magnetic data, the calculated gram-atomic paramagnetic susceptibilities, and an example of the data treatment are given in Appendix VI. The reciprocal of the gram-atomic paramagnetic susceptibility is linearly related to the absolute temperature (Fig. 20), as required by Equation (4). A least squares fit of the data from Sample IV to Equation (4) gave values of 4.216 and -6.83 for the constants $\underline{C}$ and θ, respectively. The effective magnetic moment of the ferric ion in Sample IV equaled 5.88 B.M., which is in agreement with the moment calculated from the Gouy system measurements.

Spectral Analysis

The absorption spectrum of a 1:12:41 FeTNa (0.1M Fe) solution was recorded from 8700 to 41,600 cm.$^{-1}$ (1150 to 240 nm.). A 1.200M alkaline tartrate solution, which contained 0.300 mole per liter of sodium nitrate, was used as the reference. (This nitrate concentration corresponded to the amount of nitrate contained in the FeTNa solution.) The very high tartrate-to-iron ratio in the FeTNa was employed because the calculations for Δ and β require that the iron is complexed to one ligand only. The absorption curve is shown in Fig. 21; the region from about 9000 to 23,000 cm.$^{-1}$ is plotted on an expanded scale in Fig. 22. The very strong absorption observed over the higher energies is a result of charge-transfer (40). This corresponds to electronic transitions in which an electron is transferred from a predominantly ligand molecular orbital to a predominantly metal molecular orbital.

The very weak bands shown in Fig. 22 represent d-electron transitions within the ferric ion. These transitions are very weak since they are multiplicity-forbidden and Laporte-forbidden (41); the expected molar extinctions are on the
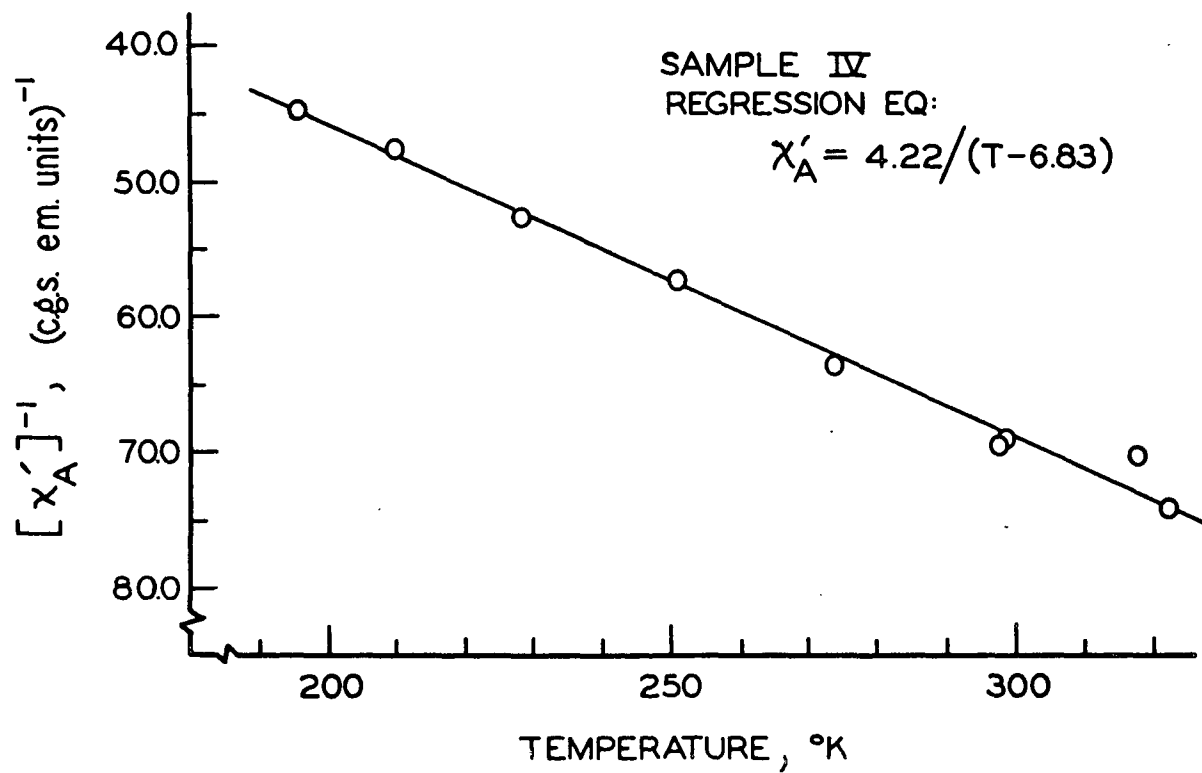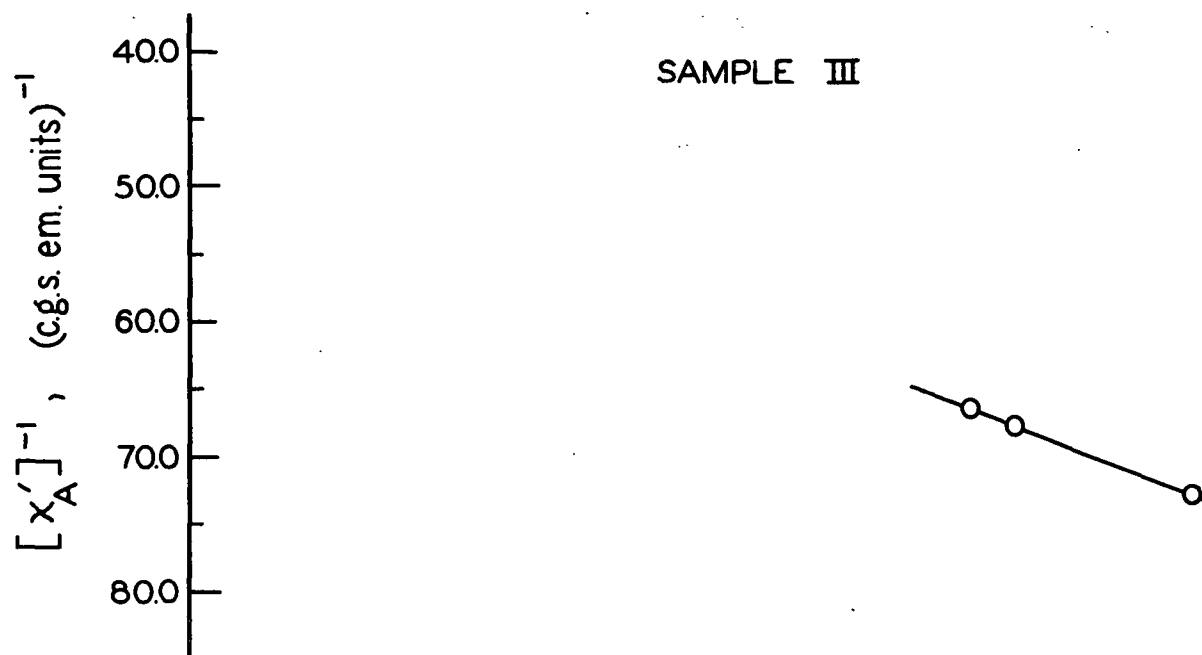
Figure 20. Temperature-Susceptibility Relations for Samples III and IV
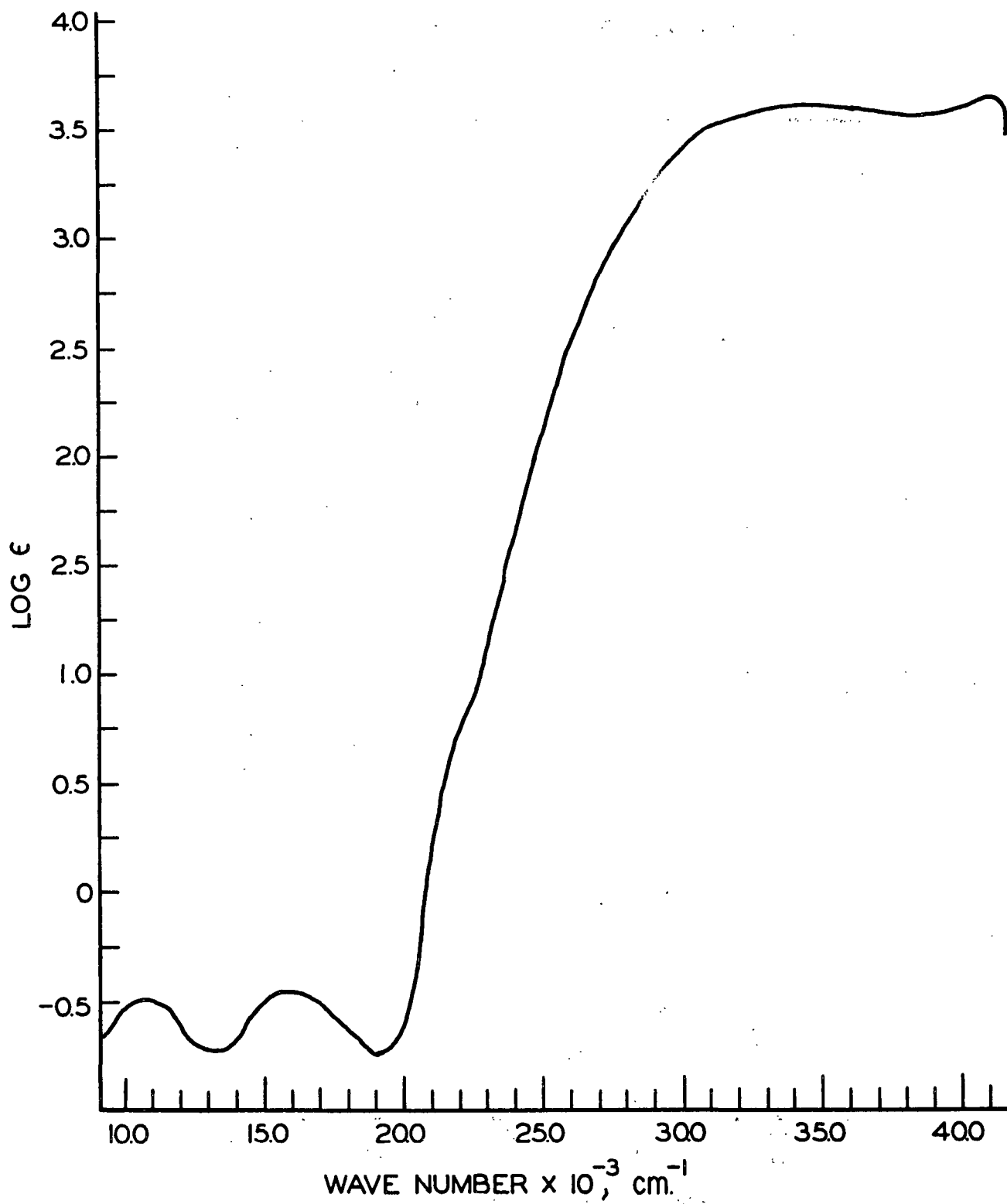
Figure 21. Absorption Spectrum of a 1:12:41 FeTNa (0.1$\underline{M}$ Fe) Solution
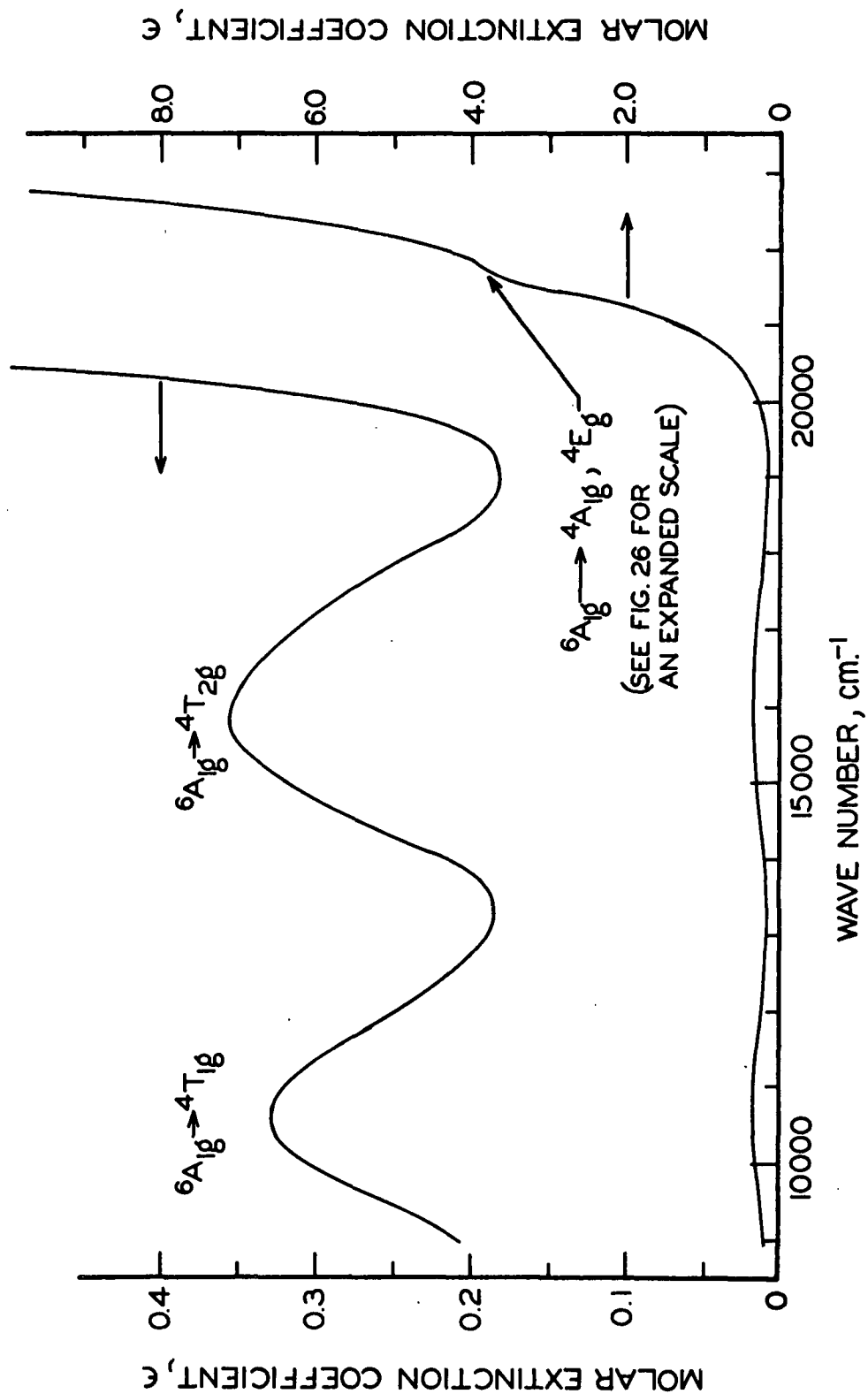
Figure 22. d-Electron Transitions in the 1:12:41 FeTNa (0.1M Fe) Spectrum

order of 0.1. Assignment of specific transitions to these bands was made after
reference to various literature sources and, in particular, to the analyses made
by Tanabe and Sugano (44) and Jørgensen (52). The spectrum of $Fe(H_2O)_6^{+3}$ (71)
was treated by Tanabe and Sugano in example calculations and the spectra of
$Fe(H_2O)_6^{+3}$ and $Fe(C_2O_4)_3^{-3}$ were recorded and analyzed by Jørgensen. The latter
spectra are reproduced in Fig. 23. The two broad bands shown in Fig. 22 and 23
are very similar, and the assignment of transitions to the FeTNa spectrum is
certain. Unfortunately, the band corresponding to the $^4A_{1g}$, ^4E_g level in the
FeTNa system is obscured by the edge of the charge-transfer band. It is assumed
that this level is represented by the small inflection on the charge-transfer band.
This assumption appears reasonable after comparison of the position of the inflec-
tion with the position of the $^4A_{1g}$, ^4E_g level in the $Fe(C_2O_4)_3^{-3}$ spectrum. (The
inflection is shown on an expanded scale in Appendix VII.)

The position of an absorption band indicates the energy difference between
the excited and ground states. The maximum value of the molar extinction coeffic-
ient usually represents this position (46). For the spectrum shown in Fig. 22,
the positions or energies of the three absorption maxima were estimated according
to the "curve analysis" methods suggested by Jørgensen (46). The methods are
described in Appendix VII, and the results are given in Table V. Similar analyses
were conducted on the spectra of additional FeTNa solutions, and the results are
included in Table V for comparison. (The solution specified by FeTGNa contains
glycerol and is defined in a later section.)

The magnitudes of the electronic parameters, Δ and β, for the 1:12:41 FeTNA
(0.1M Fe) solution were estimated from the observed absorption energies by applica-
tion of Equations (8)-(12). The interelectronic repulsion parameters, B and C, are
usually evaluated for the gaseous ion and then considered fixed (45). Tanabe and
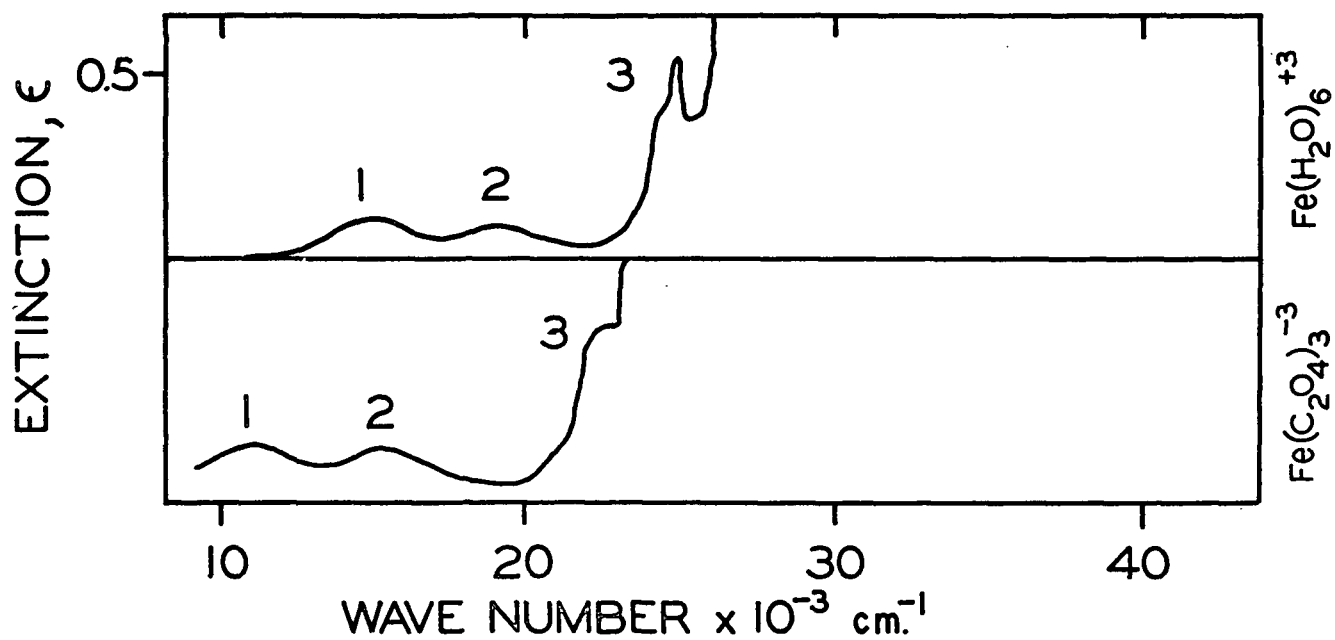
	BAND	ASSIGNMENT	POSITION, cm.$^{-1}$
$Fe(H_2O)_6^{+3}$	1	$^6A_{1g} \rightarrow {}^4T_{1g}$	12,600
	2	$^6A_{1g} \rightarrow {}^4T_{2g}$	18,500
	3	$^6A_{1g} \rightarrow {}^4A_{1g}, {}^4E_g$	24,300 , 24,600
$Fe(C_2O_4)_3^{-3}$	1	$^6A_{1g} \rightarrow {}^4T_{1g}$	10,700
	2	$^6A_{1g} \rightarrow {}^4T_{2g}$	15,200
	3	$^6A_{1g} \rightarrow {}^4A_{1g}, {}^4E_g$	22,100

Figure 23. Absorption Spectra of $Fe(H_2O)_6^{+3}$ and $Fe(C_2O_4)_3^{-3}$ (52)

TABLE V

ABSORPTION MAXIMA

Solution[a]	$^6A_{1}g \rightarrow {}^4T_{1}g$		$^6A_{1}g \rightarrow {}^4T_{2}g$		$^6A_{1}g \rightarrow {}^4A_{1}g, {}^4E_g$	
	ϵ_{max}	σ_{max}^b	ϵ_{max}	σ_{max}^b	ϵ_{max}	σ_{max}^b
1:12:41 FeTNa	0.14	10,672	0.16	15,886	1.2	21,624
1:6:20 FeTNa	0.17	10,953	0.18	15,723	nd[c]	nd
1:4:14 FeTNa	0.17	10,953	0.18	15,478	nd	nd
1:3.5:12.5 FeTNa	0.17	11,025	nd	nd	nd	nd
1:4:2:16 FeTGNa	0.14	10,764	0.16	16,207	1.1	21,671

a All solutions have an iron molarity of 0.1.

b Wave number, cm.$^{-1}$.

c Not determined as the bands were not visible.

Sugano (44) introduced the possibility of making B and C free parameters, and in this way achieved much better agreement between the experimental and calculated values for energy levels. Generally, the Tanabe-Sugano determinants are solved for $C = 4B$ (45,46). With high-spin d^5-complexes of the ferric and manganous ions, the atomic term distance, ${}^4G = {}^6S$, is directly reflected by the ${}^6A_{1g} \rightarrow {}^4A_{1g}$, ${}^4E_g$ transition. From Equations (8) and (12), the energy of this transition equals $10B + 5C = 30B$; the experimentally measured energy is 21,624 cm.$^{-1}$ (Table V). The value of B in the complex is thus given by 721 cm.$^{-1}$. For the gaseous ferric ion, an extrapolated distance of 32,800 cm.$^{-1}$ is used for the ${}^4G - {}^6S$ term separation (46). B gaseous or B_o therefore equals 1093 cm.$^{-1}$, and β, the ratio of B complex to B_o, equals 0.66. Δ is not very well defined for the high-spin d^5-complexes. Comparable results are obtained by estimating Δ from the relative positions of the ${}^4T_{1g}$ and ${}^6A_{1g}$ levels. From Equations (8) and (9) and the ${}^6A_{1g} \rightarrow {}^4T_{1g}$ transition energy, Δ was evaluated as 13,200 cm.$^{-1}$. The energy for the ${}^6A_{1g} \rightarrow {}^4T_{2g}$ transition was then calculated by substituting the values for Δ and B into Equations (8) and (10). A result of 15,350 cm.$^{-1}$ was obtained. The results from this treatment are summarized below for the 1:12:41 FeTNa (0.1M Fe) solution.

$$\Delta = 13,200 \text{ cm.}^{-1}$$

$$B = 721 \text{ cm.}^{-1}$$

$$\beta = 0.66$$

Transition	Observed Energy, cm.$^{-1}$	Calculated Energy, cm.$^{-1}$
${}^6A_{1g} \rightarrow {}^4T_{1g}$	10,700[a]	10,700
${}^6A_{1g} \rightarrow {}^4T_{2g}$	15,900	15,400
${}^6A_{1g} \rightarrow {}^4A_{1g}$, ${}^4E_g$	21,600	21,600

a
Rounded-off values from Table V.

Ligand Exchange

The data from the ligand exchange study and its treatment are presented in Appendix II. The results, which are summarized in Table VI, are given on the basis of specific activities and compared with the expected specific activities for zero and complete exchange. The analyses by the scintillation and Van Slyke methods suggest complete exchange as opposed to zero exchange.

TABLE VI

LIGAND EXCHANGE

Scintillation Analysis

Expected DPM/mM with zero exchange	$= 3.87 \times 10^5$
Expected DPM/mM with complete exchange	$= 1.93 \times 10^5$

Exchange time, min.	Observed DPM/mM
1.00	2.28×10^5
3.00	2.08×10^5
10.00	1.95×10^5

Van Slyke Analysis

Expected DPM/mM with zero exchange	$= 3.28 \times 10^5$
Expected DPM/mM with complete exchange	$= 1.64 \times 10^5$

Exchange time, min.	Observed DPM/mM
3.00	1.43×10^5
10.00	1.32×10^5

The scintillation data are probably the more reliable. This is based on the agreement between the expected specific activity of the control and the value given by the scintillation method, and on the difficulties experienced with the Van Slyke sample preparation (Appendix II). The scintillation results indicate that after 10 minutes the exchange is complete. In view of the experimental difficulties, however, it is felt that there may not be a significant difference between the values given at the three exchange times.

THE ALKALINE-FERRIC-TARTRATE-GLYCEROL SYSTEM

Examination of the alkaline-ferric-tartrate-glycerol system is broken into two sections. In the first, the interaction between glycerol and the ferric ion was studied in the absence of tartrate, and, in the second, the effect of glycerol on the bonding in the FeTNa system was investigated. Magnetic and spectral methods were employed.

FeGNa

An alkaline-ferric-glycerol (FeGNa) solution was prepared according to the procedure used for the FeTNa synthesis, except that glycerol was substituted for the tartaric acid. The 1:12:14 FeGNa (0.1$\underline{M}$ Fe) solution contained one mole of sodium hydroxide per mole of glycerol plus a 0.2$\underline{M}$ excess of the alkali. The pH of the solution was 12.3, which is essentially the same as that of FeTNa solutions which have a 0.2$\underline{M}$ excess of sodium hydroxide (Table II). This indicates that one hydroxyl group on each glycerol molecule is ionized. The color of the FeGNa solution was bronze; its absorption spectrum is shown in Fig. 24. It was noted that the intensity of the color increased with time. After a period of about 6 months, the color was very intense. There was, however, no indication of decomposition as evidenced by formation of an insoluble phase. For comparison, 1:6:20 and 1:12:36.5 FeTNa (0.1$\underline{M}$ Fe) solutions retained their characteristic green color over the same time period. The FeGNa solution was examined magnetically by the Gouy method. The data are given in Appendix IV; calculated values for the gram-atomic paramagnetic susceptibility and the effective magnetic moment were 14.11 x 10^{-3} c.g.s. em. units and 5.75 B.M., respectively.

FeTGNa

A 1:3:1.5:13 FeTGNa (0.5$\underline{M}$ Fe) solution was prepared by adding glycerol to a FeTNa solution which had not been diluted to volume. The mole ratios of iron to
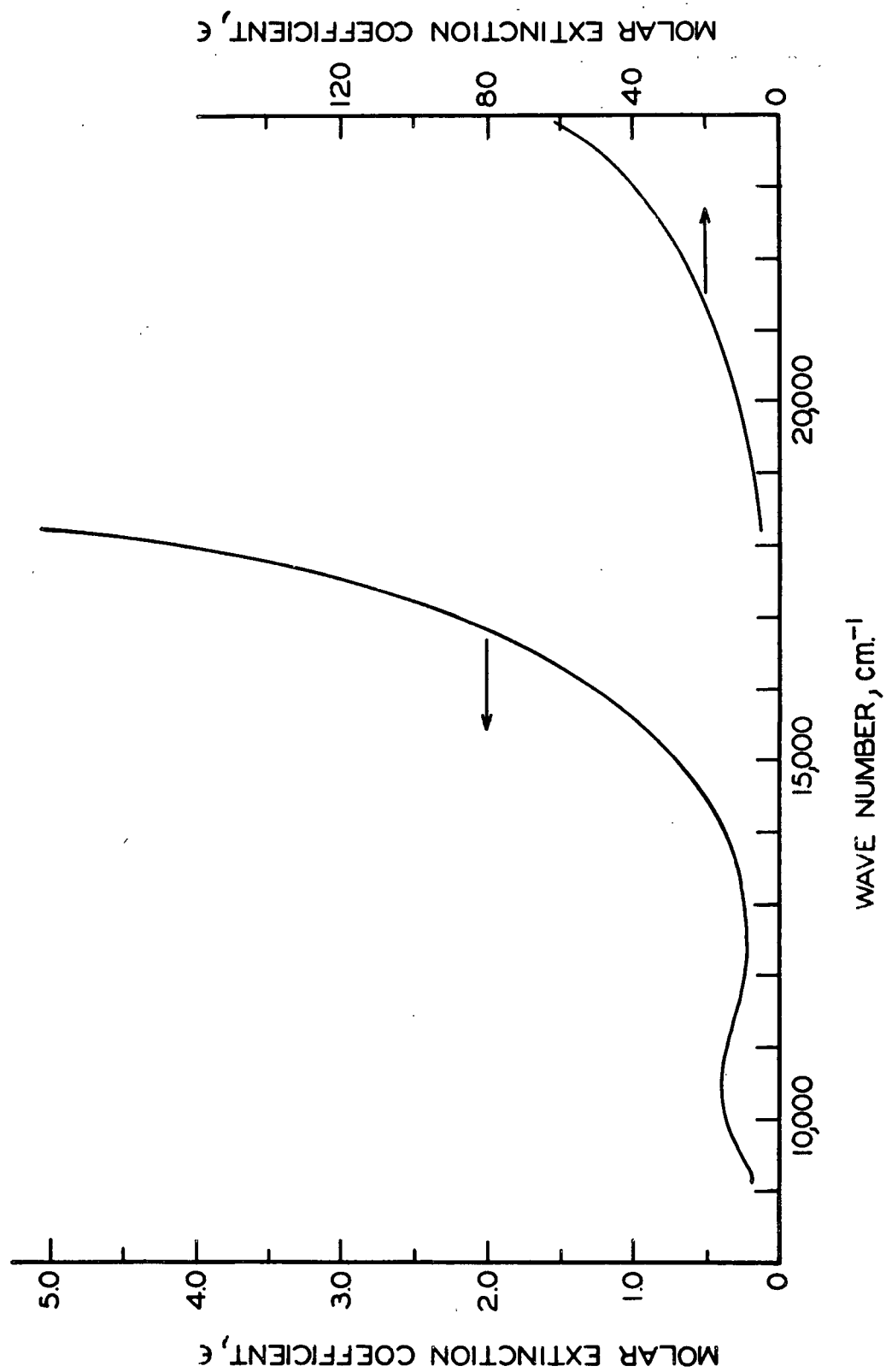
Figure 24. Absorption Spectrum of the 1:12:14 FeGNa (0.1M Fe) Solution

tartaric acid to glycerol to sodium hydroxide were 1 to 3 to 1.5 to 13. This composition is in accord with the optimum combination of 1:3:13 FeTNa (0.5$\underline{M}$ Fe) with glycerol or other suitable ligands, as reported by Bayer (23). The FeTGNa solution, which had the characteristic green color, was examined magnetically by the Gouy method. The data are tabulated in Appendix IV. The calculated gram-atomic paramagnetic susceptibility and effective magnetic moment were 14.83 x 10^{-3} c.g.s. em. units and 5.90 B.M., respectively. An iron molarity of 0.502 was used in the calculations. This value is an average of four quantitative measurements which gave results of 0.506, 0.506, 0.501, and 0.497.

The 1:3:1.5:13 FeTGNa (0.5$\underline{M}$ Fe) solution was treated with alcohol according to the precipitation technique. The resulting solid, Sample V, was dried, analyzed quantitatively, and examined by the Faraday magnetic system. The analyses were conducted for iron, tartrate, glycerol, sodium, and nitrate; the results are given in Appendix V. The magnetic data and calculated gram-atomic paramagnetic susceptibilities are listed in Appendix VI; the reciprocals of the susceptibilities are shown as a function of the absolute temperature in Fig. 25. The relation is linear, as required for a paramagnetic material by Equation (4). A least squares fit of the data to Equation (4) gave values of 4.209 and -7.59 for the constants $\underline{C}$ and θ, respectively. The effective magnetic moment of the iron in the solid equaled 5.88 B.M., which is in agreement with the results of the Gouy system measurements.

The absorption spectrum of a 1:4:2:16 FeTGNa (0.1$\underline{M}$ Fe) solution was recorded from 8700 to 24,000 cm.$^{-1}$. A corresponding alkaline-tartrate-glycerol solution was used in the reference cell. The glycerol had little effect on the spectrum, as indicated by the positions of the absorption maxima (Table V). No attempt was made to describe the absorption in terms of the parameters Δ and β since the theory requires that the central metal be coordinated to one ligand species only.
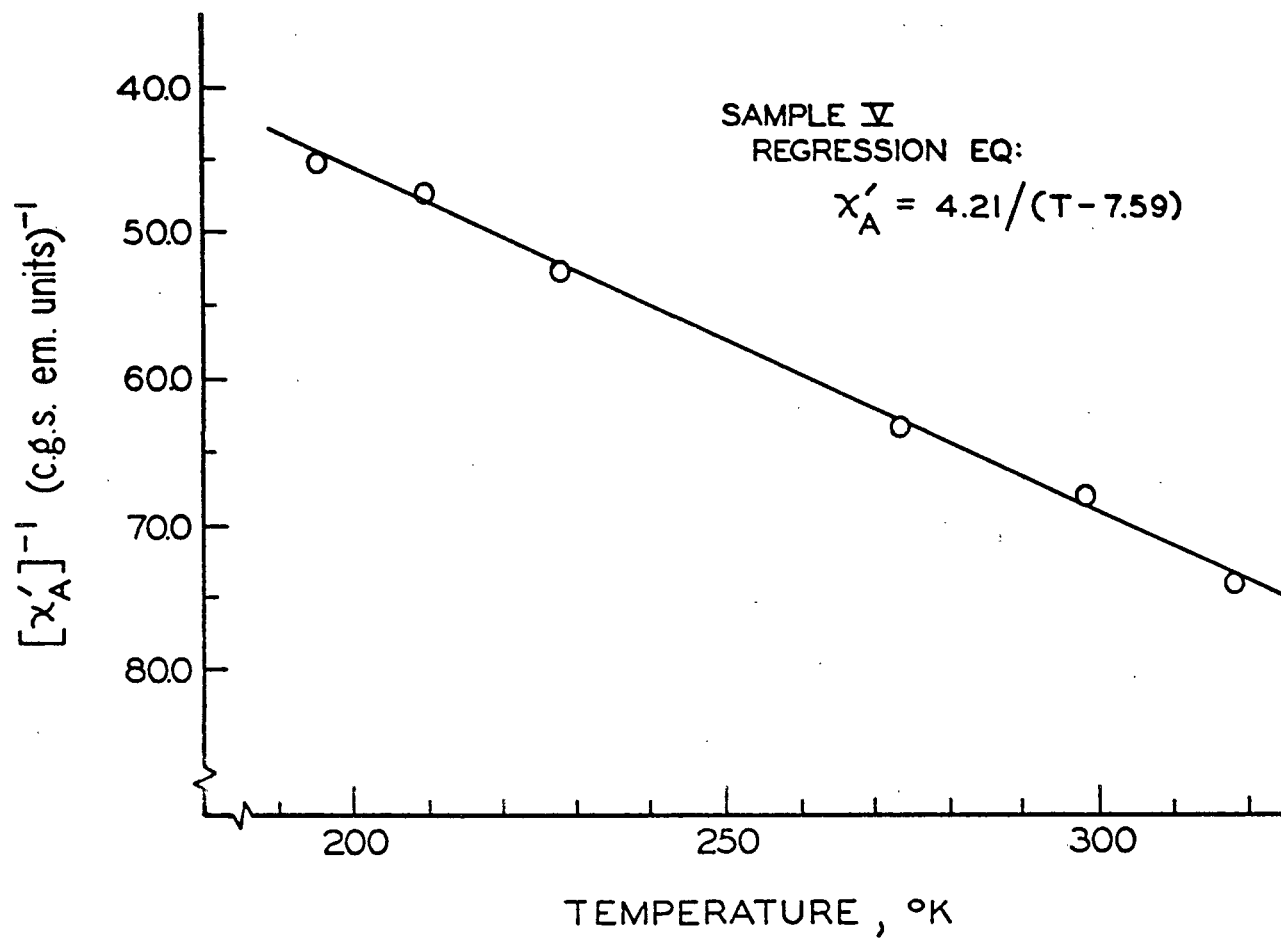
Figure 25. Temperature-Susceptibility Relation For Sample V

ADDITIONAL STUDIES

Several additional experiments were attempted with the FeTNa system which did not prove successful. These included NMR spectrophotometry, ultracentrifugation, and isolation of the complex in a pure or crystalline form.

COMPLEX ISOLATION

During the course of the experimental program, it was desired to isolate the iron-tartrate complex in a pure or, even better, in a crystalline form. Quantitative analysis of the pure form would lend information concerning the composition of the complex, and x-ray analysis of the crystals could establish the structure. An x-ray powder pattern obtained during an earlier study (72) had shown that a crystalline material is formed upon treatment of the FeTNa with a large volume of alcohol. The rate of precipitate formation, however, is very rapid with the alcohol, and the resulting solid contains all of the components found in the solution. It was attempted to lower this rate and thus allow time for crystal growth by using reduced ratios of alcohol to FeTNa. A decrease in rate was observed, but still the complex separated as a dense mass with no visible crystal structure. An additional set of FeTNa solutions was retained in contact with various ratios of alcohol for more than a year in the Institute cold room, but crystallization did not result. Finally, it was attempted to effect crystallization by concentrating a FeTNa solution within a vacuum desiccator; a solid phase was never obtained.

ULTRACENTRIFUGATION

The FeTNa system was examined with the Spinco Model E ultracentrifuge for the purpose of determining whether the iron exists in a polymeric state. The sedimentation velocity method with a synthetic boundary was employed. The

synthetic boundary was felt necessary because the complex almost certainly has a relatively low molecular weight, even if in a polymeric form. Thus, an ordinary boundary probably would not form. The synthetic boundary, single-sector, ultra-centrifuge centerpieces, which will withstand rotational speeds of 60,000 r.p.m., are constructed of an aluminum-containing material. It was found that this material reacted with the FeTNa. Centerpieces made from an all-plastic material proved inert to the FeTNa and were used in this study. With the synthetic boundary construction, however, these centerpieces are double-sectored and will withstand rotational speeds of only 42,000 r.p.m.

After trials employing various FeTNa solutions and solvents, a combination was found which produced a satisfactory boundary with the plastic centerpiece. The solvent had tartaric acid and sodium hydroxide molarities of 1.000 and 3.50, respectively. The FeTNa solution was prepared by dissolving approximately 1% by weight of the solid Sample III in this solvent. The resulting boundary, however, did not move as a function of time at 42,000 r.p.m. Since higher speeds were not possible with the centerpiece, the method was abandoned. Molecular weight data could possibly have been obtained by the sedimentation equilibrium or approach to sedimentation equilibrium methods (73). These techniques can be complete studies within themselves and were not pursued.

NMR SPECTROPHOTOMETRY

A 1:4:14 FeTNa (0.1M Fe) solution and a corresponding alkaline tartrate solution were examined by the Varian A-60A NMR spectrophotometer. Sodium deuteroxide was used in place of the sodium hydroxide and deuterium oxide was employed as the solvent. The tartrate solution showed two sharp absorption peaks, one for DHO and one for the two equivalent hydrogens attached to the tartrate anion. The FeTNa spectrum, however, showed essentially nothing. The bands were apparently broadened to the point of not being visible.

DISCUSSION AND INTERPRETATION

The discussion of the experimental results is divided into two categories: (1) the effect of pH on the ferric-tartrate system, and (2) the ferric-tartrate complex under alkaline conditions. The results are interpreted in terms of the action of the solvent FeTNa on cellulose.

EFFECT OF pH

TRIPLY IONIZED TARTRATE

The behavior of the ferric-tartrate system (one mole of iron to three moles of tartrate) as a function of pH is illustrated by the potentiometric titration curve (Fig. 12). Of particular significance is the relation between the third equivalence point of the tartaric acid and the formation of the green FeTNa solution. The third equivalence corresponds to ionization of an alcoholic function on the tartrate anion. This triply ionized species is the principal ligand in the alkaline system. With two moles of base (NaOH) per mole of tartaric acid, the iron-tartrate system shows a minimum magnetic susceptibility (Fig. 15) and a strong red color. Upon further addition of base the suscepti- bility increases, and the color gradually changes to the characteristic green. The transition is complete when the system contains three moles of base per mole of tartaric acid. Apparently, the triply ionized tartrate ligand complexes very strongly with the iron since it is able to compete with the structures which produce the red color and lower susceptibility. These latter structures form easily and are probably quite stable, especially if hydrolysis is involved.

The yellow-orange precipitate observed during the potentiometric titration was composed primarily of sodium tartrate; the iron-to-tartrate mole ratio was approximately 1 to 7.7 (Sample I, Appendix V). This indicates that less than

three moles of tartrate were coordinated with each mole of iron remaining in solution, which is in agreement with observations from other studies (24-27). The dissolution of the precipitate with continued alkali addition must then be a result of increased coordination between the iron and tartrate as the hydroxyl function on the tartrate is ionized.

THE ACIDIC REGION

Acidic solutions of the ferric ion with many weak field ligands (ligands for which Δ is small) show magnetic moments that are significantly lower than the high-spin value. The high-spin moment is usually observed when the same solutions are made highly acidic with a strong acid (74). The lower moment has been attributed to some form of hydrolysis (74). More recent evidence indicates that polynuclear complexes are formed during this hydrolysis. The electron spins of the paramagnetic ions in such complexes can sometimes interact and cause suppressed magnetic moments. This phenomenon, which is known as spin coupling, probably accounts for the behavior of many ferric ion complexes.

Dimeric complexes of the ferric ion are thought to occur through oxo or hydroxo bridging. Schugar, et al. (75) examined the complexes formed between

$$Fe \longrightarrow O \longrightarrow Fe$$

<p style="text-align:center">A</p>

$$Fe \overset{\textstyle OH}{\underset{\textstyle OH}{<>}} Fe$$
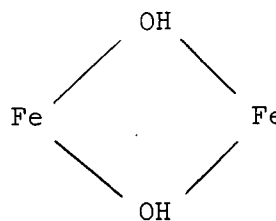
<p style="text-align:center">B</p>

the ferric ion and sodium salts of HEDTA (N-hydroxyethylethylenediaminetriacetic acid). Under proper conditions a paramagnetic dimer formed which had a magnetic moment of about 2.0 B.M. per iron atom; the monomer had a moment of 5.79 B.M.

From a characteristic strong absorption in the vicinity of 850 cm.$^{-1}$, the dimer was assigned a structure corresponding to A. Mulay and Selwood (76) studied the hydrolytic polymerization of the ferric ion in ferric perchlorate solutions. As the pH increased from 0.5 to 2.5, the magnetic moment dropped from the high-spin value to about 3.8 B.M. The decrease was attributed to the formation of a diamagnetic dimer, which was thought to have the bridged structure represented by B. Schugar, et al. (75) questioned the assumption that such a structure could be diamagnetic and showed that the experimental data could better be explained by assigning two unpaired electrons to each ferric ion in the dimer. Spiro, et al. (77) observed polymer formation in 0.3M ferric nitrate solutions after the addition of 0.50 to 0.75 equivalent of bicarbonate. These results were compatible with magnetic measurements. The magnetic moment of the ferric ion (0.197M) in excess perchloric acid showed the high-spin value and then decreased during neutralization of the acid with bicarbonate. After neutralization and addition of 0.50 to 0.75 equivalent of bicarbonate per mole of ferric perchlorate, the magnetic moment leveled out at about 3.9 B.M. Further addition of bicarbonate, up to 2.5 equivalents, darkened the color, but effected no change in the susceptibility (75). It was felt that a structure such as B likely forms before polymerization and then is incorporated into the polymer during the polymerization.

The minimum magnetic susceptibility observed in this study may be representative of a given type of structure, or it may be an average of values from different structures. More than likely, however, the reduction in the susceptibility is a result of spin coupling in polynuclear complexes. Sample I, which precipitated from the region of decreased susceptibility, was pressed into a pellet with KBr and its I.R. spectrum was recorded. An absorption peak in the vicinity of 850 cm.$^{-1}$ was not observed. With the assumption that the precipitation did not alter the structure of the complex, an oxo-bridged structure, as

specified by A, thus appears unlikely. Timberlake (26), in addition, found no absorption peak over the same region with mildly acidic ferric-tartrate solutions.

The iron-tartrate solution which showed the minimum magnetic susceptibility, Solution 16 (Tables II and III), had a magnetic moment of 3.91 B.M. Interestingly, this same value was found with 0.75 to 2.5 equivalents of bicarbonate per mole of iron, as previously discussed. The agreement may be fortuitous, or it may indicate that the same type of structures are involved in both systems. In the latter case, the hydroxo-bridged structure is probably responsible for the reduced magnetic susceptibility in the ferric-tartrate system. The work of Timberlake (26) suggests that the iron-to-tartrate mole ratio in such a complex is 1 to 1. Likely, this bridged structure is in equilibrium with a high-spin type species or incorporated into a polymer with the high-spin species. The moment of 3.91 B.M. is then an average of values from two (or more) spin states.

The results from the Faraday magnetic measurements suggest that polynuclear complex formation is probable in the acidic ferric-tartrate system. Samples I and II, which were isolated from solutions of reduced susceptibilities, gave values for the constant θ of 84.2 and 157.8 degrees, respectively. When the paramagnetic centers in the complex are independent of one another, θ equals a small temperature; a large value, such as either of the above, is indicative of interactions between these centers. Complexes of the polynuclear type frequently show these interactions (50); the phenomenon is termed "intramolecular anti-ferromagnetism."

The absorption peak observed in the vicinity of 10,300 cm.$^{-1}$ is attributed to the species which has a reduced magnetic moment. From Fig. 15 it is noted that the intensity of this absorption increases as the magnetic susceptibility of the solution decreases.

THE ALKALINE-FERRIC-TARTRATE SYSTEM

EQUILIBRIUM CONSIDERATIONS

The relation between the compositions of various alkaline-ferric-tartrate solutions and their molar extinctions in the vicinity of 19,000 cm.$^{-1}$ is illustrated in Fig. 17, 18, and 19. At a constant tartrate-to-iron ratio (which is not less than 3 to 1), the magnitude of the extinction coefficient decreases as the iron concentration increases, and, at a constant ferric ion concentration, the extinction decreases as the tartrate-to-iron ratio increases. These observations suggest the existence of an equilibrium between species. When the relative amounts of water and hydroxide are increased, the equilibrium shifts and a larger quantity of these species is incorporated into the coordination sphere of the iron. This is apparently accompanied by an increase in the absorption of the solution at about 19,000 cm.$^{-1}$. Likewise, higher ratios of tartrate again shift the equilibrium, additional tartrate enters into coordination with the iron, and the absorption decreases.

The results from the magnetic data also suggest an equilibrium mechanism. A 1:3:11 FeTNa (0.1M Fe) solution (Solution 19, Tables II and III) had a bronze color and a magnetic moment of 5.36 B.M. Solution 9, a 1:3:10.82 FeTNa (0.5M Fe) solution, showed the characteristic green color and the high-spin magnetic moment of 5.92 B.M. (Table IV). The complex in the more dilute solution; i.e., Solution 19, probably experienced a significant degree of hydrolysis with either hydroxide ions and/or water molecules. The reduced magnetic moment suggests the presence of polynuclear complexes with spin coupling.

Of principal importance is the spectrum of the cellulose-solvent 1:3:13 FeTNa (0.5M Fe). The magnitude of the absorption in the region around 19,000 cm.$^{-1}$

indicates that, in addition to tartrate ions, hydroxide ions and/or water molecules are also coordinated with the iron. Additional tartrate, or supposedly a similar ligand, should thus be able to enter the coordination sphere of the iron by replacing the hydroxide or water. Also, it has been established that this solvent FeTNa has a high-spin magnetic moment. A certain amount of hydroxide ions or water molecules can thus coordinate with the iron without causing spin coupling (Fig. 17 and p. 56).

Interestingly, the spectrum of $Fe(H_2O)_6^{+3}$, though shifted somewhat, is nonetheless quite similar to that of the alkaline-ferric-tartrate system in the vicinity of 19,000 cm.$^{-1}$ ([71]). A minimum in the absorbance of the highly acidic ferric ion solution was noted to increase in magnitude as the solution became less acidic. The higher absorbance was attributed to formation of the first hydrolysis product, $Fe(OH)(H_2O)_5^{+2}$. Extension of these results to the FeTNa system suggests that hydroxide ions enter the coordination sphere of the iron as the tartrate-to-iron ratio decreases.

Finally, it should be mentioned that the maximum complexing ratio between the tartrate and iron cannot be determined from these magnetic and spectral measurements. From reference to Fig. 1, a 3 to 1 mole ratio seems likely; this, however, is based on intuition rather than experimental evidence.

BOND STRUCTURE

It has been clearly established that the iron in the cellulose solvent FeTNa is in a high-spin state. Magnetic moments of 5.89 and 5.88 B.M. were found by the Gouy and Faraday magnetic methods, respectively. Experimentally determined moments of between 5.70 and 6.0 B.M. are characteristic of the high-spin complexes of the ferric ion ([50]).

· The value of the constant θ in the Curie-Weiss relation was found to equal -6.83 degrees for Sample IV, the solid which was precipitated from a 1:3:13 FeTNa (0.5$\underline{M}$ Fe) solution. Since this value of θ is small, the paramagnetic centers in the complex (the ferric ions) do not interact. These ions are thus suitably surrounded by ligands. This result does not eliminate the possibility of polymeric-type complexes. Such structures, however, do appear unlikely, especially since hydroxo or oxo bridging units are generally involved.

The absorption spectrum of a 1:12:41 FeTNa (0.1$\underline{M}$ Fe) solution is shown in Fig. 21 and 22. The broad, double-peaked absorption band in the ultraviolet region is attributed to charge-transfer. The lower energy end of this band largely obscures the $^6A_{1g} \rightarrow {}^4A_{1g}, {}^4E_g$ transition. This indicates that electrons are transferred from predominantly ligand molecular orbitals to predominantly metal molecular orbitals at relatively low energies, at least as compared with the $Fe(H_2O)_6^{+3}$ complex.

From the positions of the two broad bands and the inflection in the 1:12:41 FeTNa (0.1$\underline{M}$ Fe) spectrum (Fig. 22), the values of the electronic parameters, Δ and β, were estimated; the results were 13,200 cm.$^{-1}$ and 0.66, respectively. For comparison, reported values of these parameters are listed below for certain high-spin complexes of the ferric ion (46). (Presumably, none of these were analyzed in an alkaline system.) It appears that the crystal-field splitting energy, Δ, for the alkaline-ferric-tartrate complex is on the same order as the values observed with other high-spin ferric ion complexes. The value of β, however, is slightly lower than the smallest reported value, which applies to the oxalate complex and is 0.68. This indicates a relatively high degree of covalent bonding between the iron and tartrate in the FeTNa system.

Ligand	Δ, cm.$^{-1}$	β
6 F$^-$	14,000	0.78
6 Urea	13,200	0.72
3 Oxalate^{-2}	13,700	0.68
3 Malonate^{-2}	14,100	0.70
6 H$_2$O	14,300	0.75

In the calculations for Δ and β in the FeTNa system, the following assumptions were required: (1) the ferric ion exists in an undistorted octahedral environment, and (2) the inflection corresponds to the $^6A_{1g} \rightarrow {^4A_{1g}}$, ^4E_g transition. Assessment of these assumptions is difficult. It can, nonetheless, be concluded that the interactions between the iron and its environment are quite similar for the ferric-oxalate and alkaline-ferric-tartrate systems. This is based on the similarity in the positions of the two broad bands in the $Fe(C_2O_4)_3^{-3}$ and FeTNa spectra (Fig. 22 and 23).

A specimen from Sample IV was powdered and pressed into a pellet with KBr. Its I.R. spectrum showed a weak absorption at about 850 cm.$^{-1}$. An absorption in this region is supposedly characteristic of an oxo-bridged structure (75). Such a structure, however, is not expected in Sample IV because of its high-spin magnetic moment.

From the ligand exchange study, it is concluded that the exchange between complexed and uncomplexed tartrate is rapid and to a degree of 100% (Table VI). This behavior is in agreement with the high-spin type bond structure (47). The scatter in the results was caused by various experimental difficulties. Some of the scatter could have been eliminated by repeating the measurements a number of times. However, since either complete and rapid or zero exchange is expected, it was felt that further experimentation would not contribute significantly.

EFFECT OF GLYCEROL

An alkaline-ferric-glycerol solution, 1:12:14 FeGNa (0.1$\underline{M}$ Fe), was found to be stable, which establishes that glycerol will coordinate with the ferric ion in alkaline media. The absorption spectrum of the FeGNa is shown in Fig. 24. The bronze color of the solution is a result of the absorption which begins at about 15,000 cm.$^{-1}$. This absorption obscured all but the lowest energy d-electron transition. An analysis of the spectra in terms of the parameters, Δ and β, was thus not possible.

The magnetic moment of the iron in the FeGNa system equaled 5.75 B.M., which represents a slight reduction as compared to the high-spin value. This reduction was probably caused by hydrolysis of the complex. The degree of any such hydrolysis, however, was probably small since the reduction in the moment was slight. The increased absorption of the FeGNa system, as compared to the FeTNa system, is thus attributed primarily to the alkaline-ferric-glycerol complex, rather than to hydrolysis products.

Addition of glycerol to a 1:3:13 FeTNa (0.5$\underline{M}$ Fe) solution did not change the magnetic moment of the iron; values of 5.90 and 5.88 B.M. were found by the Gouy and Faraday methods, respectively. In addition, the constant θ in the Curie-Weiss relation equaled -7.59 degrees. The ferric ions in the complex therefore do not interact with one another, and the high-spin designation properly describes the system.

From the absorption of a 1:4:14 FeTNa (0.1$\underline{M}$ Fe) solution in the vicinity of 19,000 cm.$^{-1}$, it appears that additional tartrate can coordinate with the iron. A 1:4:2:16 FeTGNa (0.1$\underline{M}$ Fe) solution, which contained glycerol instead of additional tartrate, was prepared and examined spectrophotometrically. The positions of the various bands for the FeTGNa and FeTNa systems are compared in Table V.

The glycerol caused small shifts in the transitional energies, but, in general, did not appreciably affect the spectrum. These results indicate that the glycerol entered into coordination with the iron without causing a major structural change in the complex. It is expected that major structural changes would have been evidenced in the spectral and/or magnetic measurements. The small shifts are attributed to coordination between glycerol and the complex; probably the glycerol replaced hydroxide ions or water molecules which had previously been in the co-ordination sphere.

It was not possible to estimate the degree of coordination between glycerol and FeTNa by the magnitude of the extinction in the region around 19,000 cm.$^{-1}$. The alkaline-ferric-glycerol complex does not have a minimum absorption in this region of the spectrum (Fig. 24), as does the alkaline-ferric-tartrate complex. Increasing coordination between glycerol and FeTNa is therefore not evidenced by a decreasing absorption.

DISSOLUTION OF CELLULOSE BY FeTNa

Glycerol was used as a model compound for cellulose in this study. The results obtained with the glycerol are thus extended for describing the action of FeTNa on cellulose.

First, it was established by magnetic susceptibility and absorption spectro-photometry that major structural changes are not involved during the reaction of FeTNa with glycerol. The glycerol apparently enters the coordination sphere of the iron-tartrate complex in much the same manner as does additional tartrate. The reactive function on the glycerol molecule is probably a glycol pair of hydroxyl groups. In the presence of the ferric ion and alkali, one hydroxyl unit in the glycol grouping is ionized, as was shown by the pH of the FeGNa solution. The

reactive function on the glycerol thus becomes quite analogous to the glycol group on the tartrate anion, and the similarity with which the two ligands coordinate is easily visualized.

Second, it became evident that the solvent properties of the FeTNa must depend on the state of equilibrium in the system. The ferric ions can accommodate only a given amount of tartrate or tartrate-related ligands. When this amount is supplied by the tartrate in the system, the FeTNa is not a solvent. With less tartrate; i.e., a tartrate deficiency, certain positions in the coordination sphere of the iron are likely filled by water molecules or hydroxide ions. Addition of tartrate or a tartrate-related ligand to this system causes a shift in the equilibrium, and the water or hydroxide is displaced as the added ligand enters into the coordination. The driving force for the displacement is probably the thermodynamic favoring of bidentate chelation as opposed to monodentate type complexing. (Bidentate chelation refers to attachment of the ligand to the central species by two functional groups. Obviously, the water or hydroxide cannot coordinate in this manner.)

The absorption spectrum of a 1:3:13 FeTNa (0.5$\underline{M}$ Fe) solution showed that the system has a deficiency of tartrate. It should thus react with additional tartrate, glycerol, or similar species. The glycol hydroxyl groups on the glucopyranoside repeating units of cellulose are similar to the glycol groups in tartrate and glycerol. Reaction of cellulose with the 1:3:13 FeTNa (0.5$\underline{M}$ Fe) solution is therefore not surprising.

The previous discussion does not imply that each ferric ion in the 1:3:13 FeTNa (0.5$\underline{M}$ Fe) solution is coordinated with three tartrates plus additional hydroxide ions and water molecules. Instead, with an equilibrium between structures, the average number of tartrate anions complexed with each iron is less than three.

Excess tartrate (or other glycol-containing ligands) in the system then causes the equilibrium to shift so that the species with the maximum ratio of tartrate to iron is favored.

The concept of an equilibrium between structures as advanced in this study is in complete agreement with the ligand-deficiency mechanism proposed by Bayer.

SYMBOLS

$\underline{A}$	ligand
$\vec{\underline{B}}$	magnetic induction, gauss
$\underline{B}, \underline{C}$	interelectronic repulsion parameters, cm.$^{-1}$
$\underline{C}$	Curie-law constant
$\underline{E}$	energy, cm.$^{-1}$
$\underline{F}$	force, dynes
$f(\underline{H})$	magnetic pull on sample container, dynes
$\vec{\underline{H}}$	magnetic field intensity, oersteds
$\underline{k}$	Boltzmann's constant, 1.381×10^{-16} ergs/deg.
$\underline{M}$	metal ion
$\underline{m}$	mass, g.
$\underline{N}$	Avogadro's number, 6.023×10^{23}
$\underline{p}$	weight fraction
$\underline{S}$	total spin angular momentum quantum number
$\underline{s_i}$	spin angular momentum quantum number of the $\underline{i}$th electron
$\underline{T}$	absolute temperature, $^{\circ}$K.
$\underline{v}$	volume, cm.^{3}
α	cross-sectional area, cm.^{2}
β	the Bohr magneton, 0.927×10^{-20} ergs/oersted
β	ratio between $\underline{B}$ in the complex to $\underline{B}_o$ in the corresponding gaseous ion
Δ or $10\underline{Dq}$	crystal field splitting energy, cm.$^{-1}$
$\Delta\underline{w}$	apparent weight change, g.
ε	molar extinction coefficient
θ	constant in the Curie-Weiss equation, degrees

κ volumetric magnetic susceptibility, (c.g.s. em. units)(g./cm.^{3})

μ_{eff} effective magnetic moment, B.M.

ρ density, g./cm.^{3}

σ wave number, cm.$^{-1}$

χ mass or specific susceptibility, c.g.s. em. units

$\chi_{\underline{d}}$ diamagnetic specific susceptibility, c.g.s. em. units

χ' paramagnetic specific susceptibility, c.g.s. em. units

$\chi_{\underline{A}}'$ gram-atomic paramagnetic susceptibility, c.g.s. em. units

em. units = electromagnetic units

SUGGESTIONS FOR FUTURE WORK

The bonding in the alkaline-ferric-tartrate system has been well characterized by this program. At intermediate pH values, however, the bonding in the iron-tartrate complex is not at all well understood. Continued study in this direction should probably be directed toward (1) determining whether the minimum observed magnetic susceptibility represents a given structure or an average from several structures, and (2) establishing the bond type in the structure or structures, as the case may be. With more than one structure, the properties of the system should change from variations in the iron molarity and iron-to-tartrate ratio at a constant pH value. Low temperature magnetic susceptibility measurements may be useful for defining the bond type, especially if spin coupling is important. In addition, the possibility of polymerization could be investigated by ultracentrifugation. (At these intermediate pH levels, the system should not react with the aluminum-filled centerpieces.)

The solvent properties of the alkaline FeTNa system seem to depend on the state of equilibrium between species within the system. These species should be defined with respect to composition and stability. A principal difficulty in such a study will be relating measurable quantities to given species. An important aspect of any experimental program will be the ionic strength of the system, which should be maintained constant by use of an inert salt.

ACKNOWLEDGMENTS

LITERATURE CITED

1. Jayme, G., and Verburg, W., Reyon, Zellwolle u. Chemiefasern 32, no. 4:193-9; no. 5:275-9(1954).

2. Jayme, G., and Bergmann, W., Reyon, Zellwolle u. Chemiefasern 34, no. 1:27-9 (1956).

3. Jayme, G., and Bergmann, W., Das Papier 10, no. 5/6:88-90(1956).

4. Jayme, G., and Bergmann, W., Das Papier 10, no. 13/14:307-12(1956).

5. Jayme, G., and Bergmann, W., Das Papier 11, no. 13/14:280-7(1957).

6. Borruso, D., Ind. Carta 16, no. 11:383-7(1962).

7. Achwal, W. B., Narayan, T. V., and Purao, U. M., Tappi 50, no. 6:90-3A(1967).

8. Jayme, G., and Bergmann, W., Das Papier 12, no. 9/10:187-96(1958).

9. Jayme, G., and Troften, J., Melliand Textilber. 47, no. 12:1432-6(1966).

10. Jayme, G., and Kleppe, P., Das Papier 15, no. 7:272-8(1961).

11. Jayme, G., Kleppe, P., and Künschner, A., Makromol. Chem. 48:144-59(1961).

12. Jayme, G., and Brüning, D., Naturwiss. 45, no. 2:39(1958).

13. Jayme, G., and Kringstad, K., Das Papier 15, no. 10a:500-6(1961).

14. Jayme, G., and Harders-Steinhäuser, M., Das Papier 10, no. 13/14:282-6(1956).

15. Jayme, G., and Harders-Steinhäuser, M., Textil-Rundschau 19, no. 12:631-40 (1964).

16. Malm, C., Glegg, R., Young, M., and Thompson, J., Tappi 45:819-22(1962).

17. Glegg, R., Parmerter, R., Thompson, J., Ingerick, D., and Malm, C., Tappi 47:574-9(1964).

18. Centola, G., Ind. Carta (N.S.) 4, no. 2:47-54(1966).

19. Centola, G., and Borruso, D., Papier 16, no. 10a:504-12(1962).

20. Smith, D., Bampton, R., and Alexander, W., Ind. Eng. Chem., Process Design Devt. 2, no. 1:57-62(1963).

21. Künschner, A., Chemiefasern 15, no. 9:662-4, 666-8; no. 10:783-8(1965).

22. Baudisch, J., and Phillips, B., Faserforsch. Textiltech. 17, no. 10:473-4 (1966).

23. Bayer, G. F. A study of the iron-tartrate-alkali system and its complexing reaction with cellulose-related polyhydroxy compounds. Doctor's Dissertation. Appleton, Wis., The Institute of Paper Chemistry, 1964. 106 p.; Bayer, G. F., Green, J. W., and Johnson, D. C., Tappi 48, no. 10:557-61(1965).

24. Bobtelsky, M., and Jordan, J., J. Am. Chem. Soc. 69:2286-90(1947).

25. Green, R. W., and Parkins, G. A., J. Phys. Chem. 65:1658-9(1961).

26. Timberlake, C. F., J. Chem. Soc. 1964:1229-40.

27. Pyatnitskii, I. V., and Gorbataya, A. I., Ukrain. Khim. Zh. 21:182-94(1955); C.A. 50:2350i.

28. Gallet, J.-P., and Pâris, R. A., Anal. Chim. Acta 39:341-8(1967).

29. Lingane, J., J. Am. Chem. Soc. 68:2448-53(1946).

30. Yamada, A., J. Chem. Soc. Japan, Pure Chem. Sect. 83:684-93(1962).

31. Franke, W., Ann. 486:242-84(1931); C.A. 25:5145.

32. Pyatnitskii, I. V., Ukrain. Khim. Zh. 23:593-8(1957); C.A. 52:19657h.

33. Charley, P., Sarkar, B., Stitt, C., and Saltman, P., Biochim. et Biophys. Acta 69:313-21(1963).

34. Aasa, R., Malmström, B., Saltman, P., and Vänngård, T., Biochim. et Biophys. Acta 88:430-7(1964).

35. Saltman, P., J. Chem. Educ. 42:682-7(1965).

36. Fialkov, Y. A., and Davidenko, N. K., Ukrain. Khim. Zh. 25:147-54(1959); C.A. 53:21656c.

37. Tsimbler, M. E., Zhur. Neorg. Khim. 4:1081-5(1959); C.A. 54:8410i.

38. Liebhafsky, H. A., J. Chem. Ed. 23:541-2(1946).

39. Bethe, H., Ann. Physik 3:133-208(1929).

40. Orgel, L. E. An introduction to transition-metal chemistry: ligand-field theory. 2d ed. New York, John Wiley and Sons, Inc., 1966. 186 p.

41. Figgis, B. N. Introduction to ligand fields. New York, Interscience, 1966. 351 p.

42. Cotton, A. F. Chemical applications of group theory. New York, Interscience, 1963. 295 p.

43. Tanabe, Y., and Sugano, S., J. Phys. Soc. Japan 9, no. 5:753-66(1954).

44. Tanabe, Y., and Sugano, S., J. Phys. Soc. Japan 9, no. 5:766-79(1954).

45. Schäffer, C. E., and Jørgensen, C. K., J. Inorg. Nuclear Chem. 8:143-8 (1958).

46. Jørgensen, C. K. Absorption spectra and chemical bonding in complexes. Reading, Mass., Addison-Wesley Publishing Co., Inc., 1962. 352 p.

47. Martell, A. E., and Calvin, M. Chemistry of the metal chelate compounds. p. 225-37. Englewood Cliffs, N. J., Prentice-Hall, Inc., 1952.

48. Taube, H., Chem. Rev. 50:69-126(1952).

49. Selwood, P. W. Magnetochemistry. 2d ed. New York, Interscience, 1956. 435 p.

50. Figgis, B. N., and Lewis, J. The magnetochemistry of complex compounds. In Lewis and Wilkins' Modern coordination chemistry. p. 400-54. New York, Interscience, 1960.

51. Bates, L. F. Modern magnetism. 4th ed. Cambridge, University Press, 1963. 514 p.

52. Jørgensen, C. K. Orbitals in atoms and molecules. New York, Academic Press, 1962. 162 p.

53. Valtasaari, L., Paperi ja Puu 39:243-8, 250, 252(1957).

54. Nettleton, H. R., and Sugden, S., Proc. Royal Soc. (London) A173:313-23 (1939).

55. Davis, C. M. Nickel. In Furman's Standard methods of chemical analysis. 6th ed. Vol. 1. p. 700-1. Princeton, N.J., D. Van Nostrand Co., Inc., 1962.

56. Bickerdike, E. L., and Willard, H. H., Anal. Chem. 24:1026(1952).

57. Jackson, L. C., Phil. Trans. Royal Soc. (London) A224:13-15(1923).

58. Fortune, W. B., and Mellon, M. G., Ind. Eng. Chem., Anal. Ed. 10:60-4(1938).

59. Kingsbury, R. M., Tappi 34:382-4(1951).

60. Sandell, E. B. Colorimetric determination of traces of metals. p. 271-3. New York, Interscience, 1944.

61. Woods, J. T., and Mellon, M. G., Ind. Eng. Chem., Anal. Ed. 13:551-4(1941).

62. Smith, G. F. Cerate oxidimetry. Columbus, Ohio, The G. Frederick Smith Chemical Co., 1942. 123 p.

63. Smith, G. F. Periodic acid and iodic acid. 5th ed. Columbus, Ohio, The G. Frederick Smith Chemical Co., 1950. 108 p.

64. Boos, R. N., Anal. Chem. 20:964-5(1948).

65. Bricker, C. E., and Johnson, H. R., Ind. Eng. Chem., Anal. Ed. 17:400-2 (1945).

66. Bauserman, H. M., and Cerney, R. R., Anal. Chem. 25:1821-4(1953).

67. Toth, S. J., Prince, A. L., Wallace, A., and Mikkelsen, D., Soil Sci. 66:459-66(1948).

68. Dean, J. A. Flame photometry. New York, McGraw-Hill Book Co., Inc., 1960. 354 p.

69. Timell, T. E., and Purves, C. B., Svensk Papperstid. 54, no. 9:303-32(1951).

70. Van Slyke, D. D., and Folch, J., J. Biol. Chem. 136:509-41(1940).

71. Rabinowitch, E., and Stockmayer, W. H., J. Am. Chem. Soc. 64:335-47(1942).

72. Hanby, J. E. A study of the complexing reaction between the ferric-tartrate-alkali system and certain polyhydroxy compounds. Unpublished work, The Institute of Paper Chemistry, 1965.

73. Schachman, H. K. Ultracentrifugation, diffusion, and viscometry. From Methods in enzymology. Vol. 4. p. 32-103. New York, Academic Press, Inc., 1957.

74. Werbel, B., Dibeler, V. H., Vosburgh, W. C., J. Am. Chem. Soc. 65:2329-34(1943).

75. Schugar, H., Walling, C., Jones, R., and Gray, H., J. Am. Chem. Soc. 89:3712-20(1967).

76. Mulay, L. N., and Selwood, P. W., J. Am. Chem. Soc. 77:2693-701(1955).

77. Spiro, T. G., Allerton, S. E., Renner, J., Terzis, A., Bils, R., and Saltman, P., J. Am. Chem. Soc. 88:2721-6(1966).

78. Courty, C., Compt. Rend. 230:745-7(1950); C.A. 44:5661g.

79. Handbook of chemistry and physics. 41st ed. p. 2656-7. Cleveland, Ohio, Chemical Rubber Publishing Co., 1959.

80. Mittal, R. L., Univ. Rajputana Studies, Phys. Sci. 1952:193-8; C.A. 49:2136c.

APPENDIX I

ANALYTICAL PROCEDURES

IRON

The o-phenanthroline colorimetric procedure for iron was adapted from Sandell (60). An aliquot of the sample containing from 0.02 to 0.08 mg. of iron was transferred to a 25-ml. volumetric flask and acidified to a pH of about 0.5 with dilute nitric acid. A 10% hydroxylamine hydrochloride solution (2.0 ml.) was added, and the flask was agitated. After allowing several hours for complete reduction of the ferric ions, the pH of the solution was adjusted to 4.5 with dilute ammonium hydroxide and a buffer. The buffer was 1.0M in sodium acetate and acetic acid and had a pH of about 4.5. A 0.25% o-phenanthroline solution (3.0 ml.) was added, and the solution was diluted to volume. After standing for about one hour, the optical density of the solution was measured against a blank at 508 nm. The Beckman DU spectrophotometer was used with 1-cm. cells. The pH was monitored on duplicate solutions with a Beckman pH meter.

GLYCEROL

The method for glycerol analysis was adapted largely from Smith (63). An aliquot of the sample solution, containing between 1 and 9 mg. of glycerol, was introduced into a 250-ml. volumetric flask and mixed with 20 ml. of water and 20 ml. of a 0.05N periodic acid solution. The flask was stoppered (GGS) and, after allowing 80 minutes for the reaction at room temperature, 10 ml. of a 0.1N sodium arsenite solution were added. The solution was agitated intermittently over a 10-minute period and diluted to the mark. A 1-ml. aliquot was transferred from the dilute solution to a 25-ml. volumetric flask and mixed with 5 ml. of concentrated sulfuric acid and 10 drops of a 3% chromotropic acid solution. After heating for 20 minutes

on a steam bath, the solution in the 25-ml. flask was cooled and mixed with an additional 5 ml. of concentrated sulfuric acid. The solution temperature was controlled with a cold water bath during the sulfuric acid addition and then was adjusted to 20°C. After dilution to volume, the optical density was measured at 570 nm. with 1-cm. cells and the Beckman DU spectrophotometer. A blank containing the same reagents was used in the reference cell. This was especially necessary because the chromotropic acid solution discolors with time.

The periodic acid reagent solution was stored in a glass bottle (GGS) and kept out of the light. The chromotropic acid solution was contained within a darkened dropping bottle and stored under refrigeration; even then, it discolored too much for use after about 5 days. The preparation of the $0.1\underline{N}$ sodium arsenite involved dissolving 2.474 g. of arsenious acid in 25 ml. of warm, $2\underline{N}$ sodium hydroxide. The resulting solution, which was contained within a 500-ml. volumetric flask, was neutralized with dilute sulfuric acid, using phenolphthalein as indicator. Sodium bicarbonate (10 g.) was dissolved in 250 ml. of cold water and added to the 500-ml. volumetric flask. After mixing, the solution was diluted to volume.

APPENDIX II

LIGAND EXCHANGE

REACTION PROCEDURE

The exchange reaction was conducted within a 100-ml. separatory funnel and at a constant temperature of 20.1°C. The temperature was maintained with a controlled temperature bath, in which the reaction funnel and reagent solutions were immersed. A 100-ml. volume of the alkaline tartrate reagent contained 0.1200 mole (18.0108 g.) of tartaric acid plus 0.410 mole (16.400 g.) of sodium hydroxide. Approximately 0.0006 g. of the tartaric acid was the dl-tartaric acid-1,4-Cl4; the remainder was reagent d-tartaric acid. The specific activity of the C-14 tagged acid was specified as 5.09 mc./mM by the supplier. (One millicurie, 1 mc., equals 3.7×10^7 disintegrations per second.) The expected specific activity of the alkaline tartrate solution was thus about 1.67×10^{-4} mc./mM or 3.7×10^5 DPM/mM. A 1:3:10.25 FeTNa (0.4M Fe) solution supplied the iron-tartrate complex.

At the beginning of an exchange reaction, the temperatures of the FeTNa and alkaline tartrate solutions were adjusted to 20.1°C. FeTNa (5.00 ml.) was introduced into the separatory funnel, and, simultaneous with the starting of a timer, 5.00 ml. of the tagged tartrate solution were added. The funnel was immersed in the water bath and swirled. After a given time interval, 10 ml. of absolute ethyl alcohol were added, and the mixture was shaken vigorously for about 5 seconds. After allowing 1-1/2 minutes for phase separation, 10 ml. were withdrawn from the upper alcoholic phase and diluted to 25 ml. in a volumetric flask. (These solutions are referred to as the diluted alcoholic extracts.) Aliquots of 2 and 5 ml. were withdrawn from the 25-ml. flask and analyzed for iron and tartrate, respectively. The analyses were conducted as described previously, except that the alcohol in the 5-ml. aliquot was evaporated in a vacuum desiccator with heat supplied by an

infrared lamp. Additional aliquots were removed from the 25-ml. volumetric flask for C-14 analyses by the Van Slyke and liquid scintillation methods. The exchange reaction was run for times of 1.0, 3.0, and 10.0 minutes. All solution transfers were made with volumetric pipets.

DETERMINATION OF SPECIFIC ACTIVITIES

A small aliquot of the 1.200$\underline{M}$ alkaline tartrate solution was diluted by a factor of about 125 with water. The resulting solution had a tartrate concentration which was on the same order as the tartrate concentrations in the diluted alcoholic extracts. The solution is specified as the diluted control and was used for determining the specific activity of the alkaline tartrate control.

ANALYTICAL

The results from the iron and tartrate analyses are listed in Table VII. The diluted alkaline tartrate solution contained 0.976×10^{-5} mole of tartrate per milliliter.

TABLE VII

IRON AND TARTRATE ANALYSES

Sample	Exchange Time, min.	Moles Tartrate in Extract	Moles Tartrate per Mole Iron
1	1.00	3.032×10^{-4}	39.4
3	3.00	2.848×10^{-4}	38.7
10	10.00	3.633×10^{-4}	27.4

SCINTILLATION METHOD

The solutions for the scintillation measurements were prepared according to Table VIII. The specified aliquot volumes were introduced into the scintillation jars and mixed with 15 ml. of the toluene-Triton X-100 cocktail. The cocktail

volumes, which were measured by buret, were from the same reagent solution. After capping the scintillation jars and shaking the solutions vigorously for 2 minutes, the counting was begun. The gain on the Beckman DPM-100 Liquid Scintillation System was set at 5.30, and the activity from a given jar was measured for 20 minutes or to a 0.5% error, whichever came first. The results given in Table IX are averages of values recorded from 40 to 55 hours after preparation of the various solutions. The method of data treatment is illustrated below for measurements made on the diluted control.

TABLE VIII

SCINTILLATION SOLUTIONS

Test Solution	Tagged Soln.[a], ml.	Water, ml.	Standard[b], ml.
Diluted control	2.00	0	0
Diluted control-S	2.00	0	0.05
1	1.00	1.00	0
1-S.	1.00	1.00	0.05
3	1.00	1.00	0
3-S.	1.00	1.00	0.05
10	1.00	1.00	0
10-S.	1.00	1.00	0.05
Diluted control	2.00	0	0
S.	0.00	2.00	0.05
Cocktail	0.00	2.00	0

---

a
 Removed from either the diluted control or the diluted alcoholic extracts.
b
 C-14 labeled toluene with a specific activity of 2.16×10^{-5} DPM/ml. (Beckman, Inc., catalog no. 161995).

TABLE IX

SCINTILLATION RESULTS

Test Solution	Av. CPM	Counting Eff., %	Av. DPM	DPM per m$\underline{M}$ Tartrate
Dil. control	5711	75.6	7555	3.87×10^5
1	1897	68.5	2769	2.28×10^5
3	1780	75.2	2369	2.08×10^5
10	2101	74.3	2828	1.95×10^5

The background DPM was estimated from count rates recorded for the cocktail solution with and without the standard.

```
av. cocktail CPM = 68.6
av. CPM with standard = 8488
CPM from standard = 8488-69 = 8419
Activity of standard = 2.16 x 10⁵ DPM/ml. x 0.05 ml.
                     = 1.08 x 10⁴ DPM
% efficiency = (CPM/DPM) x 100
% eff. = 8419 x 10²/1.08 x 10⁴  = 77.9
DPM of cocktail (i.e., background) = 68.6/0.779 = 88
```

The measured CPM of the two diluted control solutions were 5772 and 5784, which gave an average value of 5778. The diluted control plus standard gave a count rate of 13,942 CPM.

```
CPM from standard = 13,942-5778 = 8164
% eff. = 8164 x 10²/1.08 x 10⁴  = 75.6
background CPM = 88(0.756) = 67
CPM from control = 5778-67 = 5711
DPM of control = 5711/0.756 = 7555
moles tartrate in test solution = 1.952 x 10⁻⁵
```

The specific activity of the control is thus equal to

$$\frac{7555 \text{ DPM}}{1.952 \times 10^{-2} \text{ m}\underline{M}} = 3.87 \times 10^5 \text{ DPM/m}\underline{M}.$$

VAN SLYKE METHOD

The Van Slyke method gave a specific activity of 3.28×10^5 DPM/m$\underline{M}$ for the control. This value is an average of the following determinations (Table X).

TABLE X

SPECIFIC ACTIVITIES OF CONTROL

Test	Tartrate, m$\underline{M}$	DPM	DPM/m$\underline{M}$
1	1.952×10^{-2}	6,423	3.29×10^5
2	3.904×10^{-2}	12,681	3.25×10^5
3	3.904×10^{-2}	12,924	3.31×10^5

Aliquots of the diluted alcoholic extracts gave the following specific activities with the Van Slyke method (Table XI).

TABLE XI

SPECIFIC ACTIVITIES OF TEST SOLUTIONS

Sample	Aliquot Vol., ml.	Tartrate, m$\underline{M}$	DPM	DPM/m$\underline{M}$
1	1.00	1.214×10^{-2}	1699	1.40×10^5
3	1.00	1.139×10^{-2}	1202	1.06×10^5
10	1.00	1.453×10^{-2}	1610	1.11×10^5
3	4.00	4.528×10^{-2}	6477	1.43×10^5
10	4.00	5.812×10^{-2}	7648	1.32×10^5
10	4.00	5.812×10^{-2}	7810	1.34×10^5
10	4.00	5.812×10^{-2}	7601	1.31×10^5

The amount of CO_2 produced from oxidation of the 1.00-ml. aliquots was less than the minimum which can be accurately measured by the technique. The determinations with 4.00-ml. aliquots were thus conducted. The duplicate analyses on Sample 10

gave reasonably good reproducibility for the total activity (DPM) of the samples; the manometric data, however, gave values of 2.767, 3.710, and 3.481 for the milligrams of carbon. This disparity is attributed to occlusion of small amounts of alcohol within the dried specimens. (The Van Slyke method requires that the specimens are dry.) The manometric data were therefore not used, and the calculated specific activities are based on the perchlorate-cerate determinations of tartrate. This probably caused a small error because the specimens tended to bump during the drying process, and some tartrate was certainly lost. The reported specific activities for Samples 3 and 10 are thus too low. (The drying was conducted in a vacuum desiccator with heat supplied by an infrared lamp. Attention was not given to the bumping because it was planned to base the calculations on the manometric data.)

DEGREE OF EXCHANGE

In each exchange reaction the tagged tartrate and FeTNa solutions supplied equivalent amounts of tartrate. Zero exchange is thus evidenced by a sample specific activity which equals the specific activity of the control; with complete exchange, the sample specific activity should equal one half of that of the control.

APPENDIX III

CALIBRATION OF THE MAGNETIC BALANCES

THE GOUY BALANCE

Slight modifications were made in the Gouy system sample tube at several points during the study. These changes necessitated recalibration of the system. A total of three calibrations was conducted; the results are given in Tables XII, XV, and XVI. Treatment of the experimental data is illustrated for the second calibration.

CALIBRATION ONE

Nickel chloride solutions (2.117 and 0.979$\underline{M}$) were used as the standards and gave the values shown in Table XII.

TABLE XII

CALIBRATION ONE

Current, amp.	f($\underline{H}$), dynes	$1/2\alpha(\underline{H}^2-\underline{H}_o{}^2)_{av.} \times 10^{-6}$, (oersted-cm.)^2
3.00	-0.686	4.071
5.00	-1.960	11.39
8.00	-4.990	28.76
10.00	-7.540	44.00
13.00	-11.86	68.56
15.00	-14.50	84.68
18.00	-18.71	108.7

CALIBRATION TWO

The term f($\underline{H}$) in Equation (6) was determined from the apparent weight changes of the empty sample tube at various magnetic field strengths (Table XIII).

TABLE XIII

DETERMINATION OF $f(\underline{H})$

Current, amp.	Apparent Wt. Change,[a] g.	$f(\underline{H})$, dynes
5	-0.0021	-2.059
10	-0.0079	-7.747
15	-0.0152	-14.91
18	-0.0194	-19.03

[a] An average of three determinations.

The negative signs in the above are indicative of the diamagnetic character of glass.

The function $1/2\alpha(\underline{H}^2-\underline{H}_o{}^2)$ was evaluated from $f(\underline{H})$ and the magnetic forces, $\underline{F}$ (Table XIV), observed with two nickel chloride solutions. Quantitative analysis of the solutions for nickel gave nickel molarities of 0.902 and 1.705; these are averages of the experimental values 0.903 and 0.902, and 1.703 and 1.707, respectively.

TABLE XIV

MAGNETIC FORCES

Current, amp.	$\underline{F}^a$, dynes 0.902$\underline{M}$ NiCl$_2$	$\underline{F}^a$, dynes 1.705$\underline{M}$ NiCl$_2$
5	35.11	76.39
10	135.3	293.5
15	261.5	565.0
18	335.4	724.5

[a] An average of three determinations.

Application of Equation (13) and use of 24.16×10^{-6} c.g.s. em. units ([78],[79]) as the specific susceptibility of air gave the following:

	0.902$\underline{M}$ NiCl$_2$	1.705$\underline{M}$ NiCl$_2$
$\underline{p}$ of NiCl$_2$	0.1061	0.1853
temperature	295.4°K	295.4°K
χ of NiCl$_2$	2.959×10^{-6}	5.705×10^{-6}
soln. density, ρ	1.102 g./ml.	1.193 g./ml.
$\kappa = \rho \chi$	3.261×10^{-6}	6.805×10^{-6}
air density, $\rho_{\underline{a}}$	1.16×10^{-3} g./ml.	1.16×10^{-3} g./ml.
$\kappa_{\underline{a}} = \rho_{\underline{a}} \chi_{\underline{a}}$	0.028×10^{-6}	0.028×10^{-6}
$(\kappa - \kappa_{\underline{a}})$	3.233×10^{-6}	6.777×10^{-6}

Equation (5), written in the form

$$1/2\alpha(H^2 - H_o{}^2) = [F - f(H)]/(\kappa - \kappa_a),$$

can now be used for the direct evaluation of $1/2\alpha(\underline{H}^2 - \underline{H}_o{}^2)$ (Table XV).

TABLE XV

CALIBRATION TWO

Current, amp.	Results,[a] 0.902$\underline{M}$ NiCl$_2$	Results,[a] 1.705$\underline{M}$ NiCl$_2$	Results,[a] av.
5	11.50	11.58	11.54
10	44.26	44.45	44.35
15	85.48	85.56	85.52
18	109.6	109.7	109.7

---

[a] Results for $1/2\alpha(\underline{H}^2 - \underline{H}_o{}^2) \times 10^{-6}$.

CALIBRATION THREE

A 0.667$\underline{M}$ NiCl$_2$ solution was used for this calibration. Three determinations of the nickel molarity gave values of 0.666, 0.668, and 0.667. The calibration results are given in Table XVI.

TABLE XVI

CALIBRATION THREE

Current, amp.	$f(\underline{H})$, dynes	$1/2\alpha(\underline{H}^2 - \underline{H}_o{}^2) \times 10^{-6}$ (oersted-cm.)^2
10.00	-7.355	43.93
15.00	-14.416	84.66
18.00	-18.535	108.8

THE FARADAY BALANCE

Two sets of sample bulbs and suspension fibers were used with the Faraday system. Two separate calibrations were thus required. The method of data treatment is illustrated for the first calibration.

CALIBRATION ONE

The apparent weight changes observed with the empty sample bulb and with 161.0 mg. of ferrous ammonium sulfate (f.a.s.) in the bulb are given in Table XVII. [Each value represents an average of three experimental measurements. The ferrous ammonium sulfate was used in its hexahydrated form, i.e., Fe(NH$_4$)$_2$(SO$_4$)$_2\cdot$6H$_2$O.] Conversion of the data in Table XVII to grams and multiplication by the gravitational constant gives the values for $f(\underline{H})$ and $\underline{F}$. According to Equation (7),

$$[\underline{F} - f(\underline{H})]/m\chi = H_z(dH_z/dx).$$

Measurements with the ferrous ammonium sulfate were made at 26.7°C. From Equation (14), χ equaled 31.58×10^{-6} c.g.s. em. units, and $m\chi$ became $(31.58 \times 10^{-6})(0.1610) = 5.084 \times 10^{-6}$. $H_z(dH_z/dx)$ was then calculated directly (Table XVIII).

TABLE XVII

MEASURED WEIGHT CHANGES

Current, amp.	Apparent Weight Change, mg.	
	Empty Bulb	f.a.s.
1	-0.015	0.296
2	-0.036	1.161
3	-0.057	2.344
4	-0.080	3.355
5	-0.091	4.083
6	-0.099	4.638
7	-0.105	5.089

TABLE XVIII

CALIBRATION ONE

Current, amp.	$f(H)$, dynes	$F - f(H)$, dynes	$H_z(dH_z/dx) \times 10^{-6}$, oersted^2/cm.
1	-0.0147	0.3050	0.0600
2	-0.0353	1.1739	0.2309
3	-0.0559	2.3546	0.4631
4	-0.0785	3.3686	0.6625
5	-0.0892	4.0933	0.8051
6	-0.0971	4.6454	0.9137
7	-0.1030	5.0936	1.002

CALIBRATION TWO

The results of the second calibration are listed in Table XIX.

<div align="center">

TABLE XIX

CALIBRATION TWO

</div>

Current, amp.	$f(\underline{H})$, dynes	$\underline{H}_z(d\underline{H}_z/d\underline{x}) \times 10^{-6}$, oersted^2/cm.
1	0.0029	0.0559
2	0.0029	0.2215
3	0.0000	0.4484
4	-0.0039	0.6429
5	-0.0069	0.7818
6	-0.0098	0.8858
7	-0.0118	0.9742

APPENDIX IV

GOUY SYSTEM MEASUREMENTS

The apparent weight changes observed with the Gouy magnetic system are listed in the following tables. Each value is an average of at least two, and usually three, experimental determinations. The term, $\underline{F}$, in Equation (5) equals the apparent weight change, $\Delta\underline{w}$, times the gravitational constant.

SOLUTIONS 1 THROUGH 11

The average values of $\Delta\underline{w}$ and the calculated gram-atomic paramagnetic suscepti-bilities for Solutions 1 through 11 are given in Tables XX and XXI. The calibration data in Table XII applies to these values. The method of calculation is illustrated in the next section for Solution 22.

TABLE XX

AVERAGE WEIGHT CHANGES

Current, amp.	Soln. 1 $\Delta\underline{w}$, g.	Soln. 2 $\Delta\underline{w}$, g.	Soln. 3 $\Delta\underline{w}$, g.	Soln. 4 $\Delta\underline{w}$, g.	Soln. 5 $\Delta\underline{w}$, g.
3.00	0.0196	0.0192	0.0201	0.0222	0.0239
5.00	0.0558	0.0531	0.0560	0.0612	0.0685
8.00	0.1377	0.1355	0.1407	0.1547	0.1708
10.00	0.2104	0.2073	0.2135	0.2361	0.2629
13.00	0.3275	0.3233	0.3337	0.3688	0.4084
15.00	0.4039	0.3981	0.4113	0.4548	0.5038
18.00	0.5197	0.5103	0.5283	0.5843	0.6571

Current, amp.	Soln. 8 $\Delta\underline{w}$, g.	Soln. 9 $\Delta\underline{w}$, g.	Soln. 10 $\Delta\underline{w}$, g.	Soln. 11 $\Delta\underline{w}$, g.
3.00	0.0271	0.0268	0.0268	0.0270
5.00	0.0749	0.0744	0.0747	0.0734
8.00	0.1872	0.1875	0.1883	0.1863
10.00	0.2857	0.2882	0.2855	0.2852
13.00	0.4457	0.4487	0.4453	0.4452
15.00	0.5496	0.5534	0.5512	0.5498
18.00	0.7054	0.7077	0.7055	0.7056

TABLE XXI

PARAMAGNETIC SUSCEPTIBILITIES

Soln.	Soln. Density, g./cm.^{3}	Temperature,[a] °C.	Para. Sus.[b], $\chi_A' \times 10^3$, c.g.s. em. units
1	1.271	22.9	11.36
2	1.270	20.3	11.22
3	1.273	21.1	11.64
4	1.275	21.1	12.63
5	1.278	21.1	13.78
8	1.291	21.0	14.92
9	1.307	21.1	14.95
10	1.323	21.9	14.82
11	1.348	21.9	14.80

a
 Average solution temperature during the magnetic measurements.
b
 Paramagnetic susceptibility per gram-atom of ferric ions in the complex
at 20°C.

SOLUTIONS 12 THROUGH 22

The experimentally determined values of Δw for Solutions 12 through 22 are listed in Table XXII. The calibration data in Table XVI apply to these measurements. The method for calculating the gram-atomic paramagnetic susceptibility and the effective magnetic moment is illustrated for Solution 22. The susceptibilities and magnetic moments calculated from these measurements are presented in Table III.

TABLE XXII

AVERAGE WEIGHT CHANGES

Current, amp.	Soln. 12 Δw, g.	Soln. 13 Δw, g.	Soln. 14 Δw, g.	Soln. 15 Δw, g.
10.00	0.0245	0.0243	0.0143	-0.0050
15.00	0.0473	0.0467	0.0273	-0.0100
18.00	0.0603	0.0597	0.0347	-0.0134

TABLE XXII(Continued)

AVERAGE WEIGHT CHANGES

Current, amp.	Soln. 16 Δw, g.	Soln. 17 Δw, g.	Soln. 18 Δw, g.	Soln. 19 Δw, g.
10.00	-0.0098	0.0036	0.0097	0.0130
15.00	-0.0191	0.0069	0.0185	0.0249
18.00	-0.0246	0.0089	0.0237	0.0316

Current, amp.	Soln. 20 Δw, g.	Soln. 21 Δw, g.	Soln. 22 Δw, g.
10.00	0.0227	0.0238	0.0229
15.00	0.0439	0.0461	0.0450
18.00	0.0563	0.0591	0.0578

TABLE XXIII

SOLUTION PROPERTIES

Soln.	Soln. Density, g./cm.^{3}	Temperature[a], °C.
12	1.034	21.7
13	1.036	21.4
14	1.041	20.9
15	1.043	20.1
16	1.048	22.0
17	1.051	21.7
18	1.058	20.6
19	1.065	21.0
20	1.075	21.3
21	1.082	21.7
22	1.115	23.0

[a] Average solution temperature during the magnetic measurements.

The following experimental data were recorded during the Gouy magnetic measurements on Solution 22 (Table XXIV). The values of Δw and the magnetic pull, F, were then determined (Table XXV). The terms, $[F - f(H)]$ and $(\kappa - \kappa_a) = [F - f(H)]/[1/2\alpha(H^2 - H_o^2)]$ from Equation (6), were calculated from the values of F and the "Calibration Three" data in Table XVI and are listed in

Table XXVI. The normally accepted specific susceptibility of air is 24.16×10^{-6} c.g.s. em. units ($\underline{79}$). With an air density of 1.16×10^{-3} g./ml., the volumetric susceptibility of air, $\kappa_{\underline{a}}$, equals 0.028×10^{-6} c.g.s. em. units (g./cm.^{3}). The density of the test solution was determined by weighing a tared 25-ml. volumetric flask which had been filled to the mark with the solution. A value of 1.115 g./ml. was obtained. The average specific susceptibility of the test solution was then evaluated (Table XXVII).

TABLE XXIV

EXPERIMENTAL DATA

Current, amp.	Apparent Wt., g. Test 1	Apparent Wt., g. Test 2
0.00	115.1773	115.1774
10.00	115.2003	115.2003
15.00	115.2224	115.2223
18.00	115.2353	115.2352
0.00	115.1774	115.1775

TABLE XXV

MAGNETIC PULL

Current, amp.	$\Delta\underline{w}$, g. Test 1	$\Delta\underline{w}$, g. Test 2	$\Delta\underline{w}$, g. Av.	$\underline{F}$, dynes
10.00	0.0230	0.0229	0.0229	22.457
15.00	0.0451	0.0449	0.0450	44.130
18.00	0.0579	0.0577	0.0578	56.682

TABLE XXVI

CALCULATED SUSCEPTIBILITIES

Current, amp.	$[\underline{F} - f(\underline{H})]$, dynes	$(\kappa - \kappa_{\underline{a}})$, c.g.s. em. units (g./cm.^{3})
10.00	29.812	0.679×10^{-6}
15.00	58.546	0.692×10^{-6}
18.00	75.217	0.691×10^{-6}

TABLE XXVII

AVERAGE SUSCEPTIBILITY

Current, amp.	κ, c.g.s. em. units (g./cm.^{3})	$\chi = \kappa/\rho$, c.g.s. em. units
10.00	0.707×10^{-6}	0.634×10^{-6}
15.00	0.719×10^{-6}	0.645×10^{-6}
18.00	0.719×10^{-6}	0.645×10^{-6}

$$\chi_{av.} = 0.642 \times 10^{-6}$$

The next step in the data treatment involved estimating the diamagnetic specific susceptibility, χ_d, of the test solution. This was accomplished by application of Wiedemann's additivity law (49), which states that the magnetic susceptibility of a mixture can be represented by

$$\chi = \sum_i \chi_i p_i . \qquad (15)$$

χ is the susceptibility of the mixture and χ_i and p_i are susceptibilities and weight fractions, respectively, for the components. The composition of Solution 22 is given in Table V, from which the weights of the various components per liter were calculated.

$Fe(NO_3)_3$	0.0993(241.87)	= 24.02 g.
tartaric acid	0.600(150.99)	= 90.05
NaOH	2.00(40.00)	= 80.00
	total	= 194.07 g.

(The iron content was determined colorimetrically. It is important that this value be accurate, as will be noted from a later step in the calculations.) The total solution weight per liter was estimated from the solution density, and the weight of water was determined by difference.

$$H_2O \qquad 1114.7 - 194.1 = 920.6 \text{ g.}$$

The values for the various weight fractions were then calculated.

$$p_{Fe} \quad = 0.0993(55.847)/1114.7 \quad = 0.0050$$

$$p_{NO_3} \quad = 3(0.0993)(62.01)/1114.7 \quad = 0.0166$$

$$p_{t.a.} \quad = 90.5/1114.7 \quad = 0.0808$$

$$p_{Na} \quad = 2.00(22.99)/1114.7 \quad = 0.0412$$

$$p_{OH} \quad = 2.00(17.008)/1114.7 \quad = 0.0305$$

$$p_{H_2O} \quad = 920.6/1114.7 \quad = \underline{0.8259}$$

$$1.0000$$

The diamagnetic susceptibilities of the components were obtained from the literature (49,80). Most values were expressed on a molar basis so that division by the molecular (or atomic) weight was required.

$$\chi_{d_{Fe}} \quad = -10 \times 10^{-6}/(55.847) \quad = -0.179 \times 10^{-6}$$

$$\chi_{d_{NO_3}} \quad = -20 \times 10^{-6}/(62.007) \quad = -0.323 \times 10^{-6}$$

$$\chi_{d_{t.a.}} \quad = -63.5 \times 10^{-6}/(150.09) \quad = -0.423 \times 10^{-6}$$

$$\chi_{d_{Na}} \quad = -5 \times 10^{-6}/(22.99) \quad = -0.217 \times 10^{-6}$$

$$\chi_{d_{OH}} \quad = -12 \times 10^{-6}/(17.008) \quad = -0.706 \times 10^{-6}$$

$$\chi_{d_{H_2O}} \quad = -0.722 \times 10^{-6}$$

(The above values are expressed in c.g.s. em. units.) The diamagnetic susceptibility of the solution was then evaluated from Equation (15).

$$\chi_d = -0.667 \times 10^{-6} \text{ c.g.s. em. units.}$$

The experimentally determined specific susceptibility equals χ_d plus χ', the paramagnetic specific susceptibility. After substituting and rearranging

$$\chi' = [0.642 + 0.667]10^{-6} = 1.309 \times 10^{-6} \text{ c.g.s. em. units.}$$

The paramagnetic susceptibility per gram-atom of ferric ions in the complex, χ_A', was obtained by dividing the product of χ' and 55.847, the atomic weight of iron, with p_{Fe}.

$$\chi_A' = \frac{1.309 \times 10^{-6}(55.847)}{0.0050} = 14.69 \times 10^{-3} \text{ c.g.s. em. units}$$

The magnetic moment of the ferric ion in Bohr magnetons is related to χ_A' by Equation (3),

$$\mu^2_{eff} = \left[\frac{3 \ k}{N \ \beta^2}\right] T\chi_A' \ .$$

Upon substituting $k = 1.381 \times 10^{-16}$ ergs/deg., $N = 6.023 \times 10^{23}$, and $\beta = 0.927 \times 10^{-20}$ ergs/oersted,

$$\mu^2_{eff} = 8.002(T)(\chi_A').$$

The average solution temperature during the magnetic measurements was 23.0°C. T thus equaled 296.2°K. and

$$\mu_{eff} = 5.90 \text{ B.M.}$$

Values of χ_A' reported in the various tables were adjusted to 20°C. by the temperature-susceptibility relationship of Equation (3).

In these sample calculations the diamagnetic correction was slightly larger in magnitude than the measured susceptibility. The method of correction is reliable so that this should cause little concern. Nonetheless, certain alkaline FeTNa solutions were examined specifically for determination of the magnetic moment of the iron. These solutions had iron molarities of 0.5, and the diamagnetic correction amounted to only about 10% of the measured susceptibility.

1:3:13 FeTNa (0.5$\underline{M}$ Fe) SOLUTION

The calibration results in Table XV apply to the magnetic data in Table XXVIII.

TABLE XXVIII

1:3:13 FeTNa (0.5$\underline{M}$ Fe)

Current, amp.	$\Delta\underline{w}$, g. Test 1	$\Delta\underline{w}$, g. Test 2	$\Delta\underline{w}$, g. Test 3
5.00	0.0756	0.0756	0.0753
10.00	0.2899	0.2901	0.2899
15.00	0.5568	0.5569	0.5566
18.00	0.7142	0.7141	0.7142

Average solution temperature = 22.1°C.
Solution density = 1.341 g./ml.
χ_A' = 14.69 x 10^{-3} c.g.s. em. units (at 20°C.)
μ_{eff} = 5.89 B.M.

1:12:14 FeGNa (0.1$\underline{M}$ Fe) SOLUTION

The calibration results in Table XVI apply to these measurements (Table XXIX). The specific susceptibility of glycerol was required in the calculations. Its value is -0.538 x 10^{-6} c.g.s. em. units (79).

TABLE XXIX

1:12:14 FeGNa (0.1$\underline{M}$ Fe)

Current, amp.	$\Delta\underline{w}$, g. (average)
10.00	0.0203
15.00	0.0397
18.00	0.0510

Average solution temperature = 21.9°C.
Solution density = 1.087 g./ml.
Iron molarity = 0.099 (determined analytically)
χ_A' = 14.11 x 10^{-3} c.g.s. em. units (at 20°C.)
μ_{eff} = 5.75 B.M.

1:3:1.5:13 FeTGNa (0.5$\underline{M}$ Fe) SOLUTION

The calibration results in Table XV apply to these magnetic measurements (Table XXX). Again, a specific susceptibility of -0.538 x 10^{-6} c.g.s. em. units (79) was used for the glycerol.

TABLE XXX

1:3:1.5:13 FeTGNa (0.5$\underline{M}$ Fe)

Current, amp.	$\Delta\underline{w}$, g. Test 1	$\Delta\underline{w}$, g. Test 2	$\Delta\underline{w}$, g. Test 3	$\Delta\underline{w}$, g. Test 4
5.00	0.0756	0.0759	0.0757	0.0760
10.00	0.2902	0.2906	0.2906	0.2905
15.00	0.5569	0.5571	0.5572	0.5572
18.00	0.7143	0.7139	0.7146	0.7145

Average solution temperature = 22.5°C.
Solution density = 1.351 g./ml.
$\chi_A' = 14.83$ x 10^{-3} c.g.s. em. units (at 20°C.)
$\mu_{eff} = 5.90$ B.M.

APPENDIX V

COMPOSITIONS OF IRON-TARTRATE SOLIDS

The values recorded in this section were determined by the previously described analytical methods. The results are given on an ovendry (o.d.) basis and in terms of weight percent (Tables XXXI-XXXV).

TABLE XXXI

IRON

Sample	1	2	3	4	Av.
I	3.18	3.28			3.23
II	10.09	10.06			10.08
III	8.18	8.28	8.05	8.08	8.14
IV	8.30	8.24	8.23	8.21	8.24
V	7.18	7.05	6.86	7.04	7.03

TABLE XXXII

TARTRATE

Sample	1	2	3	4	Av.
I	65.82	65.70			65.76
II	62.67	62.45			62.56
III	61.49	61.49	60.68	60.68	61.09
IV	62.22	62.35	61.60	61.41	61.89
V	52.62	52.77	52.23	51.94	52.39

TABLE XXXIII

GLYCEROL

Sample V	6.12	6.61	5.77	6.16 (av.)
	6.62	5.97	5.89	

TABLE XXXIV

SODIUM

Sample	1	2	Av.
I	16.72	16.53	16.63
II	19.08	18.92	19.00
III	25.18	24.82	25.00
IV	24.67	23.96	24.32
V	26.24	25.45	25.85

TABLE XXXV

NITRATE

| Sample | Nitrogen | | | NO_3^- |
	1	2	Av.	Av.
I	2.78	2.69	2.74	12.13
II	1.17	1.10	1.14	5.05
III	0.57	0.57	0.57	2.52
IV	0.34	0.34	0.34	1.50
V	1.11	1.11	1.11	4.91

SUMMATION

In Table XXXVI, hydroxide ions and water were added to give electric neutrality and 100% summation, respectively. From the sample calculations in Appendix VI, it can be seen that small errors in the compositions of these samples have a negligible effect on the diamagnetic corrections.

TABLE XXXVI

SUMMATION

Sample	Iron	Tartrate	Glycerol	Sodium	NO_3^-	OH^-	H_2O	Sum.
I	3.23	65.76		16.6	12.1		2.3	100.0
II	10.08	62.56		19.0	5.0	1.5	1.8	100.0
III	8.14	61.09		25.0	2.5	3.3		100.0
IV	8.24	61.89		24.3	1.5	3.7	0.4	100.0
V	7.03	52.39	6.2	25.9	4.9	3.6		100.0

MOISTURE

The moisture contents of Samples I through V were determined shortly before the Faraday magnetic measurements by drying specimens from the samples to a constant weight at 110°C. The weight percent of moisture on an ovendry basis is given in Table XXXVII.

TABLE XXXVII

MOISTURE

Sample	Moisture, %
I	0.70
II	3.42
III	2.53
IV	2.61
V	2.87

APPENDIX VI

FARADAY SYSTEM MEASUREMENTS

The apparent weight changes, Δw, and the calculated gram-atomic paramagnetic susceptibilities, χ_A', are listed in the following tables for Samples I through V. Each value is an average of usually three experimental determinations. Δw is expressed in units of milligrams and the temperature is given in °C. The method of data treatment is illustrated for Sample V.

SAMPLE I

The calibration results in Table XIX apply to these measurements (Tables XXXVIII and XXXIX). The weight of the specimen in the magnetic balance equaled 150.1 mg.

TABLE XXXVIII .

AVERAGE WEIGHT CHANGES

Current, amp.	Δw -77.6°C.	Δw -63.5°C.	Δw -45.2°C.	Δw -22.5°C.
2	0.250	0.237	0.224	0.204
3	0.500	0.474	0.445	0.407
4	0.714	0.679	0.636	0.581
5	0.867	0.825	0.772	0.706
6	0.984	0.937	0.875	0.801
7	1.078	1.028	0.959	0.876

Current, amp.	Δw 0.3°C.	Δw 24.6°C.	Δw 44.9°C.
2	0.201	0.185	0.159
3	0.406	0.370	0.329
4	0.579	0.525	0.475
5	0.702	0.641	0.577
6	0.797	0.724	0.656
7	0.872	0.794	0.718

TABLE XXXIX

SUSCEPTIBILITIES OF SAMPLE I

Temp., °C.	$\chi_{\underline{A}}{}' \times 10^3$, c.g.s. em. units
-77.6	13.37
-63.5	12.75
-45.2	11.99
-22.5	11.02
0.3	10.95
24.6	10.05
44.9	9.06

SAMPLE II

The calibration results in Table XVIII apply to these measurements (Table XL and XLI). The specimen weight equaled 158.3 mg.

TABLE XL

AVERAGE WEIGHT CHANGES

Current, amp.	Δw -77.6°C.	Δw 1.3°C.	Δw 20.0°C.	Δw 47.1°C.
2	0.789	0.627	0.607	0.572
3	1.597	1.277	1.235	1.158
4	2.283	1.831	1.765	1.662
5	2.778	2.232	2.154	2.019
6	3.152	2.536	2.447	2.294
7	3.455	2.780	2.680	2.514

TABLE XLI

SUSCEPTIBILITIES OF SAMPLE II

Temp., °C.	$\chi_{\underline{A}}{}' \times 10^3$, c.g.s. em. units
-77.6	12.89
1.3	10.44
20.0	10.11
47.1	9.53

SAMPLE III

The calibration results for the Faraday system in Table XVIII apply to these measurements (Table XLII and XLIII). The specimen weight equaled 161.0 mg.

TABLE XLII

AVERAGE WEIGHT CHANGES

Current, amp.	$\overline{\Delta w}$ 20.5°C.	$\overline{\Delta w}$ 26.9°C.	$\overline{\Delta w}$ 52.8°C.
2	0.752	0.737	0.684
3	1.523	1.494	1.381
4	2.174	2.132	1.977
5	2.646	2.593	2.403
6	3.007	2.941	2.727
7	3.296	3.222	2.988

TABLE XLIII

SUSCEPTIBILITIES OF SAMPLE III

Temp., °C.	$\underline{X_A}' \times 10^3$, c.g.s. em. units
20.5	14.99
26.9	14.70
52.8	13.68

SAMPLE IV

The calibration results in Table XVIII and a specimen weight of 158.8 mg. apply to the measurements at 25.4°C. A specimen weight of 149.3 mg. and the results in Table XIX apply to the remaining data (Tables XLIV and XLV).

TABLE XLIV

AVERAGE WEIGHT CHANGES

Current, amp.	Δw -77.6°C.	Δw -63.5°C.	Δw -45.2°C.
2	1.069	1.006	0.908
3	2.159	2.029	1.828
4	3.088	2.900	2.613
5	3.755	3.530	3.180
6	4.264	4.008	3.608
7	4.673	4.389	3.953

Current, amp.	Δw -22.5°C.	Δw 0.4°C.	Δw 24.7°C.
2	0.831	0.746	0.684
3	1.680	1.511	1.384
4	2.405	2.163	1.977
5	2.924	2.629	2.404
6	3.322	2.986	2.729
7	3.636	3.272	2.988

Current, amp.	Δw 25.4°C.	Δw 44.3°C.	Δw 49.1°C.
2	0.727	0.677	0.640
3	1.474	1.366	1.295
4	2.114	1.953	1.849
5	2.570	2.374	2.251
6	2.921	2.693	2.555
7	3.201	2.948	2.796

TABLE XLV

SUSCEPTIBILITIES OF SAMPLE IV

Temp., °C.	$\chi_A' \times 10^3$, c.g.s. em. units
-77.6	22.30
-63.5	20.98
-45.2	18.93
-22.5	17.42
0.4	15.68
24.7	14.38
25.4	14.49
44.2	14.20
49.1	13.47

SAMPLE V

The calibration results in Table XIX apply to these measurements (Tables XLVI and XLVII). A specimen weight of 149.5 mg. was used in the magnetic balance. Treatment of the experimental data is illustrated for the measurements at 25.1°C.

TABLE XLVI

AVERAGE WEIGHT CHANGES

Current, amp.	Δw -77.$\overline{6}$°C.	Δw -63.$\overline{5}$°C.	Δw -45.$\overline{2}$°C.
2	0.902	0.868	0.774
3	1.824	1.744	1.564
4	2.613	2.495	2.234
5	3.174	3.031	2.715
6	3.608	3.446	3.072
7	3.949	3.769	3.376

Current, amp.	Δw 0.3$\overline{0}$°C.	Δw 25.$\overline{1}$°C.	Δw 45.$\overline{0}$°C.
2	0.642	0.596	0.545
3	1.295	1.196	1.098
4	1.850	1.712	1.574
5	2.247	2.079	1.912
6	2.552	2.360	2.169
7	2.794	2.586	2.378

TABLE XLVII

SUSCEPTIBILITIES OF SAMPLE V

Temp., °C.	$\chi_{\underline{A}}' \times 10^3$, c.g.$\overline{s}$. em. units
-77.6	22.13
-63.5	21.18
-45.2	18.98
0.3	15.78
25.1	14.63
45.0	13.46

The specific susceptibility of Sample V at 25.1°C. was calculated from the experimental data by application of Equation (7), which states that

$$\chi = \frac{[F - f(H)]}{m[H_z(dH_z/dx)]} .$$

Upon substitution of the "Calibration Two" results and with $\underline{m} = 149.5 \times 10^{-3}$ g., the following was obtained (Table XLVIII):

TABLE XLVIII

AVERAGE SPECIFIC SUSCEPTIBILITY

Current, amp.	$[\underline{F} - f(\underline{H})]$, dynes	$\underline{m}[\underline{H}_z(\underline{dH}_z/\underline{dx})]$, g.(oersted)^2/cm.	$\chi \times 10^6$, c.g.s. em. units
2	0.5815	33.11 x 10^3	17.56
3	1.173	67.04 x 10^3	17.50
4	1.683	96.11 x 10^3	17.51
5	2.046	116.9 x 10^3	17.50
6	2.324	132.4 x 10^3	17.55
7	2.548	145.6 x 10^3	17.49

$$\chi_{av.} = 17.52$$

The diamagnetic contribution to the susceptibility was determined by application of Wiedemann's additivity law, Equation (15), as described in Appendix IV. The weight fractions of the various components, $\underline{p}_i$, were calculated from the analytical data given in Appendix V.

$$p_{Fe} = 0.0683$$

$$p_{tar.} = 0.509$$

$$p_{gly.} = 0.060$$

$$p_{Na} = 0.251$$

$$p_{NO_3} = 0.048$$

$$p_{OH^-} = 0.035$$

$$p_{H_2O} = 0.028$$

With the exception of glycerol, the specific diamagnetic susceptibilities, $\chi_{\underline{d}}$, of the above components are listed in the sample calculations for the Gouy system (Appendix IV). Glycerol has a value for $\chi_{\underline{d}}$ of -0.538 x 10^{-6} c.g.s. em. units (79). Upon substitution into Equation (15)

$$\chi_d = -0.374 \times 10^{-6} \text{ c.g.s. em. units.}$$

The paramagnetic specific susceptibility, χ', then equaled $(\chi - \chi_{\underline{d}})$, or 17.89 x 10^{-6} c.g.s. em. units. $\chi_{\underline{A}}'$ was calculated as

$$\chi_A' = \frac{17.89 \times 10^{-6}(55.487)}{p_{Fe}} = 14.63 \times 10^{-3} \text{ c.g.s. em. units,}$$

where 55.487 is the atomic weight of iron.

The experimental values of $\chi_{\underline{A}}'$ at the various temperatures were fit to Equation (4) by the method of least squares to give the relation

$$\chi_A' = 4.209/(T-7.588).$$

At a temperature of 298.0°K, $\chi_{\underline{A}}'$ equaled 14.493 x 10^{-3} c.g.s. em. units from this equation. Substitution of these values into Equation (3), as illustrated in Appendix III, gave an effective magnetic moment of 5.88 B.M.

APPENDIX VII

LOCATION OF ABSORPTION MAXIMA

The wavelength of maximum absorbance for the broad bands in the FeTNa spectrum (Fig. 22) was located by determining the limiting value of the mean wavelengths, $(\lambda_1 + \lambda_2)/2$, as the optical density of the mean approached the maximum optical density (46). (λ_1 and λ_2 are the wavelengths at either side of a band for a given optical density.) Reportedly, this method gives the wavelength of the maximum at least five times more accurately than is possible by simply looking for the highest point on the curve.

The position of the maximum which corresponded to the inflection in the absorption curve (Fig. 22) was obtained by the subtraction of the extrapolated background method (46). The region in the vicinity of the inflection was examined experimentally on a very expanded scale of the spectrophotometer for magnification. A Gaussian curve was then fit to the experimental curve on both sides of the inflection. The partly obscured band was found by subtracting points on the Gaussian curve from the absorption line. The maximum was determined as the wavelength at which the slopes of the two curves were equal. (The method is illustrated in Fig. 26.)
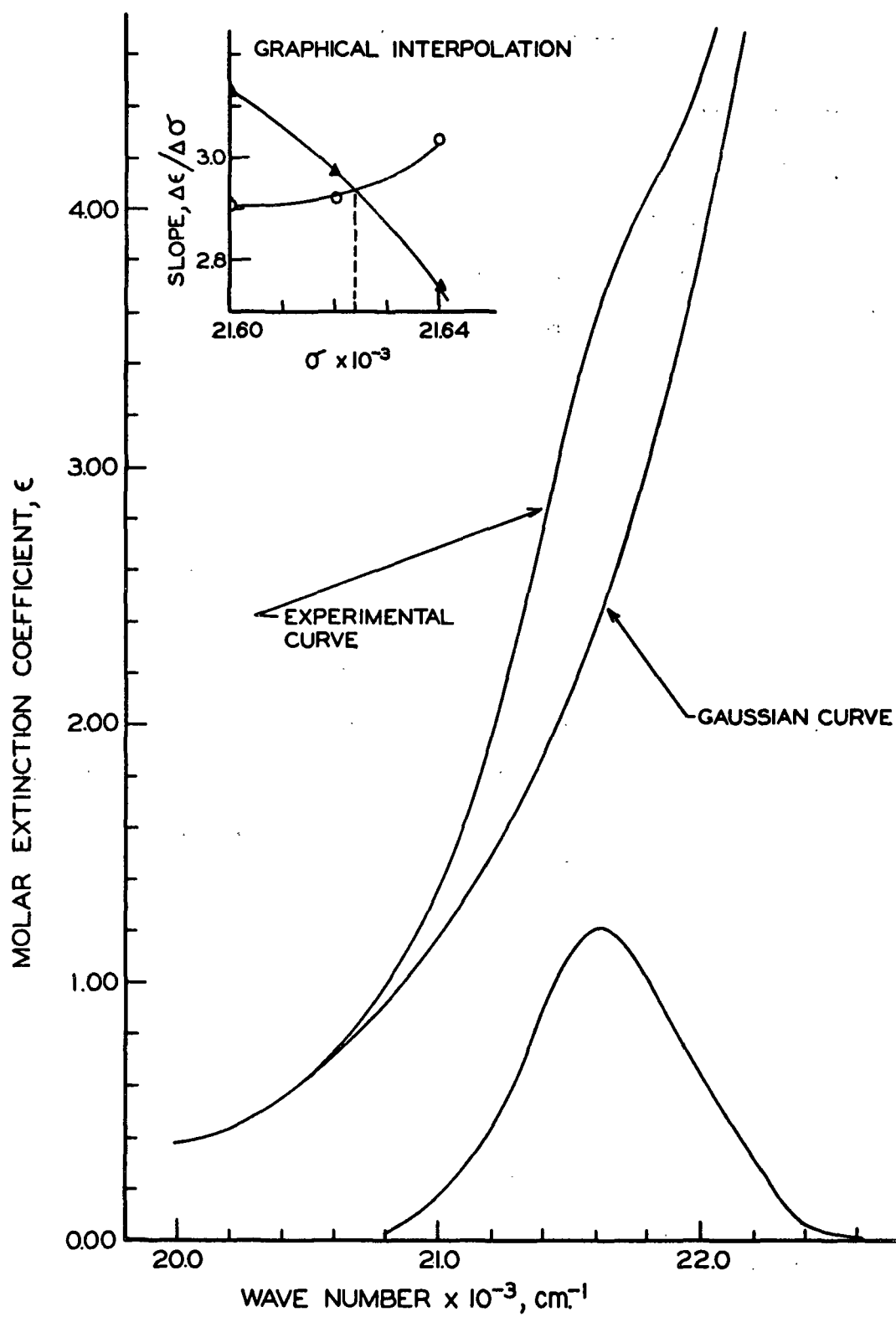
Figure 26. Position of the Inflection